Paleomagnetism of Mesoproterozoic Lavas in the Barby Formation of the Sinclair region, southern Namibia

XinXin Xu

Advisor: David A. D. Evans, Yale University
Second Reader: Richard E. Hanson, Texas Christian University

A Senior Thesis presented to the faculty of the Department of Geology and Geophysics, Yale University, in partial fulfillment of the Bachelor's Degree.

Table of Contents

Abstract

The Sinclair region, along the western margin of the Kalahari Craton, comprises several low-grade volcano-sedimentary sequences that are amenable to paleomagnetic study. The ca. 1212 Ma Barby lavas provide ample opportunity for generating a robust paleomagnetic pole. The goal of this project is to combine newly collected field data of the Barby Formation with previously published paleomagnetic results from the Sinclair region, to obtain a fuller understanding of the motion of the Kalahari craton as global paleogeography transitioned between the Nuna and Rodinia supercontinents. Chapter 1 provides geologic context and motivation for the study. In Chapter 2, new zircon U-Pb geochronology via laser-ablation ICP-MS are presented, dating the nonconformably underlying Haremub granite at ca. 1336 Ma, and providing a maximum age for the Barby sequence. Chapter 3 presents a simple structural analysis from three different fault-bounded panels of distinct general bedding attitudes (younging directions as follows): Vergenoeg (NE), Naus/Heuwelvlakte (N), and Aruab (SW). Mesoscale folds in the Aruab panel indicate a ~25-30° WNW-directed plunge; other areas have insignificant plunges. Chapter 4, the main body of this thesis, includes the Barby paleomagnetic results. Most sites have simple one- or two-component magnetizations with a magnetite- or hematite-borne characteristic remanence direction toward N or NE and shallowly to moderately downward. Whereas volcaniclastic breccia tests are either negative or inconclusive, all fold or tilt tests yield positive results; and the folding is demonstrably older than cross-cutting dikes dated at 1105 Ma. Inverse baked-contact tests on those dikes are also positive. Relative to the other two panels, Aruab has anomalous NE declinations that may indicate local ~50° clockwise vertical-axis rotation in that area, or perhaps a distinct age for those undated "Barby" lavas. The Naus/Heuwelvlakte and Vergenoeg areas show a broadly consistent north and shallow-down characteristic magnetization in tilt-corrected

coordinates, generating a paleomagnetic pole from 18 site-mean virtual geomagnetic poles at 50.5°N, 004.6°E (K=14.7, A_{95}=9.3°). Two alternative Mesoproterozoic apparent polar wander paths for Kalahari are proposed for ca. 1370 – 1000 Ma, depending on the polarity choice for the ca. 1370 Ma alkaline complexes in South Africa. Chapter 5 summarizes conclusions from the study and suggests further work.

Chapter 1: Introduction

Goals of the Study

Southern Namibia is part of the Kalahari Craton (Fig. 1-1), which is speculated to have occupied a central location the Rodinia supercontinent (Jacobs et al., 2008; Loewy et al., 2011). Along the western margin of the Kalahari Craton, the Sinclair region, in southern Namibia, comprises several Mesoproterozoic low-grade volcano-sedimentary sequences (Miller, 2012) that are amenable to paleomagnetic study. The goal of this project is to expand the Precambrian paleomagnetic database for Kalahari craton, in order to constrain its Mesoproterozoic Apparent Polar Wander Path (APWP). By combining the newly collected field data with previously published paleomagnetic results from the Sinclair region, a better understanding of the motion of the Kalahari craton can be obtained during its journey from a possible location in the Nuna Supercontinent to its ultimate location within Rodinia.

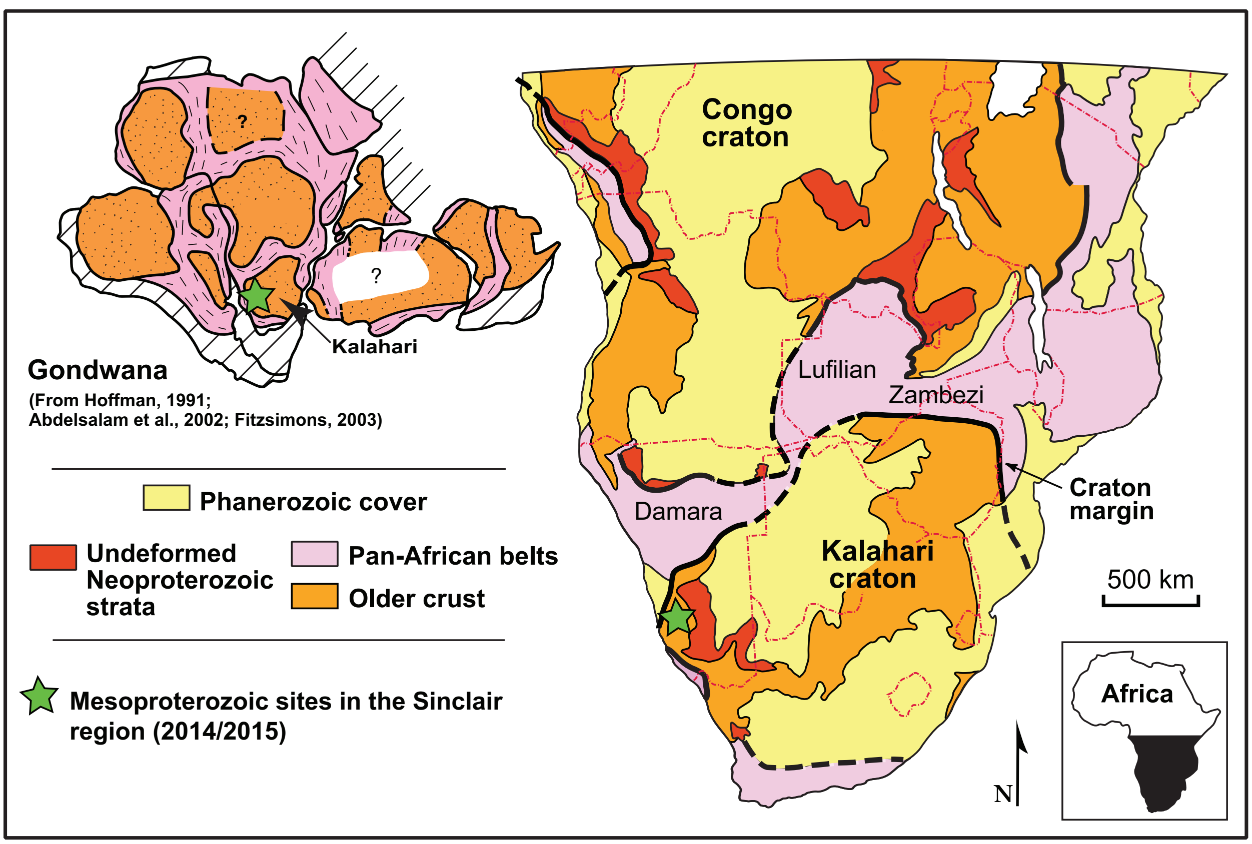

Figure 1-1: Gondwana Craton Map showing both the Kalahari and the Congo cratons with the Damara-Zambezi belt in between. The green star shows the Mesoproterozoic Barby sites from 2014-2015. (Adapted from Hanson, 2003)

Regional geology

Sinclair succession (same as that referenced in Panzik et al., 2015) is unmetamorphosed (top) to mildly metamorphosed (bottom of stratigraphy), and only mildly deformed. The youngest, least-metamorphosed units within the Sinclair stratigraphy include, in order (Fig. 1-2): Barby Formation bimodal lavas and interbedded siliciclastic sedimentary rocks (ca. 1212 Ma; David Cornell, pers. comm., 2016), Guperas Formation siliclastic sedimentary rocks and interbedded, largely felsic extrusive rocks (likely ≥ 1105 Ma; Panzik et al., 2015), post-Guperas bimodal dikes (1105 ± 1 Ma; Panzik et al., 2015), and Aubures Formation redbeds (ca. 1100 Ma; Kasbohm et al., 2015). With a stratigraphic thickness of between 3000m and 5000m, low metamorphic grade, and gentle deformation, the Barby lavas provide ample opportunity for generating a robust paleomagnetic pole, extending the Sinclair paleomagnetic record 100 million years further back in time.

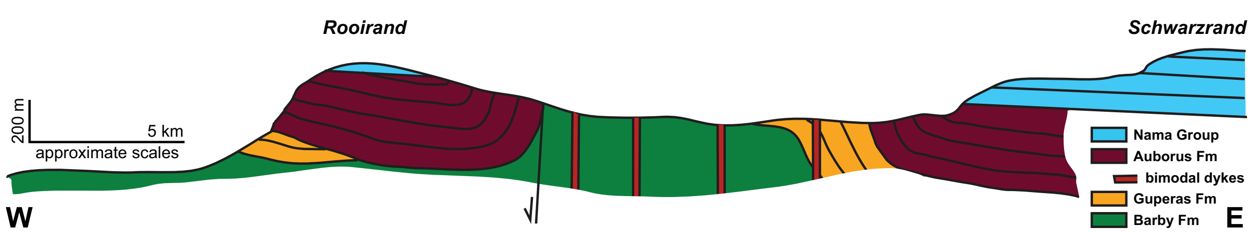

Figure 1-2: Schematic cross sectional representation of the Sinclair stratigraphy. (From Kasbohm et al., 2015).

The Barby Formation consists of variably mafic to felsic lavas and lies conformably on the Kunjas Formation, which is a sedimentary layer consisting of conglomerate, sandstone and shale (Watters, 1974). The bimodal volcanic rocks of basalts and rhyolites that make up the

Barby Formation are interspersed by bedded sediments. The base is typically a rhyolitic unit, followed by basalts and latites. Phyric andesite, large-feldspar trachyandesite (shoshonite), basaltic andesite, trachybasalt and trachyandesite make up most of the rest of the formation. The Aruab Member, a channel deposit of cross-bedded orthoquartzite, is included at the top of the Barby Formation, though its relationship to the Guperas Formation is not clear.

The Sinclair region is deformed into a broadly synclinal structure (Fig. 1-3). The Barby Formation does not outcrop continuously in one area; instead there are five distinct outcrop areas mapped with variable tilt (Von Brunn, 1969; Watters 1974). A “structural panel” is here defined as a local continuous region of outcrops with generally similar bedding attitude. These panels are named as follows, along with general younging directions: Naus/Heuwelvlatkte dipping steeply north, Aruab dipping steeply southwest (but also showing hectameter scale folds plunging shallowly northwest; see Chapter 3), Haremub dipping steeply southeast, Vergenoeg dipping moderately to shallowly northeast, and Osis dipping shallowly southwest. Different structural panels were sampled to constrain any possible local rotations associated with the deformation. It is unclear that all outcrops mapped as Barby are truly Barby; based on preliminary U-Pb ages of granites (author’s unpublished data and D. Cornell, pers. comm., 2016), there is strong suspicion that the outcrops in the Osis region might be older and therefore not correlative with Barby Formation at its type locality in the Naus/Heuwelvlakte structural panel.

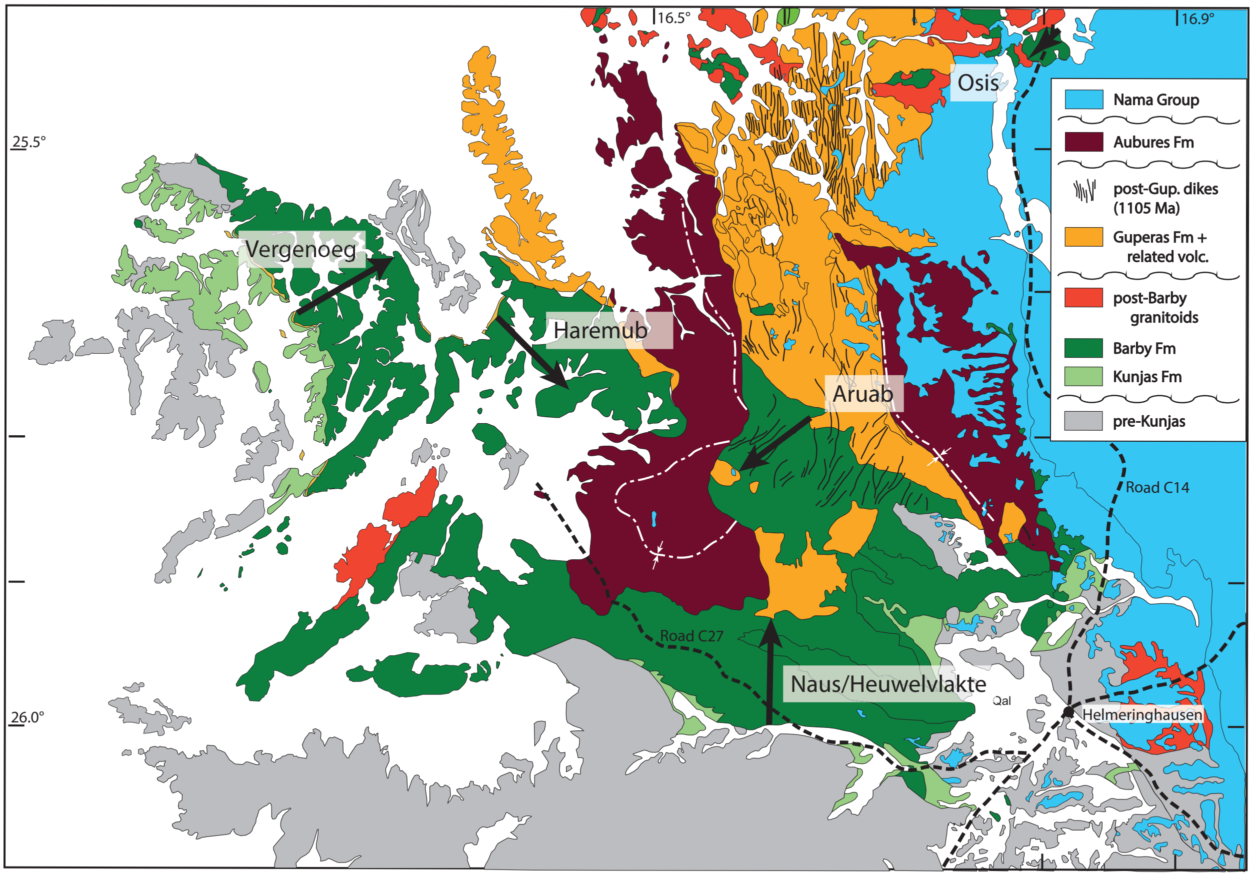

Figure 1-3: Regional map of the Sinclair region showing the five structural panels: Aruab, Naus/Heuwelvlakte, Vergenoeg, Haremub, and Osis. Black arrows denote average stratigraphic younging down sections.

<u>Previous and current paleomagnetic work</u>

There has not been a paleomagnetic study on the lavas in the Barby Formation since the early work of Piper (1975), whose analysis was limited to blanket alternating-field demagnetization of the samples. He obtained a rough clustering of shallow N-S directions from along Road C27 in the Naus/Heuwelvlakte structural panel. Hessert (2014) conducted an inverse baked contact test on the Barby Formation with a post-Guperas dike in the southern Aruab region that yielded a positive result. Unlike Piper, Hessert found a distinctive shallow NE-directed characteristic remanence from unbaked Barby Formation. Because Piper's (1975) result is similar to those of the younger Guperas and Aubures Formations (Fig. 1-4), there was suspicion before this study that Hessert's NE-shallow direction could be a better representative of the primary Barby remanence.

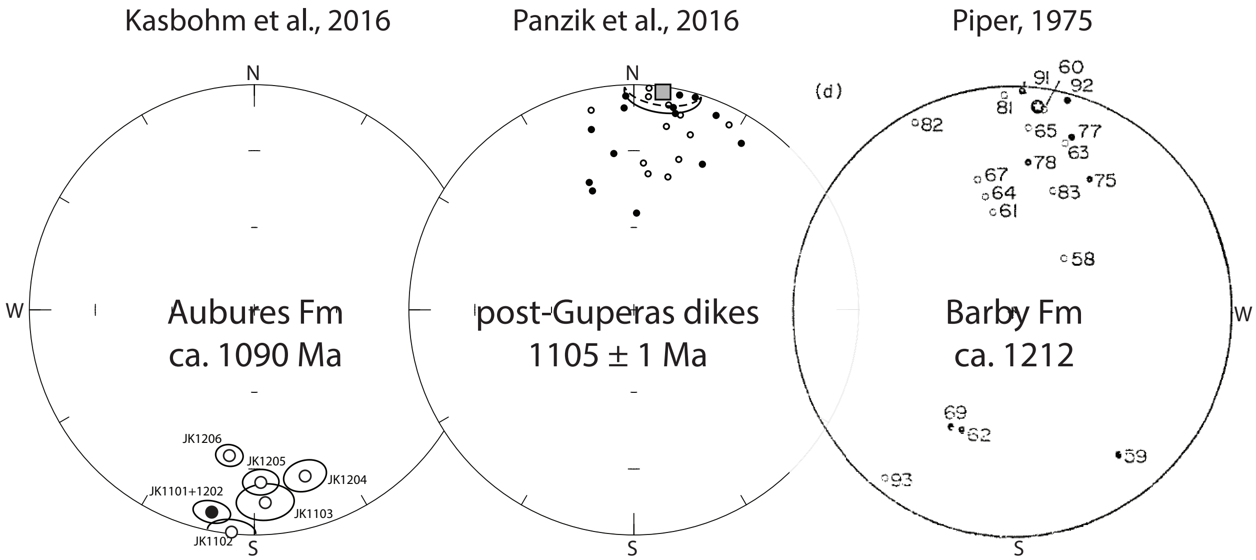

Figure 1-4 Previous paleomagnetic studies done in the Sinclair region. Aubures Formation lies unconformably on the Guperas. The Guperas lies unconformably on top of the Barby Formation, which is dated at ca. 1212 Ma (D. H. Cornell, pers. comm., 2016). Working back through time, there was a geomagnetic polarity reversal between the Aubures Fm and the Post-Guperas dikes directions. The scatter in Piper's Barby Fm data as well as the blanket AF demagnetization method render it suspicious as a possible ca. 1100 Ma overprint.

Building upon Piper's work, thermal demagnetization, statistical analysis, and field stability tests were done on a large set of almost 900 samples to yield a high quality Barby Formation paleomagnetic pole. In addition, we add new geochronological data on the Barby Formation as well as its basement units. Results found here are compared and contrasted with Piper's for a more complete understanding of the Sinclair terrane movement relative to Kalahari in the Mesoproterozoic Era. More globally, determining the position of Sinclair-Kalahari in the Mesoproterozoic can better constrain the craton relative to the location of the Congo-SF craton at the same time. This would help clarify the ideas behind the collision of Kalahari and Congo-SF during the Pan-African assembly. (Prave, 1996; Grunow, Hanson, and Wilson, 1996; Gray, et al., 2006).

Chapter 2: Geochronology

(with contributions from M. Hofmann, U. Linnenmann, Senckenberg Institute)

There are scarce published age constrains on the igneous rocks in the Sinclair region. The post-Guperas dikes which overlie the Barby Formation, sampled by Panzik et al. (2015), were dated at 1105.5 ± 0.4 Ma. This provides a younger constraint on the Barby Formation. The goal of the present study is to provide a maximum constraint on the Barby, by U-Pb dating of its granite basement at the Haremub (Fig. 2-1).

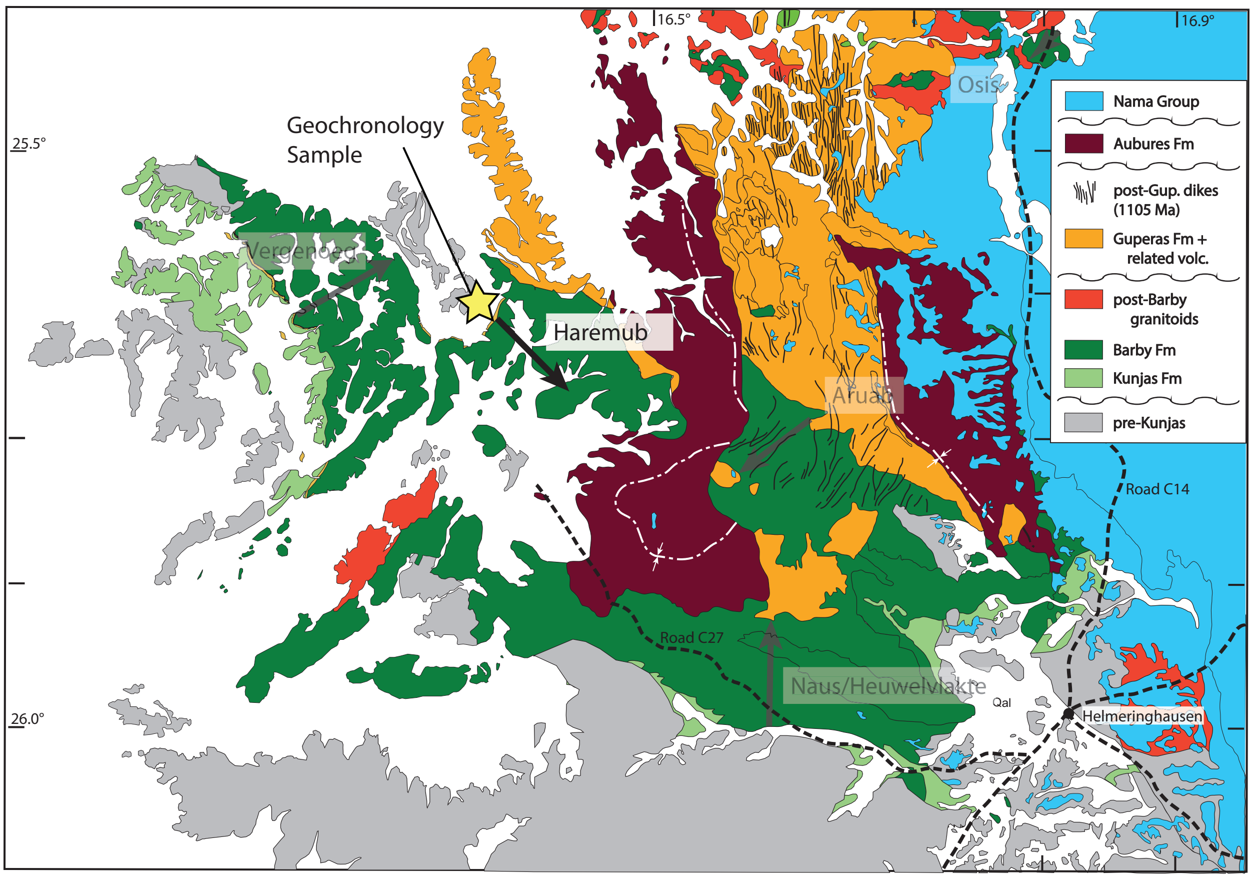

Figure 2-1: Regional map of the Sinclair region with the yellow star demonstrating the relative location of the geochronology sample relative to the Haremub structural panel.

Methods

Geochronology samples were taken from the Haremub structural panel. Site X1580X is a Haremub granite that was taken nearby the main farm house. There was a perthetic texture with brown weathering spots. There was a quartz vein with a weakly foliated direction that was dipping moderately southeast. The medium equigranular granite sample had specks of mafic mineral – biotite. Thin section analysis was not done to confirm the mineralogy of the sample.) Zircon mineral grains were separated from 2-4kg sample material at Yale and Senckenberg Naturhistorische Sammlungen Dresden (Museum für Mineralogie und Geologie) using standard methods. First, the samples was crushed milled, and sorted by density via a Wifley table and separated magnetically via a Frantz Laboratory Magnetic Separator. The non-magnetic fractions were then again separated by density via heavy liquids (LST). The final grains used for U-Pb dating were hand-picked under a binocular microscope. A wide range of grain sizes (50-150 μm) and morphological types were selected, mounted in resin, and polished to half their thicknesses.

The following U-Pb analytical methods are described with minor modifications from those presented in Kasbohm et al. (2015). LA-SF ICP-MS techniques were utilized to analyze for U, Th, and Pb isotopes at the Museum für Mineralogie und Geologie (GeoPlasma Lab, Senckenberg Naturhistorische Sammlungen Dresden); a Thermo-Scientific Element 2 XR sector field ICP-MS coupled to a New Wave UP-193 Excimer Laser System was used. The heterogeneous grains (e.g. growth zones) were sequentially sampled by a teardrop-shaped, low volume laser cell constructed by Ben Jähne (Dresden) and Axel Gerdes (Frankfurt/M.) during time-resolved data acquisition. Each analysis consisted of 15 s background acquisition followed by 30 s data acquisition, using a laser spot-size of 25 and 35 μm, respectively. A common-Pb correction based on the interference- and background-corrected 204Pb signal and a model Pb composition (Stacey and Kramers, 1975) was carried out if necessary. Background signal and other variations such as common Pb, laser induced elemental fractionation etc. were corrected via a spreadsheet program developed by Axel Gerdes (Institute of Geosciences, Johann Wolfgang Goethe-University Frankfurt, Frankfurt am Main, Germany).

Reported uncertainties were propagated by quadratic addition of the external reproducibility obtained from the standard zircon GJ-1 (~0.6% and 0.5-1% for the 207Pb/206Pb and 206Pb/238U, respectively) during individual analytical sessions and the within-run precision of each analysis. Concordia diagrams (2σ error ellipses) and concordia ages (95% confidence level) were produced using Isoplot/Ex 2.49 (Ludwig, 2001). For further details on analytical protocol and data processing see Gerdes and Zeh (2006) and Frei and Gerdes (2009). Zircons showing a degree of concordance in the range of 90-110 % in this paper are classified as concordant because of the overlap of the error ellipse with the concordia. Th/U ratios are obtained from the LA-ICP-MS measurements of investigated zircon grains. U and Pb content and Th/U ratio were calculated relative to the GJ-1 zircon standard and are accurate to approximately 10%.

Results

Zircons from the Haremub granite, which the Barby overlies, yielded concordant U-Pb data (46 out of 120 analyzed), with several modes of ages ranging from 1.6 to 1.3 Ga (Pb 207/206 ages) with individual spot uncertainties between 50-100 million years. The most prominent mode of zircon ages is between 1.4-1.3 Ga (Appendix 1). The following analyses: a10, a12, a13, a15, a17, a41, a43, a50, b19, b24, b26, b27, b30, b34, b38, b41, b42, and b60 yielded a concordia U-Pb age of 1336 ± 8 Ma (2σ; Fig. 2-2).

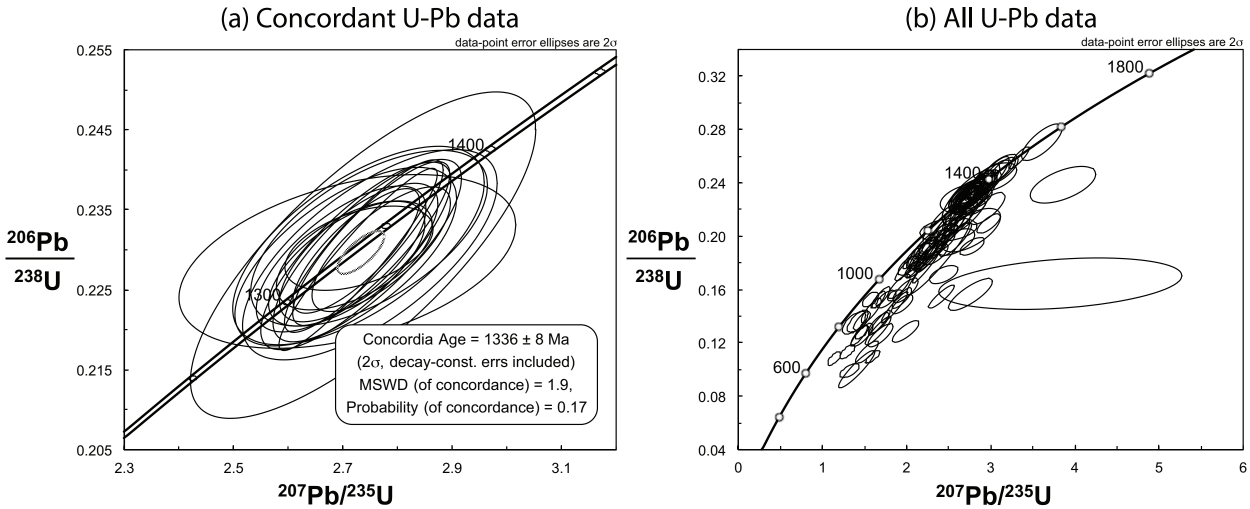

Figure 2-2: (a) Concordia plot demonstrating the Haremub granite U-Pb age with the 2σ error. (b) All U-Pb data collected from the zircons picked from the Haremub granite.

Discussion

We also collected two separate Barby Formation samples: X1549X, the lower part of Barby Formation (but well above the base), which was a pink welded tuff with minor chlorite alteration, and X1579X, the basal unit of the Barby Formation, which was a felsic lapilli tuff. However, those two samples yielded no zircons. Concurrently with our geochronological study, David Cornell (University of Gotheborg, Sweden) was able to obtain preliminary U-Pb zircon ages from the Barby Formation at Vergenoeg: 1214 ± 5 Ma from the basal rhyolite, and 1211 ± 13 Ma from the top of the exposed lava sequence (Cornell, pers. comm., 2016). These ages are consistent with those obtained by this study and Panzik et al. (2016), and henceforth we will consider the Barby Formation (at Vergenoeg) to be ca. 1212 Ma.

Chapter 3: Structural Analysis

Structural analysis was done on three of the structural panels (fault-bounded areas with similar strike): Aruab, Naus, and Vergenoeg. The investigation was done to see if there were any plunge variations in the panels. Any non-zero plunge could deflect remanence declinations (however, inclination would still be the same). Bedding was measured by way of sedimentary strata, or by flattened amygdales in the lava, the latter rarely also containing geopetal structures.

Most of the bedding measurements taken in the three different structural areas yielded a line of consistent orientation or a fold axis. This was interpreted as the geometrical characterization of a cylindrical fold. Other types of folds such as conical folds generally do not have this intersection of planes or a fold axis. The measurements were taken as strike and dip of a paleohorizontal plane assuming right hand rules (Appendix 2). These plane measurements were then converted to poles with the Stereonet program (Cardozo et al., 2013). Finally, a Bingham distribution calculation was done to find the line of common intersection to all the planes. This corresponds to the minimum eigenvector of the distribution of poles, which indicated whether the plunge of each dataset is distinguishable from zero. Uncertainty ellipses on the Bingham distribution at 95% confidence were calculated using the Paleomag software (Jones et al., 2002) after Onstott et al. (1980).

Aruab Region

The western end of the Aruab Mountain is fault-bounded. The fault brings down Aubures redbeds in contact with the Barby Formation (Fig. 3-1). Coarse conglomerates in the Aubures strata lie adjacent to the fault, suggesting motion concurrent with the redbed deposition at ca. 1090 Ma (Kasbohm et al., 2015). This fault might have had an impact on the regional plunge structure of Barby strata in its footwall. The Aruab structure may have first folded perpendicular to the strata, then tilted via the fault structure to create a plunge. To test the hypothesis that the fault may have dragged down its footwall, imparting a westward plunge, we analyzed three different sets of measurements with increasing distances away from the fault.

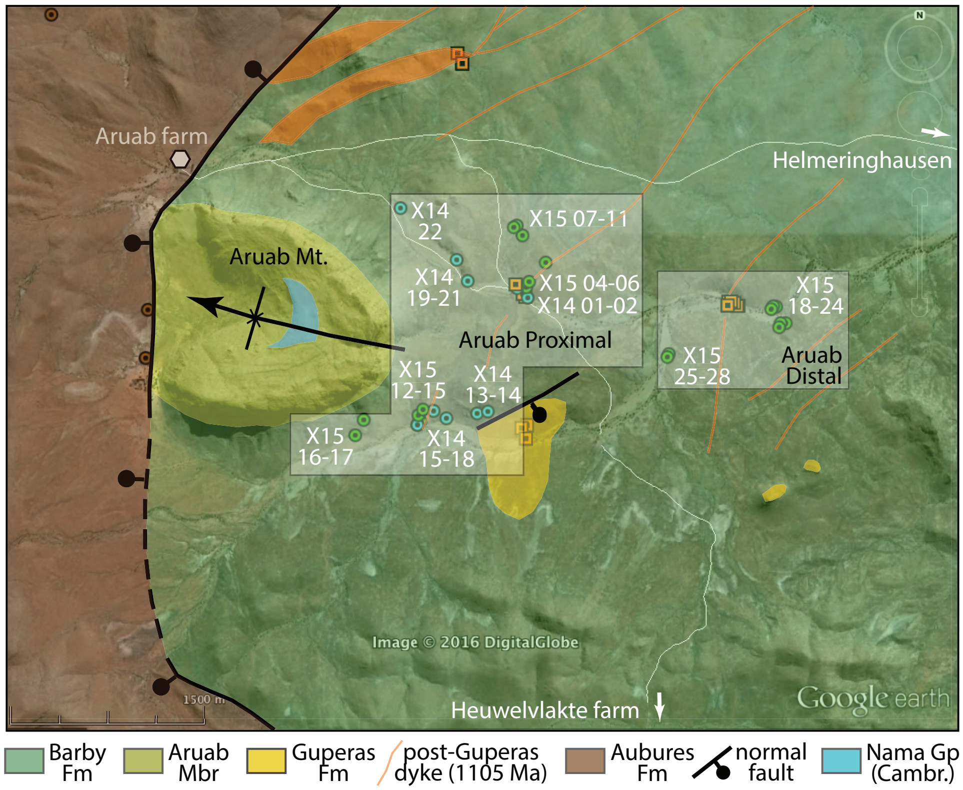

Figure 3-1: Site locations mapped. Three different areas were mapped – Aruab Mountain (or Member used interchangeably below), Aruab Poximal, and Aruab Distal. The green tint here again shows the location of the Barby Formation, yellow – the Guperas Formation, and dark red – the Aubures Formation.

First, 14 different bedding measurements were taken on the quartzitic Aruab Member, which has been included in the Barby Formation (Miller 2008). These measurements yielded a trend of 119.2° and a plunge of -27.4° for the axis of bedding plane (Fig. 3-2a). The second set of 18 measurements was taken in a ring slightly east of the mountain (Aruab Proximal). They yielded a trend of 318.9° and a plunge of 10.2° (Fig. 3-2b). The final set of six measurements was taken east of the second set (Aruab Distal). These measurements yielded a 316.4^{o} and a plunge of 26.4^{o} (Fig. 3-2c).

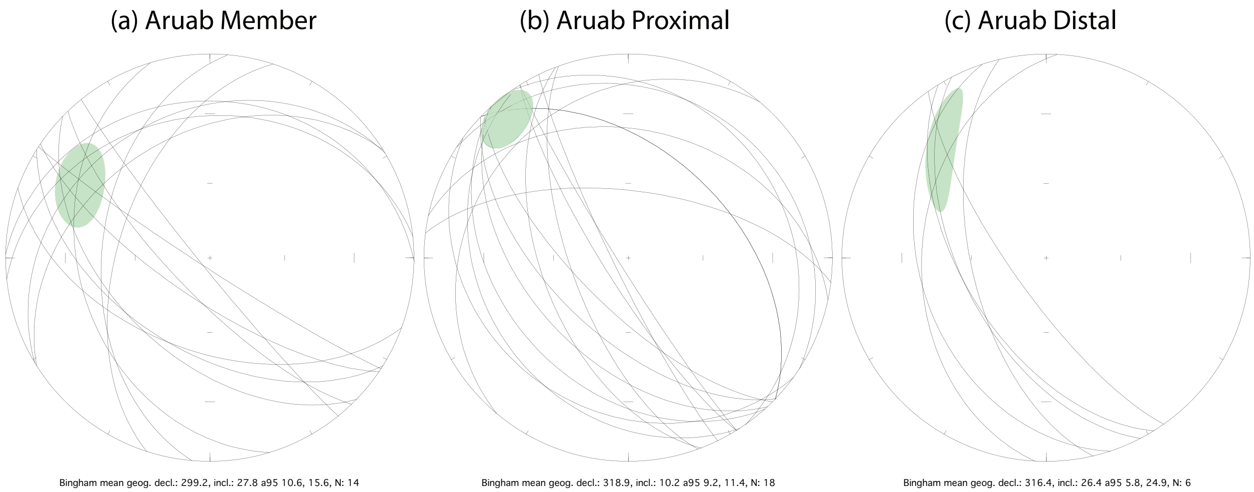

Figure 3-2: Resultant lower hemisphere stereonets from the structural analysis. The Aruab Member shows the steepest plunge, which appears to shallow eastward, away from the fault.

In addition, two smaller-scale fold tests were conducted on sedimentary rocks at sites X1513 and X1515, on a meter-decameter scale. The fold at X1513 has a trend of 308° and a plunge of 22.3°, and the fold at X1515 has a trend of 288° and a plunge of 18.5°. These are in line with the fold axis orientation of the larger first-order fold of the region. The two folds provide independent support of the shallow NW plunge structure, and also the notion that these smaller folds are parasitic to the larger fold structure, and of the same general age. Post-Guperas dikes (1105 ± 1 Ma; Panzik et al, 2015) cut across the folds with undisturbed vertical orientation.

Naus/Heuwelvlakte

We suspected that Naus structure was coaxial to that of Aruab, and we used a combination of X14 and X15 bedding measurements to investigate. Thirteen different measurements demonstrated that the structure was generally homoclinal, spanning the entire area between Naus and Heuwelvlakte farms (Fig. 3-3). Utilizing the method described above, we found that the structure panel defined a trend of 248.2° and a plunge of 20.2°, but the Bingham uncertainty ellipse extends along the common bedding plane orientation to intersect the horizontal. Therefore, the method does not clearly show a unique fold axis (that is, a point of intersection of all the bedding measurements), and the fold-plunge method is not really applicable here. The most remarkable distinction between the Aruab and Naus structural datasets is the difference in regional strike, on the order of 40-70°. Therefore, the structure in Aruab does not extend into the Naus structural area. The strike difference suggests that there could be possible relative vertical-axis rotation between the two areas, and we will consider this option when evaluating the paleomagnetic remanence data.

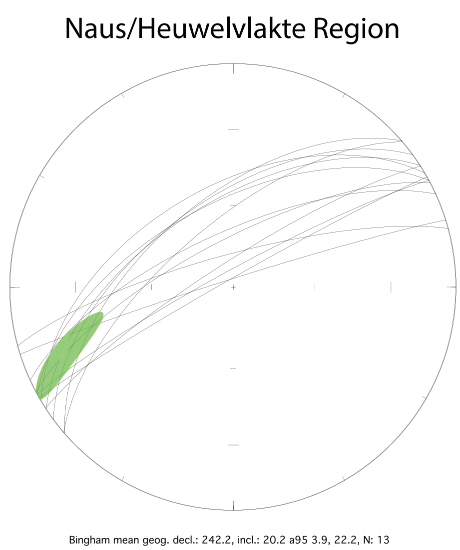

Figure 3-3: Resultant stereonet from the Naus/Heuwelvlakte region structural analysis. Since the measurements are along the same axis, the region is taken to be homoclinal.

<u>Vergenoeg</u>

In map view, the Vergenoeg structure (Fig. 3-1) could appear to be an orocline; the structure panel outcrops in a moon-shaped semicircle. This could indicate that the outcrop was originally straight before becoming curved via vertical-axis deformation (Weil, 2006). If this were the case, we would expect the strikes at the northern end of the outcrop to be northwest in direction and the strikes in the southern half of the outcrop to have a southeastern direction. If the southern structure retained an original orientation, then the northern end could have been deflected by as much as 90°. Because the paleomagnetic sites are restricted to the northern area (the southern area is invaded by a younger granite and was avoided), any oroclinal bending of the northern region can only be detected by comparison of remanence data with the other structural panels. The measured Vergenoeg bedding planes (n=12) intersect in a shallowly plunging northern trend (Fig 3-4). The data is slightly skewed since most of the measurements are shallow north northwestern or north northeastern direction. Nevertheless, the bedding is shallow; therefore, this might be indicative of a shallow domal uplift of the region.

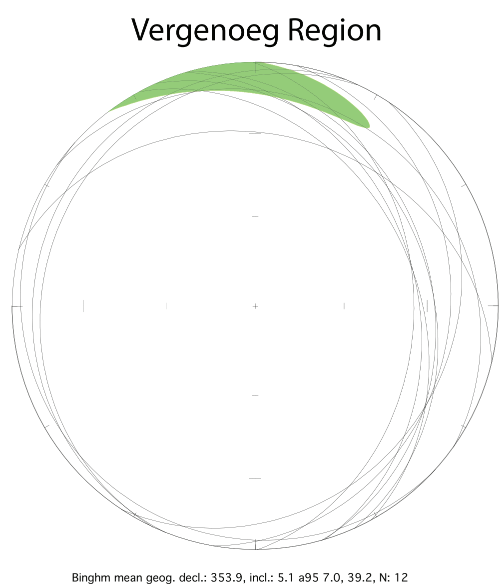

Figure 3-4: Vergenoeg resultant stereonet. Since the measurements are along the same axis, the region is taken to be homoclinal.

Chapter 4: Paleomagnetism

Methods

100 sites of the Barby Formation were collected between 2014 and 2015 in the Sinclair region of Southern Namibia. 22 sites of 194 samples were collected over two-week field season in July 2014, which was used as a preliminary basis for a three-week return sampling trip in June 2015, which entailed collection of another 78 sites. At the time of writing, 63 total sites or 543 samples were measured, of which 50 sites and 438 samples were utilized for mean directions.

Preliminary site selection was done by referencing geological maps of the region with Google Earth satellites, as well as published works (Piper et al., 1975; Watters, 1974). Further on-the-ground scouting was done to find outcrops that were suitable for paleomagnetic sampling. Sites had to petrologically fresh and lightning activity free, which was screened via a compass. Each site contained approximately eight samples; the exceptions were field test sites, which contained between 10-20 samples. These samples were cored with a diamond-tip bit, which drilled samples 2.5cm in diameter and 5-10cm in length. Samples were then oriented with a solar and magnetic compasses and a clinometer. Each site sampled a single rock type; again the exceptions being field tests, which might have taken samples from various clasts in a conglomerate or breccia (for a conglomerate or breccia test) or samples along an intrusion margin (for a [inverse] baked contact test). Site location coordinates and lithologies can be found in Table 1 in Appendix C. A variety of methods were utilized to determine paleohorizontal – sedimentary bedding, flattened vesicles/amygdales, and flow banding. Strike and dip measurements were taken from these indicators for tilt-correction calculations.

Samples were taken to the Yale Paleomagnetic Laboratory for measurement and analysis. Samples were cut from 5-10cm in length to be about 1-2cm in length. The metadata information (site location, paleohoriztonal, orientation) were documented electronically. Prepped samples were then analyzed using a cryogenic DC-SQuID magnetometer with automated sample changer (Kirschvink et al., 2008). Initial natural remanent magnetization (NRM) measurements were recorded. Then samples were immersed in liquid nitrogen and measured again at room temperature. After that, samples were then heated to 100°C for about 10 min. in a magnetically shielded oven before measurement on the magnetometer. The samples were heated in the shielded ovens thereafter in a nitrogen atmosphere to increasingly higher temperatures. Temperature steps decreased as samples approached the Curie temperatures (580°C for magnetite, 670°C for hematite). Samples remained in this cycle until completely demagnetized.

After the samples were demagnetized, least squares analysis (Kirschvink,1980; Jones, 2002) was done to fit lines to the characteristic remanent magnetization. Components were labeled using a system of abbreviations including MAG (magnetite curie temperature component), HTH (high thermal), MTO (magnetite-to-origin), HTO (hematite-to-origin), DTO (decay-to-origin), and SEP (stable endpoint). After fits were made for each sample, a single data point representing the characteristic remanence direction was plotted on an equal-area projection of the unit sphere (Butler, 1992). For each site, these data points were analyzed with Fisher (1953) statistics to determine common component directions that agree with each other, and these were used to calculate final Barby mean direction. Appendix 3 has diagrams detailing every sample mean in geographic and tilt-corrected coordinates as well as a representative sample's Zijderveld and equal area plots.

<u>Site Descriptions/Results</u>

Below are descriptions of the sites that were drilled including the lithology, initial magnetic moment behavior, resultant ChRM equal area, and remanent components. The results are organized via geographic regions in the following order: North Aruab, South Aruab, Heuwelvlakte, Naus, and Vergenoeg.

North Aruab

X1401

Seventeen samples were taken from a layer of volcaniclastic breccia complex, near the western baked contact test of Hessert (2014). A breccia test was done on 13 clasts. Samples B1 and B2, D1 and D2, and F1 and F2 were three pairs drilled from the same clasts. All the samples had a single hematite component with clear decay-to-origin behavior. The initial magnetic moments of the samples in the site were moderate at 1e-03 to 1e-04 emu with no indication of lightning activity. The resultant ChRM was quite well clustered equal area plot. The alpha 95 of the Fisher statistics was 2.7°. The cluster was an upward shallow northeastern direction in geographic coordinates. In tilt-corrected coordinates, the cluster became a shallower downward northeastern direction. Since the directions were well clustered, the breccia test is negative: magnetization was acquired after incorporation of the clasts into the breccia.

X1402

This site was another breccia test a few meters downstream from X1401 and the Hessert (2014) baked contact test. The site had similar composition as X1401, with a mafic volcaniclastic composition. Eleven samples were taken from 10 clasts; sample F1 and F2 were from the same clast. All the samples exhibited clear decay-to-origin and single component behavior. The initial magnetic moment of the samples in the site was moderate at 1e-03 to 1e-04 emu with no indication of lightning activity. The ChRM results were well clustered (Fisher statistics alpha 95 of 4.5°) in a very shallow upwards-northeastern direction in geographic coordinates; tilt-corrected, this direction was a shallow downward northeastern direction. Sample J was an outlier in both geographic and tilt-corrected coordinates. Since the site was well clustered, the breccia test is negative: magnetization was acquired after incorporation of the clasts into the breccia.

X1419

Eight samples were taken from a chocolate-brown lava flow with banded dark layers (which was used as paleohorizontal). The samples began with weak magnetic moments from 1e-03 to 1e-05 emu. The samples all had two components and decay-to-origin behavior. The ChRM of the samples had a shallow upwards east northeastern direction in geographic coordinates with an alpha 95 of 4.7°. In tilt-corrected coordinates, the cluster had a shallow downwards east northeastern direction

X1420

Seven samples were taken from a felsic lava on a ridge to the east of Aruab, approximately 1km west of X1419. The lavas are conformably overlain by silty sediments that provided paleohorizontal for the site. The samples began with weak magnetic moments from 1e-04 to 1e-05 emu. The samples all had two components and decay-to-origin behavior with the exception of sample H, which exhibited a high-temperature stable endpoint. The ChRM of the samples had a steep upwards east northeastern direction in geographic coordinates with an alpha 95 of 5.0°. In tilt-corrected coordinates, the cluster had a shallow downwards northeastern direction.

X1421

Eight samples were taken from the silty sediments above X1420. The samples began with moderate magnetic moments from 1e-04 to 1e-03 emu. The samples all had two components with the exception of H, which had a single component, and all samples exhibited decay-to-origin behavior. The ChRM of the samples had a steep upwards east northeastern direction in geographic coordinates with an alpha 95 of 4.0°. In tilt-corrected coordinates, the cluster had a shallow downwards northeastern direction.

South Aruab

X1413

Eight samples were taken from the eastern flank of Aruab Mountain, across the fault from the Guperas section (JP1128). Numerous fractures and quartz veins cut this coherent mafic lava, which is a dark chocolate brown color. The samples began with weak magnetic moments from 1e-04 to 1e-05 emu. The samples all had two components and either decay-to-origin or stable high-temperature end point behavior. The ChRM clustered in a shallow upwards north northeastern direction with an alpha 95 of 10.0° in geographic coordinates. Sample C was excluded as an outlier (its direction was a shallow upwards eastern direction in geographic coordinates). In tilt-corrected coordinates, this direction was a shallow downwards north northeastern direction.

X1414

Eight samples were taken on the western flank of Aruab Mountain. There was evidence of bedding in the sandstone that was consistent with the paleohorizontal indicators in X1413. The samples were from a mafic lava flow that was visually similar to X1413, which is slightly above the sandstone layer. There is also evidence of a small fault nearby but the site was drilled approximately 10 meters north of the fault. The samples began with weak magnetic moments from 1e-04 to 1e-05 emu. The samples all had two components and either decay-to-origin or stable high-temperature end point behavior. The ChRM clustered in a shallow upwards north northeastern direction with an alpha 95 of 12.9° in geographic coordinates. In tilt-corrected coordinates, this direction was a shallow downwards north northeastern direction.

X1415

Eight samples were taken from a sediment layer approximately 1km north of X1413 and X1414. The samples began with weak magnetic moments from 1e-04 to 1e-05 emu. The samples all had two components and exhibited high temperature stable-end-point behavior. The ChRM clustered in a mid-shallow upwards northern direction with an alpha 95 of 17.7° in geographic coordinates. In tilt-corrected coordinates, this direction was a shallow upwards/downwards northeastern direction.

X1416

Eight samples were taken from visually similar chocolate brown lava that was next to X1415. The site was slightly downhill and southeast of X1415. The samples began with weak magnetic moments from 1e-04 to 1e-06 emu. All samples had two components and either decay-to-origin or high temperature stable-end-point behavior. The ChRM of the samples had a mid-shallow upwards north northeastern direction in geographic coordinates with an alpha 95 of 5.9°. In tilt-corrected coordinates, the cluster had a mid-shallow downwards north northeastern direction.

X1417

Seven samples were taken from a lava flow below X1416. The lava flow was a dark brown heavily weathered with small vesicles. The samples began with weak magnetic moments from 1e-04 to 1e-06 emu. All samples had single components and clear decay-to-origin behavior. The ChRM of the samples had a steep downwards north northeastern direction in geographic coordinates with an alpha 95 of 5.4°. In tilt-corrected coordinates, the cluster had a shallow downwards northeastern direction

X1418

Nine samples were taken approximately 10m above X1417 in a siltstone/fine-grained sandstone. There were numerous reduction spots and the site was heavily weathered with fractures parallel to the bedding planes. The samples began with weak magnetic moments from 1e-04 to 1e-05 emu. The samples all had two components and high temperature stable-end-point behavior with the exceptions of: sample C, which had a clear mid-temperature component, sample D, which had a decay-to-origin behavior, and sample E, which had a clear high-temperature component. The ChRM of the samples had a shallow downwards north northeastern direction in geographic coordinates with an alpha 95 of 13.9°. In tilt-corrected coordinates, the cluster had a shallow upwards north northeastern direction

X1422

Eight samples were taken from a banded lava flow; the banding in the lava is variable but dipped generally steeply to the west. The samples began with weak magnetic moments from 1e-04 to 1e-05 emu. The samples all had two components and exhibited decay-to-origin behavior, with the exception of sample H, which had a high temperature stable-end-point. The ChRM of the samples had a shallow upwards north northeastern direction in geographic coordinates with an alpha 95 of 10.3°. In tilt-corrected coordinates, the cluster had a steep downwards northern direction.

X1512

The site was a breccia on the southeastern side of Aruab. Only regional bedding was used to tilt-correct the 15 samples taken. Sample specific strike and dip were taken; however, it was unnecessary to use these measurements, since the data clustered together well in geographic coordinates. The Z-feld diagrams show generally two to three components. The low temperature component was also clearly shown as a north or northeastern direction in both geographic and tilt-corrected coordinates. The ChRM plotted on the equal area LSQ diagram show a group in this northeastern direction as well – there was almost no scatter on the stereonet. With an alpha 95 of 16.5, the breccia test is negative. This indicates overprinting of the site after the brecciation event. The direction could still be 'primary' for the purposes of tectonic reconstruction if such overprinting corrode during the emplacement of the Barby succession.

X1513

12 samples were taken in sediments overlain by lava over two different bedding altitudes for a fold test. Samples A through H were on the eastern side of the fold axis with samples I through L on the Western side of the fold axis. All samples began with magnetic moments around 1e-04 or 1e-05 emu. There was no indication of lightning activity in site. Nine of the 12 samples had two-component demagnetization behavior (B, C, E-I, K, L); the rest had single component behavior (A, D, J). All the samples seem to have a well-clustered single direction on the equal area view. The samples yielded consistent directions with stable decay-to-origins; only sample K had a stable endpoint. The site in geographic coordinates yielded two clusters both in downward northeastern directions, one cluster shallower than the other (with a single outliner – sample H, which was excluded). In tilt-corrected coordinates, the clusters grouped together in a shallow downward northeastern, passing the fold test. In addition, the er statistics provide additional evidence for passing the fold test. The alpha 95 was 14.4 for geographic coordinates; in tilt-corrected coordinates, the alpha 95 decreased to 5.3. There was also a clear low temperature component in the majority of the samples (with the exception of Sample A and D which were excluded). This low component was the opposite polarity of the stable end/decay-to-origin direction of X1517. Sample F, which is chosen as the representative sample, had the strongest

representation of this low temperature component in both the equal area and orthographic views. (This might be reminiscent of a 1000 Ma overprint).

X1514

Eight samples were taken from a small outcrop of brown vesicular lava lying conformably atop sediments from X1513. All samples began with magnetic moments around 1e-05 emu. Because of this, decay to the origin was difficult to discern, and measurements were mostly scattered in orthographic view. Samples C to H had clear two-component demgantetization behavior, while samples A and B had more complex behavior. Low temperature components had a mid-shallow northeastern direction for samples D-H. Samples A and C had a mid-steep Northern direction, and Sample B had a steep Southern direction. The ChRM (most high temperature) directions of the samples did not cluster well. Samples F, G, and H had a tight cluster in a mid-steep upper northerly direction in geographic coordinates. The rest were scattered in shallow downward and upward northerly directions. A second slightly lower temperature component was also recorded for samples C-H. These did end up clustering well together in a very shallow northeastern direction for tilt-corrected coordinates, and a steeper downward northeastern direction for geographic coordinates. The alpha 95 for this Fisher distribution is 7.6. There are indications that the higher temperature stable endpoints and decay-to-origins were a later hematite CRM overprint, while the lower temperature were a primary magnetite direction.

X1515

18 samples were taken from a layer of red-brown, fine to medium grained, Barby sandstone. Samples A to H were taken 20m SSW and over a fold axis from samples I to P for a fold test within the site. All samples began with magnetic moments around 1e-04 or 1e-05 emu – there was no indication of lightning activity in site. The decay to the origin for samples B, F, G, L, and

M were difficult to discern, so stable-end-point measurements were taken instead. The samples had generally scattered mid to shallow north directions in both geographic and tilt-corrected coordinates. Fisher statistics were done on the data and alpha 95 for geographic coordinates was 18.5 but increased to 20.8 in tilt-corrected coordinates, resulting in an inconclusive fold test.

X1516

Seven samples were taken lava overlying light-brown mafic sandstone at the base of Aruab Mountain. Samples were taken approximately 5m above the sandstone layer. Bedding measurements were taken from the flattened vesicles above the flow. All samples began with magnetic moments around 1e-04 or 1e-05 emu. Samples A-F had two-component demagnetization behavior while samples G and H had a single component behavior. All the samples except G had a huge decrease in remanent magnetization in between the 450˚ and 500˚. Samples C, and F had lower high-temperature end points, and samples G and H had high temperature decay-to-origins; both these sets of points had end points in the hematite temperature range. Samples A, B, and E had a distinct magnetite component. This least squares produced two antiparallel clusters which using autoreversed to calculate a coherent direction (Swanson-Hysell 2015). The least square equal area plot in geographic coordinates had a shallow downward northern direction with an alpha 95 of 34°. In tilt-corrected, this direction was a shallow upwards northern direction.

X1517

Eight samples were taken from a dark brown vesicular lava flow approximately 200m uphill from the previous site. All samples began with magnetic moments around 1e-04 emu. The samples had single component demagnetization behavior with clear decay-to-origins. The samples were well clustered with an alpha 95 of 4.2 in a mid-shallow downward eastern direction in geographic coordinates that tilt-corrects to an east northeastern direction. This direction was antiparallel to the low temperature component from X1513. This deviated from the other site means and was excluded from the mean of site means calculations.

Naus

X1546

Eight samples were taken from a small outcrop of medium grained mafic sandstone near the gate on Naus farm. All samples began with magnetic moments around 1e-04 emu, with no clear indication of lightning activity. The samples did not have clear decay-to-origin paths, and low-temperature components were mostly scattered in direction, ranging from shallow west to north and down. The samples all did have clear ChRM stable-end-points at high temperatures. All samples exhibited two-component demagnetization behavior. The ChRm had a clear cluster in a steep downward eastern direction in geographic coordinates with an alpha 95 of 7.4°. With tilt-correction, this cluster was shifted to a very shallow downward north northwestern direction with the same alpha 95 of 7.4°.

X1547

Eight samples were taken about 50m north of Site 46 on the Naus farm from a mafic sediment layer, which is conformably overlain by mafic lava. These were well-behaved samples which all had single component demagnetization behavior and clear decay-to-origin. There was a large decrease in intensity between the 660˚ and 685˚. All but two samples also had a parallel magnetic component. Samples did begin with moderate magnetic moments around 1e-03 emu. Nevertheless, the resulting direction cluster was well-clustered steep downward eastern direction in geographic coordinates with an alpha 95 of 4.8. In tilt-corrected coordinates, the tight cluster had a shallow downward north northeastern direction with the same alpha 95 of 4.8°.

X1548

This site contains eight samples taken from a steep mafic dike-like intrusion approximately 12cm wide. The 'dike', which could be more sill-like upon restoration of the Naus section to paleohorizontal, intrudes rhyolite lava and is about 25m upstream from the previous site (X1547). This site had moderate initial magnetic moments ranging from 1e-03 to 1e-05 emu. The samples had slightly complex demagnetization behavior (two-component or single component with messier orthographic plot in higher temperatures). Nevertheless, there are clear stable-end-points for almost all the samples with a clear decay-to-origin for sample C. The resultant ChRM are scattered in the northeastern/northwestern shallow upwards and downwards direction in geographic coordinates (alpha 95: 26.1). This group is shifted to a steep northern direction (center of the stereonet) in tilt-corrected coordinates with the same alpha 95.

X1549

For a baked-contact test, eight samples were taken from the rhyolite in immediate contact with the narrow mafic dike of site X1548. Distance from each sample to the dike margin was recorded—the closest samples A, B, and C are all within 5 centimeters of the boundary, while the farthest are G and H at ~60 and ~50 centimeters away, respectively. All samples began with moderate magnetic moments around 1e-03 or 1e-04 emu. The samples exhibited clear single component behavior. Most samples lost the most intensity between steps 675˚ and 695˚. The ChRM of the data was very tightly clustered in geographic coordinates in a steep downward Eastern direction. This was tilt-corrected to a shallow downward north northeastern direction with an alpha 95 of 2.3°. The ChRM directions for this area of Naus are more consistent with the remainder of the Barby dataset in tilt-corrected coordinates, although a fold test is not possible here due to the nearly homoclinal nature of the structure. Indeed, the ratio of Fisher concentration parameters of in-site versus tilt-corrected Heuwelvlakte and Naus means (12.8 vs 9.5) is substantially less than the critical ratio (2.36) at the 95% significance level (Fisher et al., 1987, p. 217). Overall, the baked-contact test appears negative, though the 'dike' (X1548) might be a sill like intrusion of Barby age. Thus the test is inconclusive.

X1550

Eight samples were taken from mafic lava with flattened amygdales. These were well-behaved samples which all had two-component component demagnetization behavior and clear high temperature stable-end-points. There was a large decrease in intensity between the NRM and LN2 steps. Samples did begin with moderate magnetic moments around 1e-03 emu. Nevertheless, the resulting direction cluster was well-clustered steep downward northeastern direction in geographic coordinates with an alpha 95 of 9.7 (if the outlier sample D was excluded, the alpha 95 decreases to 7.9). In tilt-corrected coordinates, the tight cluster had a shallow downward north northeastern direction with the same alpha 95 of 9.7 (7.9 without sample D).

X1551

Approximately 50 m down section from X1550, eight samples were taken from mafic lava with hard large xenoliths. (The xenoliths were avoided when drilling for the samples and therefore not included in any of the samples). The data had clear single component and decay-to-origin behavior. There was a large intensity decrease from temperature steps 645˚ to 685˚. Samples began with moderate magnetic moments around 1e-04 emu. In geographic coordinates the ChRM clustered over a very steep upwards northern direction. When tilt-corrected, the cluster was a mid-shallow upward southeastern direction with an alpha 95 of 6.7. When the outlier, Sample A, was excluded, the alpha 95 dropped to 4.5.

Heuwelvlakte

X1403

This is the first site on Heuwelvlakte. Ten samples were taken from a sill dipping north that is cutting into a quartzite layer. There is evidence of columnar jointing and has the appearance of a Barby layer. The initial magnetic moment of the samples in the site was moderate at 1e-03 to 1e-04 emu with no indication of lightning activity. All samples had two components with a clear well-clustered mid-temperature component. In geographic coordinates, this component was a steep downward north northeastern direction with alpha 95 of 3.9°. In tilt-corrected direction, this component had a shallow downward northwestern direction. Samples A, B, D, G, and H had a clear high temperature component. In geographic coordinates, these samples produced a steep upwards southeastern direction with an alpha 95 of 12.6°. In tilt-corrected coordinates, these directions produced a very shallow upwards/downwards southeastern direction.

X1404

This site sampled 10 samples the less than 1 km away from X1403 in another Barby lava sill intruding a quartzite layer. The sill structure was confirmed by looking at the exposed contact with interrupted sedimentary layers. The initial magnetic moment of the samples in the site was moderate at 1e-03 to 1e-05 emu with no indication of lightning activity. All samples had two components and exhibited high temperature stable endpoint behavior. There were two major clusters of direction – Samples C, E, F, and J had a very steep upwards northeastern direction while samples B, G, H, and I had a shallow upwards southeastern direction. Samples A and D were outliers. In orthographic view and geographic coordinates, we see that samples C-F, and J were trending towards the shallow southeastern direction before losing all magnetism. We choose the shallow upwards south southeastern direction as representative of the site. This cluster had an alpha 95 of 7.1°. This cluster was a slightly steeper downwards south southeastern direction.

X1405

Nine samples were taken from a banded rhyolite that was silica rich. Specifically, sample F had horizontal vein structure rimmed by ochreous hematite. The initial magnetic moment of the samples in the site was weak at 1e-04 to 1e-05 emu with no indication of lightning activity. The samples all had two components and high temperature stable-end-point behavior with the exception of samples G and I. Samples G and I were excluded from the least squares mean. In geographic coordinates, the direction was an upwards mid-shallow south southwestern direction with an alpha 95 of 18.4°. In tilt-corrected coordinates, the cluster was a shallow downwards southern direction.

X1406

Seven samples were taken from a flow-banded rhyolite that was fine-grained and visually similar to X1405. The initial magnetic moment of the samples in the site was moderate at 1e-04 to 1e-03 emu with no indication of lightning activity. The samples all had two components and high temperature stable-end-point or decay-to-origin behavior. In geographic coordinates, the direction was a downwards steep eastern direction with an alpha 95 of 12.8°. In tilt-corrected coordinates, the cluster was a mid-shallow downwards north northwestern direction.

X1407

Eight samples were taken from a mafic quartzite that was in contact with a quartzite layer. There are indications that the layer is a shallow igneous body since large sections of peperite were found scattered along the unit. The initial magnetic moment of the samples in the site was moderate at 1e-02 to 1e-03 emu with no indication of lightning activity. The samples all had two components and decay-to-origin behavior with the exception of sample A, which had a high temperature stable-end-point. In geographic coordinates, ChRM had a steep downwards northeastern direction with an alpha 95 of 10.1°. In geographic coordinates, the ChRM had a shallow downwards northwestern direction.

X1408

Eight samples were taken form a Barby sill that intrudes older quartzite. This is the first site of three that comprise a baked contact test (with a sill), with this site as the host rock away from the contact. The initial magnetic moment of the samples in the site was strong at 1e-01 to 1e-02 emu. The samples all had a single component and decay-to-origin behavior. However, there was scatter on the ChRM least squares. With an alpha 95 of 22.7°, the samples had a mid-shallow downward northern direction in geographic coordinates, and a shallow upwards/downwards northwestern direction in tilt-corrected coordinates.

X1409

Approximately 10m down creek, eight samples were taken from a melanocratic microsyenite sill that was slightly harder than surrounding rock. The sill had red ochreous streaks in the matrix, and this site is the second of the three sites for the baked contact test. The initial magnetic moment of the samples in the site ranged from 1e-01 to 1e-04 emu. The samples all had complex multi-components and no clear high temperature behavior. There was significant scatter in the ChRM least squares and no clear cluster or direction could be discerned.

X1410

Eight samples were taken approximately one meter down creek from X1409. This is mafic exocontact of the sill. Samples A-D were the ‘immediate contact’ to the sill and samples E-H were slightly farther away. Samples A-F had reddish feldspar crystals that were not present in the previous two sites, and samples G and H had greenish feldspars. The samples began with moderate magnetic moments from 1e-02 to 1e-03 emu. The samples all had two components and decay-to-origin behavior. The results were a very steep tight downwards cluster in a northwestern direction in geographic coordinates, and a shallow downwards northwestern direction in tilt-corrected coordinates. The alpha 95 from the Fisher statistics was 5.0°. This direction is very similar to that of X1408. This indicates that the sill did not have an impact on the magnetic direction of X1410. The baked contact test is inconclusive. The sill and the surrounding rock might be similar in age (there is no age constraints on the sill) which might indicate that the sill, contact, and host rock all cooled at approximately the same time retaining the same magnetic direction.

X1411

Eight samples were taken from another microsyenite sill intruding medium grained trachyandesite. Like the previous syenite sill, this sill has flattened amygdales weathering out. The intrusion contact next to the site is more irregular than the previous baked contact test. The samples began with moderate magnetic moments from 1e-02 to 1e-03 emu. The samples all had two components and either decay-to-origin or stable high-temperature end point behavior. There was significant scatter in the ChRM least squares and no clear cluster or direction could be discerned.

X1412

Eight samples were taken from the medium-coarse grained trachyandesite host to the sill at site X1411. The samples began with moderate magnetic moments from 1e-02 to 1e-03 emu with the exception of samples G and H, which had strong magnetic moments on the order of 1e-01. These samples had indications of lightning activity and were excluded from the least squares means calculation. All samples (with the exception of G and H which had a single component) had two components and a decay-to-origin behavior in magnetite. The ChRM of the remaining samples had a steep downwards eastern direction in geographic coordinates with an alpha 95 of 9.1°. In tilt-corrected coordinates, the cluster had a shallower northern direction.

Vergenoeg

X1552

Eight samples were taken from a layer of massive felsic lava with quartz filled amygdales at the base of the hill near Vergenoeg farm. Most of the samples exhibited two-component behavior with the exception of Sample B and D. All the samples except C and F had a clear decay-to-origin behavior with the exceptions showing high temperature stable-end-points. The initial magnetic moment of the samples in the site was moderate at 1e-03 to 1e-04 emu with no indication of lightning activity. The resultant ChRM was quite scattered on the equal area plot. The alpha 95 of the Fisher statistics is 57.2° and the site is excluded from further discussion.

X1553

This site is the first of a set of three sites that make up a baked contact test. The eight samples from this site were taken from a mafic dike approximately 2m wide trending Southwest with a strike 235˚ and dip of 90°. The next site (X1554) sampled host Barby rhyolite dike from near the margin to farther away in host rock. Site X1555 represents the host rock far from the dike. The dike at site X1553 appears to be a satellite intrusion of a larger mafic dike just a few meters to the east; however, no direct junction was observed. The dike samples started with a strong magnetic moment from 1e-02 to 1e-03 emu. All the samples exhibited clear decay-to-origin and single component behavior. This is consistent with the dike carrying a thermal remanent magnetization from initial cooling after intrusion. The ChRM results were well clustered (Fisher statistics alpha 95 of 5.5°) in a very shallow upwards-northeastern direction; tilt-corrected, this direction was slightly steeper in an upwards northeastern direction.

X1554

The eight samples from this site were in silicified Barby rhyolite porphyry in exocontact, from very close to the margin of the dike at site X1553 (Sample A – 2cm from margin) to far from the dike (Sample H, 92cm from the margin). The samples generally exhibited two components with a LN2-dominated low stability component of large directional scatter. All samples except C exhibited decay-to-origin behavior with C exhibiting a high temperature stable-end-point. All the samples had moderate initial magnetic moments of 1e-03 to 1e-04 emu with the exception of Sample F. Sample A was an outlier in the resultant direction. The sample had to be held in place to be oriented and marked; therefore its exclusion from the site mean is justified. The site ChRM was a shallow downwards north northeastern direction. Tilt-corrected, the site had a shallow upwards north northeastern direction similar to X1553 (the adjacent dike). The Fisher statistics showed an alpha 95 of 6.9° with the exclusion of Sample A.

X1555

This site sampled the distant (approximately 5m from the dike) Barby host porphyry for the baked contact test. Eutaxitic foliation was present with a similar orientation as X1552; X1554 should thus be stratigraphically higher. The seven samples generally had slightly complex two-component behavior with the exception of Sample F and H, which had single component behavior. All the samples had moderate initial magnetic moment of 1e-02 to 1e-03 emu. Samples C, F-H exhibited decay-to-origin while the other samples had high temperature stable endpoints that are indicative of ChRM. Samples C and F were outliers that had stronger NRM (1e-02 emu) component and an LN2 component that was parallel to the high temperature component. This is indicative of lightning activity. The resultant least squares ChRM was not well clustered and had a mid-shallow upwards and downwards southeastern direction in geographic coordinates. In tilt-corrected coordinates, the direction was mid-shallow upwards (except samples F &C), and downwards (samples F&C) directions with an alpha 95 of 39.3. If samples F and C were excluded, the direction is a coherent upwards mid-shallow south southeastern direction with an alpha 95 of 16.5°. Overall, X1553-X1555 was a positive baked contact test. Based on dike remanence, we suspect that reheating occurred around 1100 Ma (Panzik et al., 2015).

X1556

Seven samples were taken from a Barby lava flow approximately 500m from the baked contact test and at a higher stratigraphic level. There was eutaxitic foliation and flattened amygdales present at the site. Five samples had clear single component with decay-to-origin behavior with samples F and H exhibiting two components. Samples F and H did display at high temperatures a stable-end-point. All the samples had moderate initial magnetic moment of about 1e-03 emu. There seemed to be two clusters of directions: in geographic coordinates a steep upwards north northwestern direction (samples A, B, and D) and a mid-steep upwards south southeastern direction (samples E, F, G, and H). In tilt-corrected coordinates, the first cluster shifts to the mid-steep west northwestern direction, and the second cluster shifts to a mi-steep southwestern direction. Samples E-G form an especially tight cluster with an alpha 95 of 4.8. Looking at the equal area plots for the rest of the samples, the samples seem to be ending up in the area around the E-G cluster before losing all magnetism. Therefore, the southwestern cluster (in tilt-corrected coordinates) was taken as the primary direction for this site.

X1558

Eight samples were taken from a dark gray rhyolite with eutaxitic foliation. All samples with the exception of sample F had a single component; sample F had two components. Nevertheless, all the samples exhibited decay-to-origin behavior. Most samples had moderate initial magnetic moments of 1e-03 emu with samples A, B, and C with larger initial magnetic moments of 1e-02 emu. This might be indication of local lightning activity. In the least squares equal area plot, which displayed the ChRM results, samples A and B were outliers – mid-shallow upwards eastern direction in geographic coordinates, while the other samples had a shallow upwards north northeastern direction. There was very little difference between the tilt-corrected and geographic coordinate directions. After Fisher statistics was done on the site, with the exclusion of sample A and B, the alpha 95 is 8.6°.

X1559

Eight samples were taken from a lava flow below a small dam overlain by conformably bedded sediments. Samples' magnetic moments ranged from 1e-03 emu to 1e-05 emu. Samples had generally two clear components. The low temperature component had a generally western and down direction but with a lot of scatter. Samples did have high-temperature stable-end-points and those were taken to be the ChRMs. The site produced a shallow upwards southern direction in geographic coordinates and a slightly steeper southern direction in tilt-corrected coordinates. The alpha 95 from the Fisher statistics was 10.1°.

X1560

Approximately 500m from the last site, eight samples were taken from massive lava overlain by sediments. The lava contained flattened amygdales, which provided the paleo-horizontal for the site. Samples A and B had a single component; samples C, D, and E, had two components; samples G and H had more complex low temperature behavior, but also a clearly defined ChRM. The decay-to-origin was easily observable for most samples. All the samples began with magnetic moments on the order of 1e-02 to 1e-03 emu. The results were scattered across the stereonet with two broadly defined clusters. They range from downwards steep west (n=5) to shallow north northeastern (n=2) in geographic coordinates. The directions barely change in tilt-corrected coordinates. The west direction group had LN2 parallel to ChRM and a generally stronger NRM, which is suggestive of lighting. The North and shallow group may indicate a better estimate of the lightning-free ChRM; but since there are only two samples, the mean is not accurate enough to be taken as a representative direction.

X1561

Approximately 20m uphill from the previous site, eight samples were taken from a coarse Barby trachyandesite. This flow was directly above a sedimentary layer with clear bedding. All the samples began with magnetic moments on the order of 1e-03 emu. The samples all had two components. Samples D-H had clear decay-to-origin behavior while A, B, and C had a high temperature stable-end-point that was taken as ChRM. The results were a very shallow (upwards and downwards) cluster in the north northeastern direction in geographic coordinates, and the same for tilt-corrected coordinates. The alpha 95 from the Fisher statistics was 12.3°,

X1562

Eight samples were taken from brown weathered vesicular lava. From the crest of a hill at eastern Vergenoeg Farm, the samples began with weak magnetic moments from 1e-06 to 1e-04 emu. In addition to a LN2 component with random directions, the samples all had two components. Measurements were mostly scattered in orthographic view, and decay to the origin was difficult to discern. Samples did have high-temperature stable-end-points (at ≤ 580°C) and those were taken to be the ChRMs. The results were a very shallow cluster in the south southeastern direction in geographic coordinates, and almost the same for tilt-corrected coordinates. The alpha 95 from the Fisher statistics was 24.9°; too large to be included in the overall mean, but indicative of polarity at this stratigraphic level.

X1563

Approximately 100m downhill from site X1562, eight samples were taken from a red-brown rhyolite. The layer was mildly weathered and contained flattened vesicles and flow banding. Chlorite/epidote alteration was present with samples E and F in particular containing significant epidote staining. The samples began with weak magnetic moments from 1e-05 to 1e-04 emu with no indications of lightning activity. The samples all had two components, the first being removed at LN2 and low thermal steps with random orientations. Thereafter, samples B, E, and H had observable decay-to-origin behavior while the other samples had high temperature stable-end-points. The resultant equal-area ChRM plot shows a tight cluster in an upwards mid-shallow south southeastern direction in geographic coordinates; in tilt-corrected coordinates, the cluster has a shallow upwards southern direction. The alpha 95 from the Fisher statistics was 7.8°. Sample C could be seen as an outlier in the site; with its exclusion, the alpha 95 drops to 5.6°, but we retained all 8 samples as the more conservative approach.

X1564

This is the first site in the Vergenoeg river section. Eight samples were taken from a mafic massive lava flow that was primarily grey-green in color. Slight hints of brown weathering were present at the surface with numerous fractures. Samples A, B, C, and H started with large magnetic moments on the order of 1e-02emu; the other samples had moderate magnetic moments around 1e-03emu. All the samples were single component; the samples lost the most intensity between the NRM and the LN2 steps. When heating the samples along with sites X1559-X1562 and X1565-X1566, the oven malfunctioned and overheated these sites. The resumption of decay at 568°C suggests that the runaway attained that temperature before emergency termination of the heating. Despite these technical issues, the decay-to-origin was easily discernable. The results were well clustered in a shallow downwards northwestern direction in geographic coordinates; in tilt-corrected coordinates, the cluster was very shallow northwestern direction. The alpha 95 from the Fisher statistics was 9.0°. Sample H could be seen as an outlier in the site; with its exclusion, the alpha 95 drops to 6.4°. As before with X1563, sample H was included to be consistent with the conservative approach.

X1565

A mafic lava flow was sampled eight times approximately 30m up the streambed from X1564. The composition at this site is similar to that of the previous site. Samples A and D started with large magnetic moments on the order of 1e-02emu; the other samples had moderate magnetic moments around 1e-03emu. All the samples had single components with large intensity decreases between NRM and LN2 as well as between the 200˚C and 250˚C temperature steps. Because it was well behaved on the orthographic view, the decay-to-origin was easily discernable in each sample; however, the results were scattered along the least square equal area view strung along from a mid-shallow upwards southern direction to a shallow upwards north northeastern direction in geographic coordinates; in tilt-corrected coordinates, the sample directions barely changed. The alpha 95 from the Fisher statistics is 32.4°, and the site is excluded from the mean due to probable lightning influence.

X1566

A breccia test was done on site X1566. Rounded light bluish-grey volcanic clasts with a lighter colored magmatic matrix were sampled approximately 8-10m upsection from X1565. Some clasts contained vesicles and amygdales. Samples D1 and D2, G1 and G2, and I1 and I2 were from the same clasts. The samples had weak to magnetic moments around 1e-05 to 1e-03 emu. All the samples have multiple components. Samples D2, G2, I1, I2, and J were not well behaved in orthographic view; therefore, their decay-to-origin wasn't clearly observable. There was considerable scatter in the resultant least squares equal area plot. All the samples except D1 and E had an upwards direction. The majority of the samples had a southwestern direction but with a lot of scatter. Samples D1 and D2 had very different directions (thought they were from the same clast): D1 had a shallow downwards northern direction; D2 had a shallow upwards east northeastern direction. Sample G1 and G2, and I1 and I2 had generally the same shallow upwards east southeastern and steep southeastern direction respectively (G2 is steeper than G2, and I2 is steeper than I1). This site presents evidence for an inconclusive breccia test, for the following reasons: (1) lightning had a major effect on the underlying coherent lava flow, and it seems influential at this site as well. (2) Although scattered, the stable endpoint components have a dominant direction similar to the reverse polarity sites from other areas in Vergenoeg. We envisage partial overprinting at this site following the emplacement of the breccia, but such overprinting could be indicative of early hydrothermal alteration coincident with the Barby deposition.

X1567

Approximately 15m upsection from X1566, a dark basalt flow was sampled eight times. The flow was approximately 3m thick and contained quartz filled amygdales at the top of the flow. Samples were from the base of the flow. The flow protrudes out from the more weathered underlying succession of shales. The samples had moderate NRM moments around 1e-03emu. All samples had LN2 loss followed by one or two components. The site was a included in the oven malfunction and probably heated to 568°C after the 250°C step; it exhibits the same demagnetization behavior as site X1563. Therefore, stable-end-points (up to 568°C) were taken to be ChRM. The resulting least square equal area shows a very shallow tight cluster in subhorizontal southeastern direction in geographic coordinates. The cluster is shallow upwards southeastern direction in tilt-corrected coordinates. The alpha 95 from the Fisher statistics is 5.9°.

Plunge Corrections

After the structural analysis was done, there was a non-insignificant plunge measurement was found for Aruab proximal structural area. There were 5 North Aruab sites captured by that area – X1401, X1402, X1419, X1420, and X1421, and 6 South Aruab sites – X1416, X1417, X1612, Z1513, X1514, and X1516. In order to calculate the most accurate declination and inclination for those sites, a plunge correction on that area was done. We utilize the preciously calculated trend of 318.9° and a plunge of 10.2°.

The previous site means declination and inclinations were utilized along with the average magnetic declinations, the paleohorizontal measurement, and the trend and plunge values to calculate the corrected inclination declination values. For site X1513, this was extended to be a two-part process. X1513 was a fold test, so there were two different bedding measurements.

Each group of samples with the same paleohorizontal was unplunged separately and averaged to calculate an unplunged site mean. The alpha 95 was calculated manually for accuracy. We end up with a corrected 45.1° inclination and 18.5° declination for the Aruab structural panel mean. This was quite similar to the 44.6° and 18.2° values that were found after the same sites were only tilt-corrected. Since the difference between the two means is too small, the effect of plunge can be excluded.

Discussion

Aruab

The ChRMs of South Aruab have a moderate downward north northeastern trend. In geographic coordinates, there is wide distribution of inclinations in a girdle distribution in geographic coordinates, which could indicate partial overprint typical of the 1100 Ma post-Guperas dikes (Panzik et al., 2015). However, after tilting correcting, there is a well-clustered NE direction indicating a positive fold test (X1401, X1402, X1413-22, X1504-17). Positive fold test is when folding occurs after magnetization is emplaced, so magnetization is regarded as pre-fold. The direction would cluster post-tilt-correction

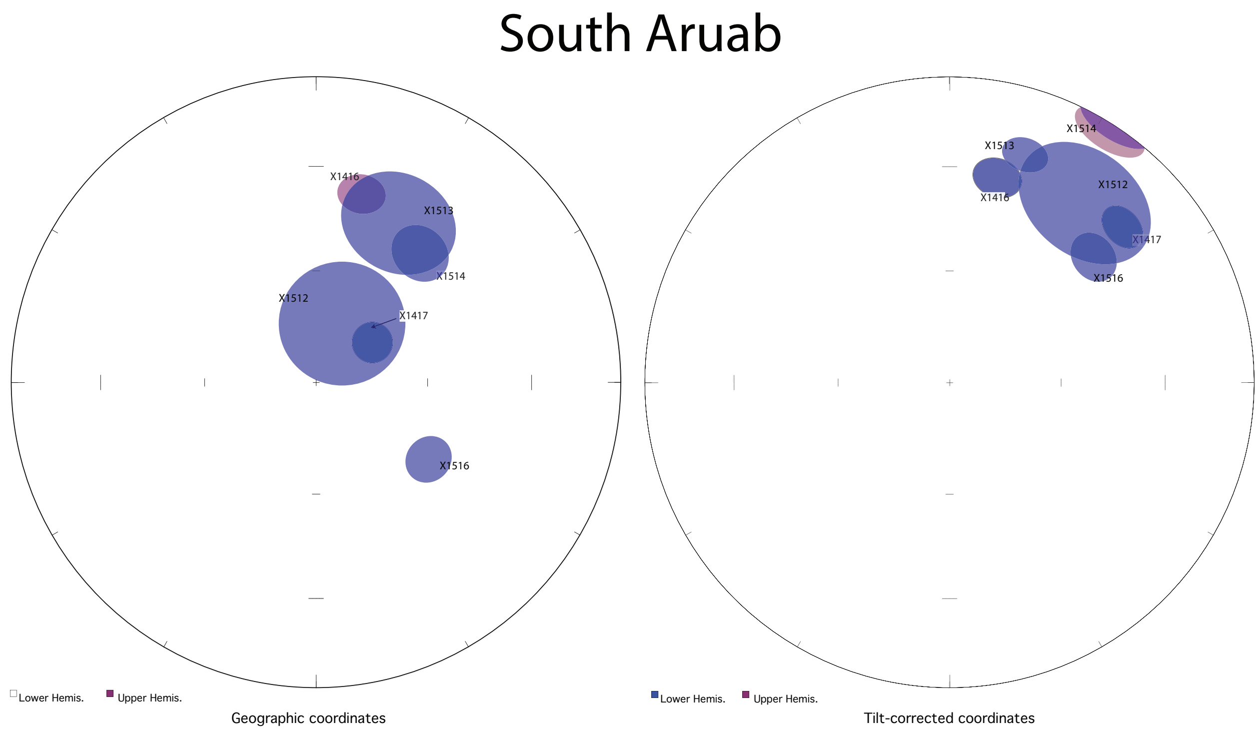

Figure 4-1: Site means displayed in both geographic coordinates (left) and tilt-corrected coordinates (right). Upper hemisphere directions are represented by the red-purple color and lower hemisphere directions are represented by a dark blue color.

This trend is consistent with a smaller positive fold test on a magnetite component from site X1513. This provides further evidence that the remanent magnetization that was measured at these sites occurred pre-fold and was possibly primary. These ChRM mean directions are again supported by positive inverse baked contact tests from Hessert et al., (2014) and Panzik et al., (2015).

In North Aruab, sites X1401, X1402, and X1512 had negative breccia tests; however, these results were inconclusive as the direction could still be primary since the overprint could have occurred concurrent with the emplacement of the Barby succession. The North Aruab sites also passed a fold test. In geographic coordinates, there was a variety of direction in the site means; these sites, however, formed a tight NE shallow and downward direction in tilt-corrected coordinates.

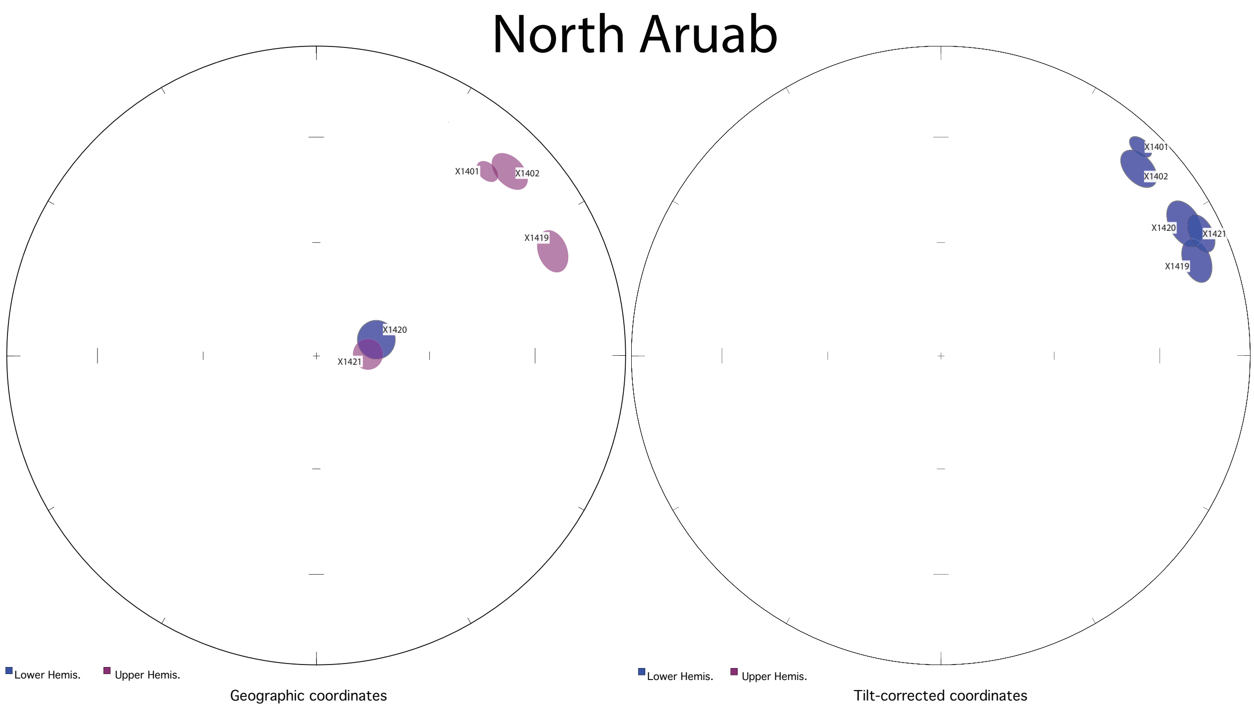

Figure 4-2: Resultant stereonets from North Aruab showing a clear shallow NE and down direction.

Naus/Heuwelvlakte

The structural panel closest to Aruab would be Naus/Heuwelvlakte. The site means in both geographic and tilt-corrected coordinates of this panel is different than that of Aruab, with a moderate downward north northwestern trend. There were two major magnetic components within almost all samples: a coherent lower temperature magnetite direction from all sites in this structure panel and a consistent higher temperature hematite direction in three of the sites. We interpret the magnetite direction to be primary and the hematite direction to be secondary, since more sites display the magnetite demagnetization behavior clearly. The hematite direction is also anti-parallel in geographic coordinates to the magnetite direction in tilt-corrected coordinates, which implies that the hematite direction could be a chemical remanent magnetization after an early episode of tilting. The alpha 95 of the pole and the local space have opposite fold test indicators (i.e. the local space demonstrating a negative fold test with higher alpha 95 values when unfolded and the pole space demonstrating a positive fold test with lower alpha 95 values when unfolded). The statistical variation of these non-linear transformations from local to pole space outweigh the small variation in bedding attitudes, demonstrating that this structural panel is probably homoclinal.

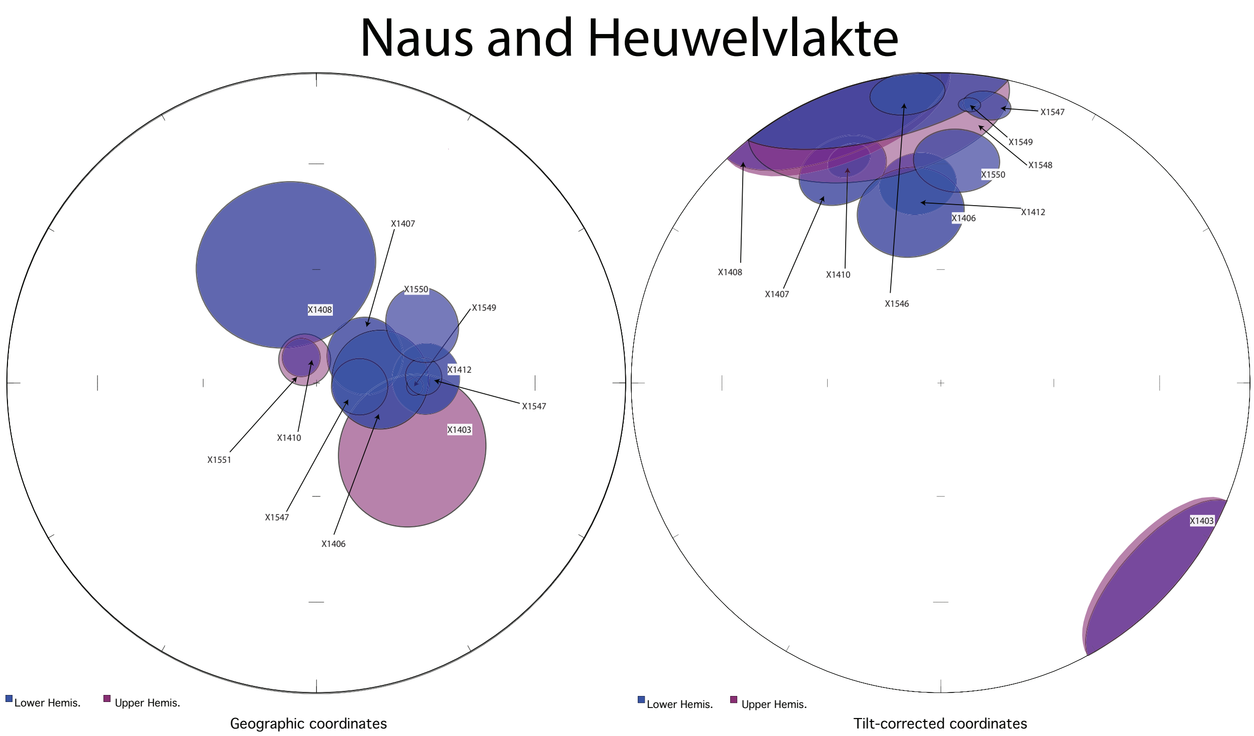

Figure 4-3: Resultant stereonets from Naus/Heuwelvlakte showing a very shallow NNW direction.

There are now two sets of moderate and downwards generally northerly ChRM measurement directions: in Aruab, the trend is northeast, in Naus/Heuwelvlakte, the trend is northwest. We suspect that there will be local vertical axis rotation in one of these structural panels; this rotation would also have to be prior to the post-Guperas dikes of 1105 Ma as per the field tests from the Aruab structural panels.

Vergenoeg

Vergenoeg provides 15 more site of evidence indicating that the northwestern trend is probably primary. The site means are variable in geographic coordinates, but clean up to show a dual polarity North/NNW trend in tilt-corrected coordinates, which is consistent to that of the Naus/Heuwelvlakte structural panel.

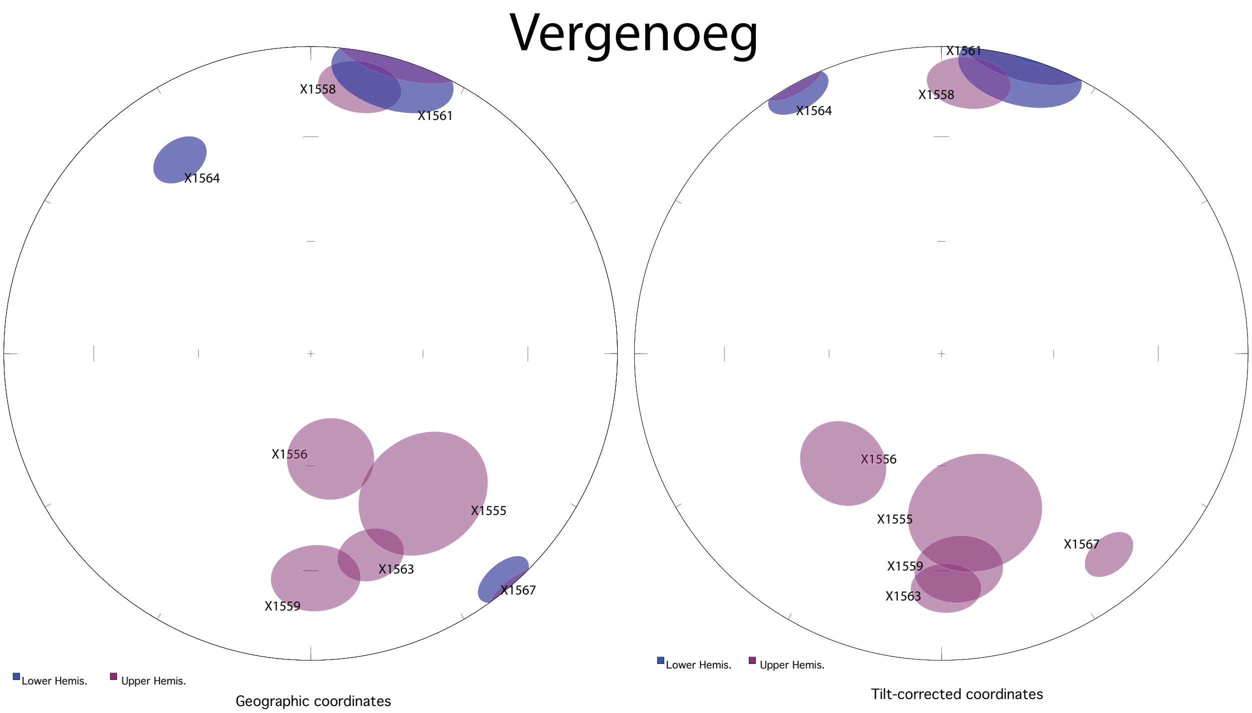

Figure 4-4: Resultant stereonets from Vergenoeg showing a shallow N/NNW direction.
In addition, there are additional field tests in Vergenoeg that substantiate that the Vergenoeg direction could be primary. X1553 – X1555 yielded a positive baked contact test, where the dike and the Barby Formation showed very different directions.

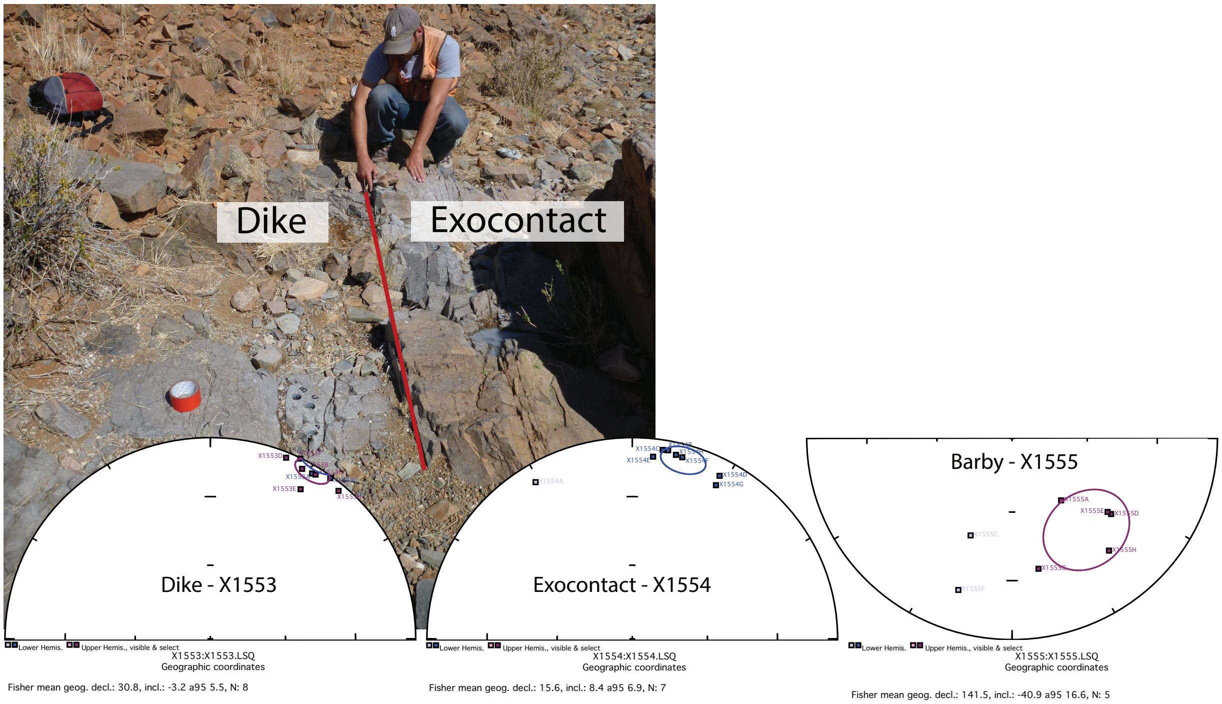

Figure 4-5: The differences in directions between the dike, transition, and the Barby Fm proper in geographic coordinates.

The dike orientation from site X1553 and its exocontact X1554 have similar directions as that of the post-Guperas dikes from Panzik et al., (2015); this indicates that it could be from that same dike swarm (which is dated at 1105) though this dike has not yet been dated.

Summary of Paleomagnetic Discussion

Vergenoeg and Naus/Heuwelvlakte samples passed a tilt test. The two different structural panels that show very different directions in geographic coordinates show similar tilt-corrected coordinates, Magnetization was emplaced before any of the strata were tilted.

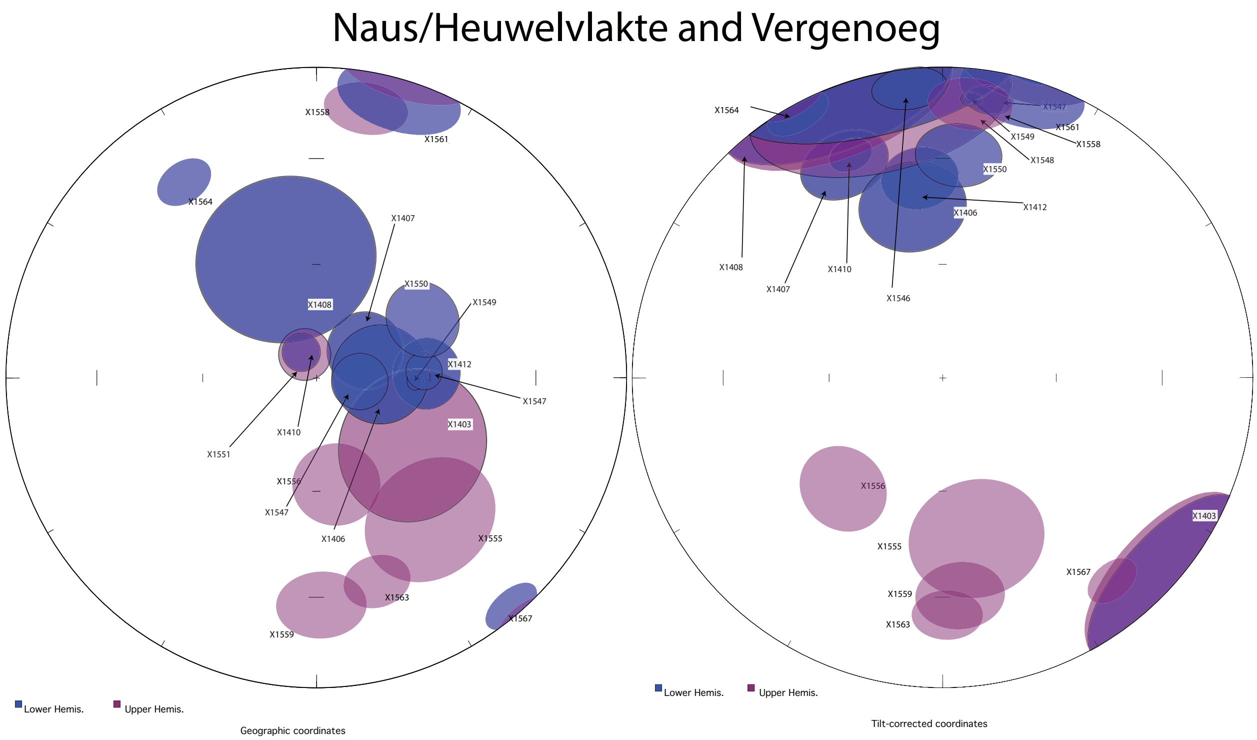

Figure 4-6: Positive tilt test with the Naus/Heu. and Vergenoeg site means in geographic coordinates on the left and the site means in tilt-corrected coordinates on the right.
In order to compute the mean pole, we have taken the sites from Naus, Heuwelvlakte, and Vergenoeg. The Aruab structural panel site means were excluded from the calculation.

Since the sites from both Vergenoeg and Naus/Heuwelvlakte show a consistent direction in tilt-corrected coordinates, this indicates that there was either local vertical axis rotation in the Aruab structural panel or the Barby Formation from Aruab structural panel is not 1212 Ma (the age derived from samples from the Vergenoeg structural panel). The Aruab sites yielded a pole of 34.3°N and 073.0°E. This pole position would overlap with the Premier pole dated at 1150 Ma. This would imply that the Barby Fm at Aruab would have been emplaced, folded, eroded, overlain by the Guperas Formation, and intruded by the post-Guperas dikes between 1150 Ma and 1212 Ma. The more plausible scenario is probably local vertical axis rotation in the Aruab panel.

Chapter 5: Tectonic implications and suggestions for further work

The Barby means pole would already add to a bank of other paleomagnetic poles that demonstrate the position of Kalahari in the formation of Rodinia. This Barby paleomagnetic pole is taken to be primary. The two independent structural panels – Naus/Heuwelvlakte and Vergenoeg exhibit consistent direction after tilt-correction, broadly passing a regional tilt test. In addition, there has been a positive baked contact test (X1553-X1555) in the Vergenoeg region hat further supports this result.

The Aruab pole result demonstrates a slightly different direction in all the sites sampled. There was a positive inverse baked contact test done in Northern Aruab which indicates that the Barby Formation in Aruab was emplaced pre-1105 Ma, the age of the post-Guperas dike in the field test. The resultant magnetic direction is also very shallowly downwards and northeast, with approximately 30° difference between the Naus/Heuwelvlakte and Vergenoeg direction. Therefore, we interpret that the Aruab region, though having retained its primary remanent magnetization, has experienced local vertical axis rotation. This would account for the declination changes and the lack of inclination changes. The Aruab mean was not included in the calculation of the final Barby mean pole.

Despite these tests, the resultant Barby pole direction shows consistency with previous poles, especially the post-Guperas and the Aubures poles (from Panzik et al., 2015 and Kasbohm et al., 2015). However, from the positive inverse baked contact test we have validation that the Barby direction was pre-1105 Ma. There is a possibility that during this time interval of Barby emplacement (1212 Ma) and the post-Guperas dikes (1105 Ma) was a magnetically static interval of time.

The polarity interpretation of the poles from Kasbohm et al., (2015), Panzik et al., (2015), and Swanson-Hysell (2015) has been that poles representing Kalahari younger than Barby has been in the Southern hemisphere which would conform to previous Rodinia reconstruction models. Here, fitting in the Barby pole in the general APW path shows that two different pole positions that have very different implications for the path that Kalahari takes.

The first option demonstrates that Kalahari would always stay in the southern hemisphere. The Kalahari Alkaline Means pole here is the pole as illustrated in Gose et al., (2013); hereafter referred to simply as the 'Kalahari Alkaline Means pole' as opposed to the anti-pole of that as illustrated by Fig. 5-2.

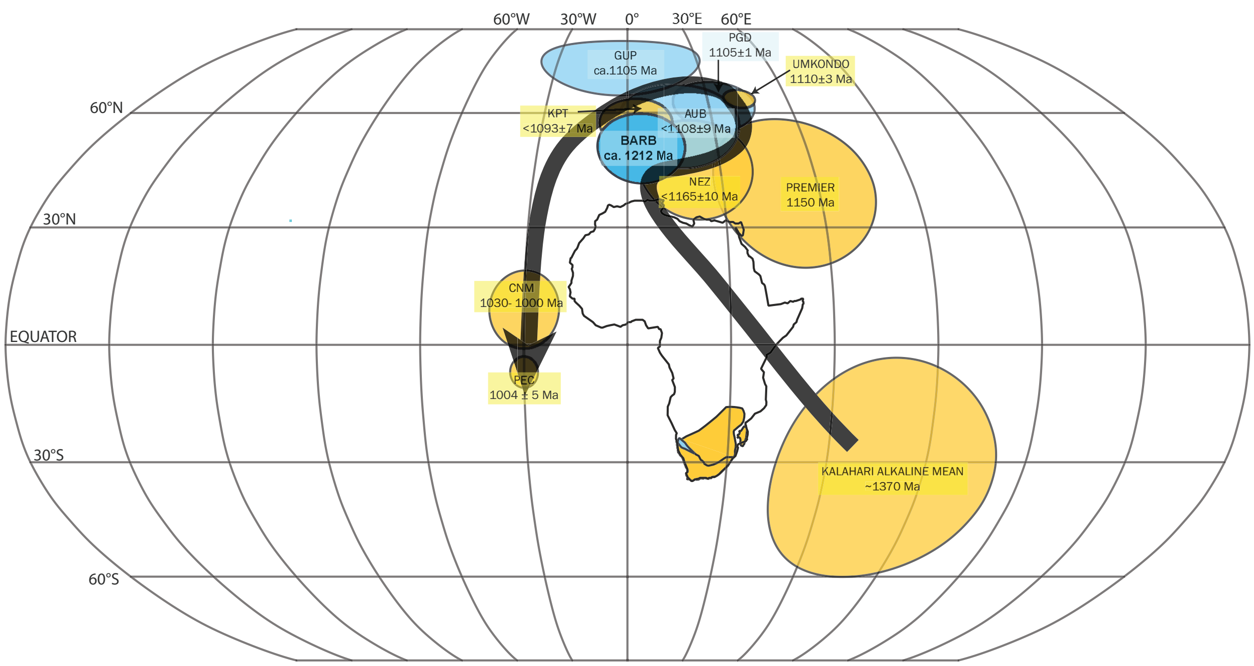

Figure 5-1: First of two APWP where the pole (as illustrated by Gose et al., 2013) is shown.

The second option, using the Kalahari anti-pole as the pole for 1370 Ma, would predict that Kalahari crosses the equator between 1300 Ma and 1212 Ma. By this time, according to the Miller 2012 model, Sinclair has already sutured into Kalahari.

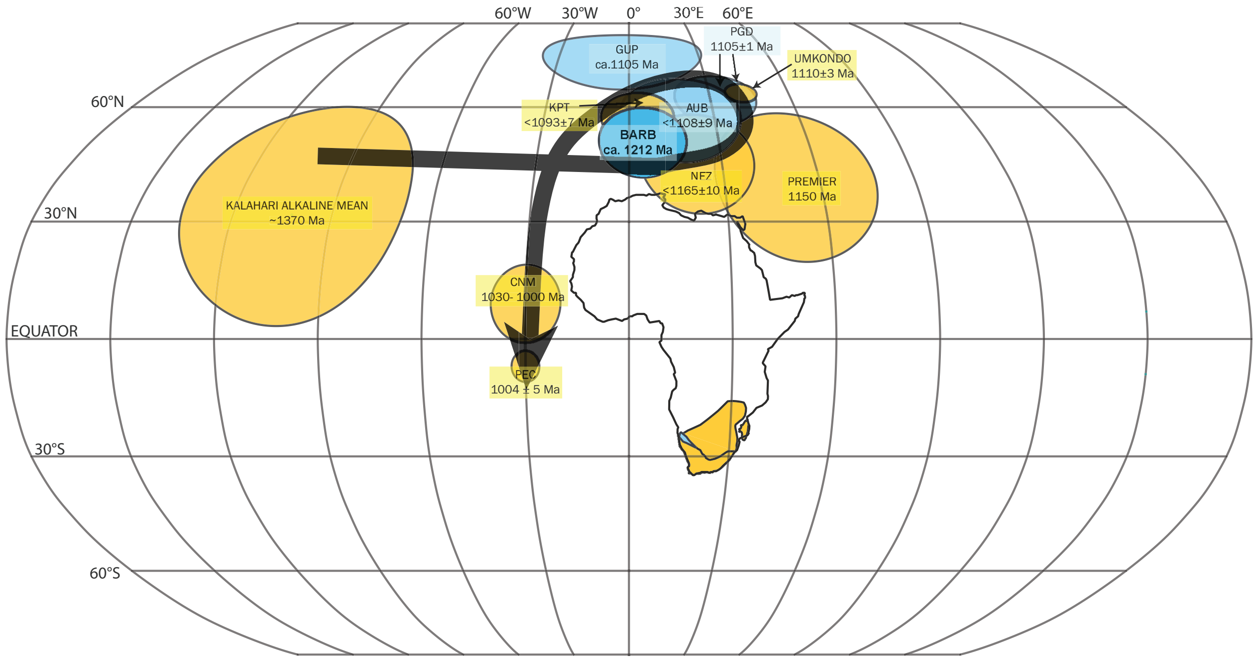

Figure 5-2: Second of the two proposed APWP.

Conclusions and further study

This study has presented new geochronological age constraint and paleomagnetic pole for the Barby Formation within the Sinclair region. A maximum age constraint for the Barby from the Haremub granite has been found at 1336 ± 8 Ma via U-Pb dating. This age is stratigraphically in line with concurrent geochronology age of Barby at ca. 1212 Ma.

Structural analysis was also done on the paleomagnetic data from the three structural panels: Aruab, Vergenoeg, and Naus/Heuwevlakte. The Aruab panel was clearly synclinal at the Aruab Member but shallowed eastwards. Therefore, the paleomagnetic data from the Aruab structural panel was not impacted by plunge corrections. Vergenoeg and Naus/Heuwelvlakte was found to be homoclinal, and no plunge corrections was needed for the paleomagnetic data.

With a positive tilt test and a positive baked contact test, a new virtual geomagnetic pole was calculated from 18 sites and two structural panels, Vergenoeg and Naus/Heuwelvlakte to be at 50.5°N, 004.6°E. The Aruab structural panel was determined to have been either have been locally vertical-axis rotated or is of a different age than ca. 1212 Ma (the age of the Barby from the Vergenoeg structural panel).

Two new APW paths were proposed utilizing both the pole and the anti-pole of the Kalahari Alkaline Means. This path agrees with previous studies' Kalahari paths in Rodinia reconstructions post-Barby (ca.1212 Ma.). If the pole of the Kalahari Alkaline Means (as illustrated by Gose et al., 2013) is taken to be a part of the APWP, Kalahari would be in the Southern hemisphere between 1370-1212 Ma; with the anti-pole, Kalahari would cross the equator between that period of time. Further work to look at basement of the Barby Formation would probably provide better constraints as to the position of the Kalahari. The Kunjas Formation is basement to Barby; however, this Formation is not amenable to paleomagnetic study as it is made up mainly of poorly sorted and immature clastic rocks (Miller, 2008). The Nagatis Formation, which underlies the Kunjas uncomformably, though not dated, is thought to be in the range of 1300 Ma in age (Miller, 2008). If paleomagnetic study was done on the Nagatis Formation, it would elucidate which APW path was more likely. For example if the first option were more likely, we would expect the direction to be close to the Alkaline Complex 'pole'. Further study into the older strata is necessary to understand the position of Kalahari leading up to the construction of Rodinia.

Acknowledgements

I would like to thank first and foremost my advisor David Evans for being a wonderful mentor for the past three years and introducing me to paleomagnetism and the Barby Formation. The field team for both 2014 and 2015: Tierney Larson, Joe Panzik, Johanna Salminen, Richard Hanson, and Olivia Walker, was integral in making this project a success. Thank you so much for helping to collect these amazing samples, and I’m very luck to have had the chance to work with y’all in the field. Mandy Hofmann and Ulf Linnenmann from the Senckenberg Institute were amazing in teaching me U-Pb dating methods and allowing me to call their lab home for two weeks. Finally, Von Damm Fellowship, Saybrook College Summer Summer Fellowship, and Bruce M. Babcock ’62 Saybrook College Travel Fellowship have helped to support this project throughout the past two years.

References

Butler, R. F. & Butler, R. F. *Paleomagnetism: magnetic domains to geologic terranes*. Vol. 319 (Blackwell Scientific Publications Boston, 1992).

Cardozo, N. & Allmendinger, R. W. Spherical projections with OSXStereonet. *Computers & Geosciences* **51**, 193-205 (2013).

Fisher, D. H. Knowledge acquisition via incremental conceptual clustering. *Machine learning* **2**, 139-172 (1987).

Fisher, R. A. The Expansion of Statistics. (1953).

Frei, D. & Gerdes, A. Precise and accurate in situ U–Pb dating of zircon with high sample throughput by automated LA-SF-ICP-MS. *Chem Geol* **261**, 261-270 (2009).

Gerdes, A. & Zeh, A. Combined U–Pb and Hf isotope LA-(MC-) ICP-MS analyses of detrital zircons: comparison with SHRIMP and new constraints for the provenance and age of an Armorican metasediment in Central Germany. *Earth Planet Sc Lett* **249**, 47-61 (2006).

Gose, W. A., Helper, M. A., Connelly, J. N., Hutson, F. E., & Dalziel, I. W. (1997). Paleomagnetic data and U‐Pb isotopic age determinations from Coats Land, Antarctica: implications for late Proterozoic plate reconstructions. *Journal of Geophysical Research: Solid Earth*, *102*(B4), 7887-7902.

Gray, D. R., Foster, D. A., Goscombe, B., Passchier, C. W. & Trouw, R. A. 40 Ar/39 Ar thermochronology of the Pan-African Damara Orogen, Namibia, with implications for tectonothermal and geodynamic evolution. *Precambrian research* **150**, 49-72 (2006).

Grunow, A., Hanson, R. & Wilson, T. Were aspects of Pan-African deformation linked to Iapetus opening? *Geology* **24**, 1063-1066 (1996).

Jacobs, J., Pisarevsky, S., Thomas, R. J. & Becker, T. The Kalahari Craton during the assembly and dispersal of Rodinia. *Precambrian Research* **160**, 142-158 (2008).

Jones, C. H. User-driven integrated software lives:“Paleomag” paleomagnetics analysis on the Macintosh. *Computers & Geosciences* **28**, 1145-1151 (2002).

Kasbohm, J., Evans, D. A., Panzik, J. E., Hofmann, M. & Linnemann, U. Palaeomagnetic and geochronological data from Late Mesoproterozoic redbed sedimentary rocks on the western margin of Kalahari craton. *Geological Society, London, Special Publications* **424**, SP424. 424 (2015).

Kirschvink, J. The least-squares line and plane and the analysis of palaeomagnetic data. *Geophysical Journal International* **62**, 699-718 (1980).

Kirschvink, J. L., Kopp, R. E., Raub, T. D., Baumgartner, C. T. & Holt, J. W. Rapid, precise, and high-sensitivity acquisition of paleomagnetic and rock-magnetic data: Development of a low-noise automatic sample changing system for superconducting rock magnetometers. *Geochemistry, Geophysics, Geosystems* **9** (2008).

Loewy, S. *et al.* Coats Land crustal block, East Antarctica: A tectonic tracer for Laurentia? *Geology* **39**, 859-862 (2011).

Ludwig, K. User's manual for Isoplot/Ex v. 2.47. A geochronological toolkit for Microsoft Excel. *BGC Special Publ. 1a, Berkeley* (2001).

Miller, R. M. The geology of Namibia. *Geological Survey of Namibia, Windhoek* (2008).

Miller, R. M. Review of Mesoproterozoic magmatism, sedimentation and terrane amalgamation in southwestern Africa. *South African Journal of Geology* **115**, 417-448 (2012).

Onstott, T. C. Application of the Bingham distribution function in paleomagnetic studies. *Journal of Geophysical Research: Solid Earth* **85**, 1500-1510 (1980).

Panzik, J. *et al.* Using palaeomagnetism to determine late Mesoproterozoic palaeogeographic history and tectonic relations of the Sinclair terrane, Namaqua orogen, Namibia. *Geological Society, London, Special Publications* **424**, SP424. 410 (2015).

Piper, J. The palaeomagnetism of Precambrian igneous and sedimentary rocks of the Orange River belt in South Africa and South West Africa. *Geophysical Journal International* **40**, 313-344 (1975).

Prave, A. R. Tale of three cratons: Tectonostratigraphic anatomy of the Damara orogen in northwestern Namibia and the assembly of Gondwana. *Geology* **24**, 1115-1118 (1996).

Stacey, J. t. & Kramers, J. Approximation of terrestrial lead isotope evolution by a two-stage model. *Earth Planet Sc Lett* **26**, 207-221 (1975).

Swanson-Hysell, N. L. *et al.* Stratigraphy and geochronology of the Tambien Group, Ethiopia: Evidence for globally synchronous carbon isotope change in the Neoproterozoic. *Geology* **43**, 323-326 (2015).

Von Brunn, V. *Igneous Rocks of the Nagatis and Sinclair Formations North-East of Luderitz, South West Africa*, University of Cape Town, (1969).

Watters, B. R. *Stratigraphy, Igneous Petrology, and Evolution of the Sinclair Group in Southern South West Africa*. (University of Cape Town, Department of Geology, 1974).

Weil, A. B. Kinematics of orocline tightening in the core of an arc: Paleomagnetic analysis of the Ponga Unit, Cantabrian Arc, northern Spain. *Tectonics* **25**, n/a-n/a, doi:10.1029/2005TC001861 (2006).

Appendix a: Geochronology measurements

Table X1580X:

Number	^{207}Pb[a] (cps)	U[b] (ppm)	Pb[b] (ppm)	Th[b]/U	^{206}Pb[c]/^{204}Pb	^{206}Pb[c]/^{238}U	2 σ %	^{207}Pb[c]/^{235}U	2 σ %	^{207}Pb[c]/^{206}Pb	2 σ %	rho[d]	^{206}Pb/^{238}U	2 σ (Ma)	^{207}Pb/^{235}U	2 σ (Ma)	^{207}Pb/^{206}Pb	2 σ (Ma)	conc %
a48	60562	809	131	1.04	437	0.13512	5.2	1.37599	8.1	0.07386	6.3	0.64	817	40	879	49	1038	127	79
b18	73002	845	148	0.58	199	0.15273	3.0	1.57376	4.9	0.07473	3.9	0.60	916	25	960	31	1061	79	86
a23	20563	288	45	0.70	1668	0.13630	5.0	1.41865	7.2	0.07549	5.2	0.70	824	39	897	44	1081	104	76
a24	37486	513	66	0.80	494	0.10809	3.9	1.13917	5.6	0.07644	4.0	0.69	662	24	772	30	1107	80	60
a2	34172	445	68	0.94	5431	0.13662	4.2	1.47047	5.6	0.07806	3.6	0.76	826	33	918	34	1148	72	72
b2	37464	445	79	1.06	1054	0.15226	3.4	1.66410	4.2	0.07927	2.5	0.81	914	29	995	27	1179	49	78
b4	20442	276	49	1.09	5468	0.14422	5.2	1.57913	6.2	0.07941	3.4	0.84	868	42	962	39	1182	67	73
b7	29863	378	65	0.78	1169	0.15403	4.3	1.69511	5.1	0.07982	2.8	0.84	924	37	1007	33	1192	56	77
b20	23536	235	53	0.99	1186	0.18327	3.5	2.05835	4.0	0.08146	2.0	0.87	1085	35	1135	28	1232	40	88
b49	29067	411	88	1.35	2555	0.17483	3.9	1.97318	4.5	0.08186	2.3	0.87	1039	38	1106	31	1242	44	84
b5	21849	200	40	0.61	765	0.17802	3.4	2.02221	5.0	0.08239	3.7	0.67	1056	33	1123	34	1255	72	84
b10	37939	370	87	0.99	8369	0.20384	3.6	2.33240	4.8	0.08299	3.2	0.75	1196	40	1222	35	1269	62	94
b52	13947	335	43	0.50	1475	0.11341	3.8	1.29895	5.5	0.08307	3.9	0.70	693	25	845	32	1271	77	54
a46	29152	559	79	0.84	1769	0.12539	5.0	1.43866	5.7	0.08321	2.7	0.88	762	36	905	35	1274	53	60
a21	30094	546	81	1.07	1252	0.12786	3.3	1.46766	4.5	0.08325	3.1	0.72	776	24	917	28	1275	61	61
a6	31278	350	63	1.01	3121	0.15281	3.5	1.75532	5.4	0.08331	4.2	0.64	917	30	1029	36	1277	81	72
a47	25878	250	57	0.93	962	0.18978	5.6	2.19086	6.5	0.08373	3.4	0.86	1120	58	1178	47	1286	66	87
a5	24552	170	41	0.78	1336	0.21152	4.8	2.45318	6.4	0.08412	4.3	0.75	1237	54	1258	47	1295	83	95
b45	8162	59	15	1.47	3979	0.18152	2.6	2.10748	4.4	0.08420	3.5	0.59	1075	26	1151	31	1297	69	83
b57	28547	395	96	1.25	4909	0.19097	3.4	2.22471	4.3	0.08449	2.6	0.79	1127	35	1189	30	1304	51	86
b53	35977	516	126	1.26	5079	0.19414	3.8	2.26426	4.4	0.08459	2.3	0.86	1144	39	1201	31	1306	44	88
b55	46790	1202	158	0.28	1004	0.12595	5.6	1.46954	7.3	0.08462	4.6	0.77	765	41	918	45	1307	90	59
a59	25871	218	50	0.85	327	0.18872	2.5	2.20822	5.4	0.08486	4.7	0.47	1114	26	1184	38	1312	92	85
a3	42394	380	79	0.75	18378	0.18643	5.4	2.18876	6.2	0.08515	3.1	0.87	1102	55	1177	44	1319	59	84
a45	9974	89	19	1.18	3045	0.16225	4.5	1.91093	5.6	0.08542	3.4	0.80	969	41	1085	38	1325	66	73
a12	25021	187	51	1.00	3059	0.22887	3.3	2.69667	4.7	0.08546	3.4	0.69	1329	39	1328	35	1326	66	100

a4	10245	55	18	2.15	2897	0.22049	4.4	2.59997	5.1	0.08552	2.6	0.86	1284	51	1301	38	1327	51	97
b42	6603	77	20	0.79	7888	0.22916	4.0	2.70509	6.1	0.08561	4.7	0.65	1330	48	1330	46	1329	90	100
b60	12849	159	43	0.67	3494	0.23054	4.4	2.72844	6.9	0.08583	5.3	0.64	1337	53	1336	53	1334	103	100
a10	22792	159	41	0.87	1640	0.22987	2.8	2.72426	3.5	0.08595	2.1	0.80	1334	33	1335	26	1337	41	100
a13	13859	62	20	1.22	295	0.22856	3.9	2.70806	9.3	0.08593	8.5	0.42	1327	47	1331	71	1337	163	99
a26	8484	61	18	1.49	6171	0.23102	5.0	2.73806	6.0	0.08596	3.3	0.83	1340	61	1339	46	1337	64	100
b27	7863	76	22	1.36	9334	0.22828	2.8	2.70692	4.3	0.08600	3.3	0.65	1325	33	1330	33	1338	64	99
b34	5426	78	20	0.97	6494	0.23021	1.9	2.72942	4.1	0.08599	3.6	0.46	1336	23	1336	31	1338	70	100
b41	8228	98	26	0.85	1849	0.22932	2.4	2.72081	4.3	0.08605	3.5	0.57	1331	29	1334	32	1339	68	99
b19	10167	92	27	1.37	12109	0.23145	3.9	2.74789	6.4	0.08611	5.1	0.60	1342	47	1342	49	1341	99	100
a41	22496	253	69	1.23	18202	0.23047	3.8	2.73816	4.3	0.08617	2.0	0.88	1337	46	1339	33	1342	40	100
b26	12759	120	31	0.73	10298	0.22925	4.2	2.72362	5.2	0.08617	3.1	0.80	1331	50	1335	40	1342	61	99
b38	12086	118	33	1.20	4155	0.22967	3.1	2.72883	4.3	0.08617	3.1	0.71	1333	37	1336	33	1342	59	99
a55	12677	92	25	1.57	14994	0.20203	4.1	2.40115	4.6	0.08620	2.2	0.88	1186	45	1243	34	1343	42	88
a32	26858	290	60	0.80	3370	0.17903	4.6	2.13165	4.9	0.08636	1.7	0.94	1062	45	1159	34	1346	32	79
b35	11275	181	36	1.23	3072	0.17559	3.2	2.09021	4.4	0.08634	3.0	0.73	1043	31	1146	31	1346	58	77
a1	18874	142	31	0.66	1011	0.19022	3.1	2.26538	6.3	0.08637	5.5	0.49	1123	32	1202	46	1347	107	83
a44	7448	71	17	0.99	4704	0.20352	2.0	2.42586	3.8	0.08645	3.2	0.53	1194	22	1250	28	1348	62	89
a17	16779	134	36	1.01	2022	0.22881	4.1	2.72778	4.3	0.08646	1.5	0.94	1328	49	1336	33	1349	29	98
b30	22575	215	65	1.62	13045	0.23079	3.6	2.75171	4.3	0.08648	2.3	0.85	1339	44	1343	32	1349	44	99
a15	16919	123	37	1.63	10760	0.22991	4.0	2.74438	5.1	0.08657	3.2	0.79	1334	49	1341	39	1351	61	99
a43	21324	215	58	0.97	1398	0.22934	7.3	2.73687	9.4	0.08655	6.0	0.77	1331	88	1339	73	1351	116	99
b1	22029	170	34	1.04	8609	0.15564	2.3	1.85845	3.9	0.08660	3.1	0.59	932	20	1066	26	1352	61	69
b50	4003	26	9	3.19	4709	0.20214	9.0	2.41556	9.7	0.08667	3.5	0.93	1187	99	1247	72	1353	67	88
a50	27182	173	59	2.50	2893	0.22940	4.7	2.74920	6.9	0.08692	5.1	0.68	1331	57	1342	53	1359	98	98
a28	23762	208	52	0.99	10869	0.21336	3.6	2.56258	4.3	0.08711	2.4	0.83	1247	41	1290	32	1363	46	91
a38	17978	190	49	0.67	3970	0.23688	2.6	2.84607	3.2	0.08714	1.9	0.80	1370	32	1368	24	1364	37	101
a8	25451	191	48	0.95	3913	0.21844	2.6	2.62448	3.3	0.08714	2.1	0.77	1274	30	1308	25	1364	41	93
a40	10421	114	32	1.23	6216	0.23670	3.1	2.84582	4.6	0.08720	3.4	0.67	1370	39	1368	35	1365	66	100
a39	18640	146	42	1.32	5096	0.23561	2.6	2.83481	3.6	0.08726	2.5	0.71	1364	32	1365	28	1366	49	100
b24	6632	53	15	1.24	4269	0.23009	2.8	2.77000	3.7	0.08731	2.5	0.74	1335	33	1347	28	1367	48	98
a49	23948	302	63	0.82	2849	0.18525	5.0	2.23143	5.4	0.08736	2.2	0.92	1096	50	1191	39	1368	42	80

a9	8522	56	16	1.16	9913	0.23543	4.7	2.83546	5.7	0.08735	3.2	0.83	1363	58	1365	43	1368	62	100
b51	12440	149	43	1.21	3310	0.23749	3.4	2.86360	5.2	0.08745	4.0	0.65	1374	42	1372	40	1370	76	100
a42	15644	146	37	0.95	2136	0.20905	4.6	2.52349	6.1	0.08755	4.0	0.76	1224	52	1279	45	1373	77	89
b56	12334	154	53	2.24	14440	0.23713	2.9	2.86319	4.0	0.08757	2.7	0.73	1372	36	1372	30	1373	52	100
a25	16150	134	38	0.98	3386	0.23723	5.8	2.86820	6.8	0.08769	3.6	0.85	1372	72	1374	53	1376	69	100
a33	22290	204	54	0.83	12723	0.23575	3.4	2.85405	4.7	0.08780	3.3	0.72	1365	41	1370	36	1378	63	99
b25	9906	117	25	0.66	5006	0.19614	3.9	2.38100	6.7	0.08804	5.4	0.59	1155	42	1237	49	1383	104	83
b13	25125	243	52	0.84	29213	0.18363	3.6	2.22959	4.4	0.08806	2.4	0.83	1087	36	1190	31	1384	47	79
b39	23165	257	66	0.66	17944	0.23623	3.2	2.86826	4.2	0.08806	2.7	0.76	1367	39	1374	32	1384	53	99
a20	3404	26	7	1.23	3927	0.22852	3.0	2.77712	5.6	0.08814	4.8	0.54	1327	36	1349	43	1386	91	96
b21	27571	125	37	0.99	159	0.20495	3.5	2.49834	11.1	0.08841	10.5	0.31	1202	38	1272	84	1391	202	86
b6	73161	431	120	1.05	3079	0.23951	3.6	2.92231	3.8	0.08849	1.2	0.95	1384	44	1388	29	1393	23	99
b14	20492	176	47	0.75	6298	0.24038	3.2	2.93393	5.3	0.08852	4.3	0.60	1389	40	1391	41	1394	82	100
a60	49313	628	133	0.65	1488	0.18862	6.5	2.30881	7.2	0.08878	3.0	0.91	1114	67	1215	52	1399	58	80
b15	18681	171	46	0.77	1774	0.24248	5.8	2.97516	6.6	0.08899	3.2	0.87	1400	73	1401	52	1404	62	100
b43	29871	399	91	0.80	2438	0.20131	3.0	2.47281	4.5	0.08909	3.3	0.67	1182	33	1264	33	1406	63	84
a22	12205	100	30	1.61	2594	0.23129	5.2	2.84383	6.6	0.08918	4.1	0.79	1341	63	1367	51	1408	78	95
b54	14017	199	47	0.81	2857	0.20810	2.9	2.55967	3.8	0.08921	2.5	0.76	1219	32	1289	28	1409	47	87
a37	46397	459	100	0.89	2494	0.18437	5.2	2.26908	5.7	0.08926	2.4	0.91	1091	52	1203	41	1410	46	77
a53	13143	168	45	1.21	5956	0.22165	2.0	2.73297	3.3	0.08942	2.6	0.61	1291	24	1337	25	1413	50	91
b29	18682	198	43	0.71	2761	0.19045	3.4	2.35417	4.4	0.08965	2.8	0.77	1124	35	1229	32	1418	53	79
a34	42377	617	103	1.02	1009	0.13489	4.7	1.66924	6.0	0.08975	3.7	0.78	816	36	997	39	1420	71	57
b59	19903	278	70	1.00	4978	0.21399	3.8	2.64734	5.0	0.08972	3.3	0.76	1250	43	1314	37	1420	62	88
b3	27583	335	53	0.79	1749	0.13520	5.8	1.67743	6.4	0.08998	2.6	0.92	817	45	1000	41	1425	49	57
a27	18006	157	43	0.71	4874	0.24870	2.9	3.09002	4.1	0.09011	3.0	0.70	1432	37	1430	32	1428	56	100
a19	21472	167	47	1.22	2881	0.23738	2.9	2.95066	3.6	0.09015	2.1	0.81	1373	36	1395	28	1429	40	96
a36	33848	266	64	0.70	7597	0.21366	7.1	2.65789	7.7	0.09022	3.0	0.92	1248	81	1317	58	1430	57	87
b17	32638	363	80	0.68	1782	0.19906	3.7	2.47687	4.1	0.09024	1.9	0.89	1170	40	1265	30	1431	35	82
b12	6579	57	17	1.17	1449	0.25023	3.6	3.11791	5.4	0.09037	4.1	0.66	1440	47	1437	43	1433	77	100
b44	51290	758	144	0.94	1023	0.15928	4.7	1.98659	6.2	0.09046	4.0	0.76	953	42	1111	43	1435	76	66
b11	4155	34	10	0.97	2635	0.24436	3.6	3.05150	6.9	0.09057	5.9	0.52	1409	45	1421	54	1438	112	98
a18	31769	375	91	2.21	2904	0.18676	3.6	2.34420	5.2	0.09104	3.8	0.69	1104	36	1226	38	1447	72	76

a31	12382	100	32	1.60	2765	0.25002	3.0	3.14183	4.0	0.09114	2.6	0.76	1439	39	1443	31	1449	49	99
b40	35702	510	106	1.04	1141	0.17708	5.7	2.22970	5.9	0.09132	1.6	0.96	1051	56	1190	42	1453	31	72
a35	16575	175	31	0.92	1288	0.14672	6.5	1.85533	7.0	0.09171	2.4	0.94	883	54	1065	47	1461	46	60
b33	33989	309	81	1.04	3869	0.22170	2.1	2.80344	3.9	0.09171	3.3	0.55	1291	25	1356	30	1461	62	88
a30	37232	383	77	1.34	942	0.15359	4.1	1.94533	4.9	0.09186	2.7	0.83	921	35	1097	34	1464	52	63
b48	26577	398	100	1.01	1365	0.21771	5.3	2.76601	6.1	0.09215	3.0	0.87	1270	61	1346	46	1470	57	86
a14	30005	289	68	0.99	1177	0.20828	3.3	2.65697	4.6	0.09252	3.2	0.72	1220	37	1317	35	1478	61	83
b9	42684	548	96	1.54	783	0.12919	6.7	1.66205	7.5	0.09331	3.3	0.90	783	50	994	49	1494	62	52
b31	46151	428	125	0.96	1369	0.25883	2.6	3.33538	3.0	0.09346	1.5	0.87	1484	34	1489	24	1497	28	99
b32	14806	144	30	0.97	1348	0.18342	12	2.37427	12.8	0.09388	4.1	0.95	1086	123	1235	96	1506	78	72
a16	30390	318	55	0.77	1315	0.14911	4.0	1.94921	5.4	0.09481	3.7	0.74	896	33	1098	37	1524	69	59
b37	14807	162	37	0.82	1049	0.19733	5.2	2.57982	6.1	0.09482	3.1	0.86	1161	56	1295	45	1524	58	76
a29	15531	164	33	0.42	1852	0.19565	4.2	2.58091	7.2	0.09567	5.9	0.57	1152	44	1295	54	1541	112	75
a11	8723	78	19	0.98	1550	0.20894	3.3	2.76968	5.1	0.09614	3.8	0.66	1223	37	1347	39	1551	72	79
b36	14985	315	36	0.64	839	0.09913	4.2	1.32050	7.0	0.09661	5.5	0.61	609	25	855	41	1560	104	39
a54	9783	91	31	1.49	1128	0.27051	4.1	3.60740	5.5	0.09672	3.6	0.76	1543	57	1551	44	1562	67	99
a58	22033	245	61	0.96	1985	0.22082	4.4	2.95796	5.9	0.09715	3.8	0.76	1286	52	1397	45	1570	72	82
b8	20333	188	30	0.94	1109	0.12572	5.6	1.69021	7.2	0.09751	4.5	0.78	763	40	1005	47	1577	84	48
a56	3765	42	9	0.55	750	0.20455	6.5	2.76291	10.5	0.09796	8.2	0.62	1200	72	1346	81	1586	153	76
a57	28768	484	69	1.01	667	0.11302	6.2	1.52765	7.4	0.09803	4.1	0.84	690	40	942	46	1587	76	43
b47	23185	445	56	0.88	770	0.10040	12	1.40751	12.5	0.10168	4.9	0.92	617	68	892	77	1655	91	37
b58	27367	331	83	0.91	632	0.20946	2.9	2.97582	3.8	0.10304	2.5	0.76	1226	32	1401	29	1680	46	73
b16	14459	156	30	0.62	847	0.17125	3.2	2.43877	5.7	0.10329	4.7	0.57	1019	31	1254	42	1684	86	61
b23	28269	240	58	1.06	779	0.19234	2.8	2.77707	4.3	0.10471	3.3	0.65	1134	29	1349	33	1709	61	66
a51	24319	361	50	0.91	619	0.10957	3.6	1.59742	4.5	0.10574	2.6	0.81	670	23	969	28	1727	48	39
b46	21915	273	44	0.83	395	0.12865	5.2	1.98949	6.5	0.11216	4.0	0.79	780	38	1112	45	1835	72	43
b28	23133	250	46	0.61	588	0.15470	4.6	2.41397	5.2	0.11318	2.3	0.90	927	40	1247	38	1851	41	50
a52	4688	35	10	0.70	506	0.23860	4.7	3.85826	8.2	0.11728	6.8	0.57	1379	59	1605	69	1915	121	72
b22	31567	308	58	0.61	363	0.15626	6.2	2.75922	7.7	0.12806	4.5	0.81	936	55	1345	59	2072	80	45
a7	56271	420	143	1.10	330	0.16443	9.6	3.82751	30.8	0.16883	29.3	0.31	981	88	1599	285	2546	491	39

[a] within-run background-corrected mean ^{207}Pb signal in counts per second
[b] U and Pb content and Th/U ratio were calculated relative to GJ-1 and are accurate to approximately 10%.
[c] corrected for background, mass bias, laser induced U-Pb fractionation and common Pb (if detectable, see analytical method) using Stacey & Kramers (1975) model Pb composition. ^{207}Pb/^{235}U calculated using ^{207}Pb/^{206}Pb/(^{238}U/^{206}Pb × 1/137.88). Errors are propagated by quadratic addition of within-run errors (2SE) and the reproducibility of GJ-1 (2SD).
[d] Rho is the error correlation defined as err^{206}Pb/^{238}U/err^{207}Pb/^{235}

Appendix b: Structure measurements

Aruab Member		
Measurement number	Strike (in degrees)	Dip (in degrees)
1	141	86
2	136	75
3	110	52
4	123	86
5	124	73
6	122	52
7	134	50
8	185	46
9	163	36
10	198	53
11	271	24
12	264	31
13	238	39
14	239	29

Aruab Proximal			
Site	Strike (in degrees)	Dip (in degrees)	Notes
x1401	147	28	
x1402	145	28	repeat
x1413	126	26	
x1414	137	49	
x1415	160	67	
x1416	94	69	near fault
x1417	315	47	repeat
x1418	314	47	
x1419	227	74	near fault
x1420	146	86	repeat
x1421	148	86	
x1422	154	84	
x1504	148.4	28	repeat
x1505	148.4	28	repeat
x1506	133.8	59	
x1507	135	70	
x1508	159.1	55	
x1509	148	80	
x1510	148	80	repeat
x1511	148	80	repeat
x1512	314	47	
x1513a	220	23	
x1514	288	49	repeat
x1515a	138	37	

x1516	277	63	
x1517	282	37	
x1513b	287	49	
x1515b	255	32	

Aruab Distal			
Site	Strike (in degrees)	Dip (in degrees)	Notes
x1518	152.4	56	
x1521a	166.7	60	
x1521b	161.7	38	
x1522	183.2	39	repeat
x1523	183.1	39	
x1524	183.1	39	repeat
x1525	144.8	76	
x1527	148.1	56.5	

Naus			
Site	Strike (in degrees)	Dip (in degrees)	Notes
X1541	241.4	84	
X1542	237.2	81	
X1543	234.3	81	repeat
X1544	254.8	78	
X1545	256.7	78	repeat
X1546	252.5	87	
X1547	251.4	87	repeat
X1548	252.5	87	repeat
X1549	250.8	87	repeat
X1550	237	59	
X1551	238	59	repeat
X1403	229.1	58	
X1404	245.4	70	
X1405	242.1	73	
X1406	239.4	53	
X1407	229.4	67	
X1408	241.5	59	
X1409	241.2	59	repeat
X1410	248.7	59	repeat
X1411	240.4	87	
X1412	233.7	68	

Vergenoeg			
Site	Strike (in degrees)	Dip (in degrees)	Notes
x1552	343.4	34	
x1553	345.2	28	repeat
x1555	344.2	28	
x1557	3.4	28	Avg. of sites 56+58
x1558	10	21	
x1559	152.2	6	
x1560	204.9	14	
x1561	201.6	10	
x1562	331.6	35	
x1563	336.1	29	
x1564	283.4	30	
x1565	305.4	15	
x1566	305.4	15	repeat
x1567	33.5	20	
X1556	359.5	35	

Aruab Structural Panel

Name	Location Latitude (S)	Location Longitude (E)	Lithology	n/N	Geog. Dec°	Geog. Inc°	Geo a95 °	TC Dec°	TC Inc°	TC a95°	VGP Lat°N	VGP Long°E
NORTH ARUAB												
X1401	25.725	16.578	Volcaniclastic breccia (mafic)	17/17	042.9	-19.8	2.7	043.7	07.4	2.6	38.461	78.298
X1402	25.725	16.579	Volcaniclastic breccia (mafic)	11/11	046.4	-14.7	4.5	046.4	13.0	4.5	34.581	77.500
X1419	25.724	16.574	Basalt flow	8/8	066.1	-17.5	4.7	069.6	12.6	4.7	15.306	91.559
X1420	25.722	16.573	Felsic lava	7/8	075.0	-73.7	5.0	061.6	11.4	5.0	22.514	87.937
X1421	25.722	16.573	Red siltstone	8/8	088.4	-76.4	4.0	064.8	07.7	4.0	20.704	91.416
Mean for North Aruab				5 sites	056.2	-40.8	34.4	057.2	10.6	25.7		
SOUTH ARUAB												
X1416	25.734	16.572	Basalt	9/9	013.7	-36.6	5.9	013.2	31.7	5.9	45.256	34.656
X1417	25.735	16.57	Basalt	7/8	054.3	71.5	5.4	048.0	24.7	5.4	29.367	72.805
X1512	25.734	16.57	Volcaniclastic breccia (mafic)	15/15	023.8	72.5	16.5	037.1	26.4	16.5	36.374	63.245
X1513	25.734	16.57	Red sandstone	11/11	027.3	40.5	14.4	018.5	22.4	5.3	48.538	44.593
X1514 (M)	25.734	16.57	Vesicular basalt	6/8	038.8	45.0	7.6	032.7	-02.1	7.6	50.004	73.781
X1516	25.736	16.565	Basalt	7/8	124.0	53.3	6.2	049.1	37.3	6.2	23.389	66.917
Mean for South Aruab				6 sites	017.2	32.4	66.3	032.9	24.1	16.0		
Mean for both South and North Aruab				11 sites	037.8	-09.4	45.5	044.6	18.2	11.9		

Other Aruab components

X1413 veined	25.734	16.576	Basalt	7/8	009.2	-14.9	10.0	009.9	08.4	10.0	58.574	35.799
X1414 porous	25.734	16.575	Basalt	8/8	010.9	-28.7	12.9	015.0	12.9	12.9	54.625	42.970
X1415	25.734	16.571	Red sandstone	7/8	353.5	-35.3	17.7	017.4	-02.9	17.7	60.522	54.010
X1418 red sed.	25.735	16.57	Fine grained red sandstone	8/8	016.7	25.7	13.9	018.5	-16.7	14.0	65.421	65.574
X1422 red sed.	25.719	16.567	Banded basalt flow	8/8	018.8	-10.6	9.8	353.9	42.5	9.8	39.340	9.424
X1515 red sed.	25.734	16.57	Red sandstone	16/16	004.1	-03.7	18.5	004.8	-04.4	20.8	66.053	28.489
Mean for other Aruab components				6 sites	009.2	-11.6	19.7	010.6	06.4	18.8		

Naus and Heuwelvlakte Structural panel

Name	Location Latitude (S)	Location Longitude (E)	Lithology	n/N	Geog. Dec°	Geog. Inc°	Geo a95 °	TC Dec°	TC Inc°	TC a95°	VGP Lat°N	VGP Long°E
NAUS												
X1546	25.821	16.482	Mafic sandstone	8/8	093.6	78.8	7.4	353.2	07.0	7.4	59.955	2.847
X1547	25.821	16.482	Mafic sandstone	8/8	086.5	61.6	4.8	009.3	09.7	4.8	58.016	34.197
X1548*	25.821	16.482	Dike (basalt)	8/8	009.7	80.0	26.1	347.1	-05.9	26.1	64.012	-14.085
X1549	25.821	16.482	Rhyolite	8/8	091.1	63.9	2.3	005.8	11.5	2.3	57.894	27.404
X1550	25.844	16.521	Basalt (with amygdales)	8/8	061.4	57.8	9.7	004.1	28.1	9.7	49.057	22.551
X1551	25.844	16.522	Basalt (with xenoliths)	8/8	334.2	-83.5	6.8	147.1	-37.5	6.8	33.358	-20.884
HEUWELVLAKTE												
X1403 (M)	25.859	16.668	Sill (Basalt)	9/9	022.3	73.5	3.9	335.2	23.5	3.9	44.843	-18.615
X1403* (H)	25.859	16.668	Sill (Basalt)	5/9	135.8	-53.8	12.6	137.2	04.1	12.6	42.474	-50.311
X1404* (H)	25.854	16.668	Sill (Basalt)	4/10	169.7	-34.5	7.1	169.5	33.8	7.1	77.796	-38.135
X1405* (H)	25.849	16.667	Flow banded rhyolite	7/8	190.8	-43.4	18.4	181.0	20.0	18.4	74.485	20.380
X1406 (M)	25.847	16.666	Flow banded rhyolite	7/8	087.1	73.1	12.8	350.0	43.1	12.8	38.216	5.152
X1407 (M)	25.843	16.668	Sill (Basalt)	8/8	060.8	75.3	10.1	335.3	25.1	10.1	44.198	-17.876
X1408* (M)	25.836	16.657	Sill (Basalt)	8/8	345.5	57.0	22.7	339.1	-01.2	22.7	57.736	-25.231
X1410 (M)	25.836	16.657	Sill - exocontact (basalt)	8/8	330.5	82.3	5.0	337.5	23.4	5.0	46.132	-15.965
X1412 (M)	25.833	16.647	Medium to coarse grained trachyandesite	6/8	087.7	60.8	9.1	353.4	35.4	9.1	44.187	7.913
NAUS+HEUWELVL. mean				10 sites	075.3	73.6	8.3	349.6	25.1	11.0		

Vergenoeg Structural Panel

Name	Location Latitude (S)	Location Longitude (E)	Lithology	n/N	Geog. Dec°	Geog. Inc°	Geo a95 °	TC Dec°	TC Inc°	TC a95°	VGP Lat°N	VGP Long°E
VERGENOEG												
X1553*	25.593	16.214	Dike (Basalt)	8/8	030.8	-03.2	5.5	026.1	-22.6	5.5	61.758	81.745
X1554*	25.593	16.214	Exocontact (Silicified Porphyry)	7/8	015.6	08.4	6.9	016.2	-05.9	6.9	62.527	53.364
X1555	25.593	16.214	Silicified porphyry	5/7	141.5	-40.0	16.6	168.3	-45.0	16.6	36.639	3.146
X1556	25.586	16.22	Basalt	4/8	169.0	-61.1	11.2	221.8	-50.2	11.2	20.747	53.893
X1558	25.586	16.223	Rhyolite (with eutaxitic foliation)	6/8	010.3	-12.8	8.6	005.7	-12.0	8.6	69.730	32.783
X1559	25.607	16.27	Basalt	8/8	178.6	-27.7	10.1	175.6	-30.2	10.1	47.946	9.956
X1560 (G+H)	25.607	16.267	Basalt	2/8	009.1	10.3	13.0	007.2	06.2	13.0	60.445	30.968
X1561	25.607	16.266	Coarse Trachyandesite	8/8	016.4	05.5	12.3	015.6	04.3	12.3	58.396	47.120
X1562	25.59	16.297	Vesicular basalt	8/8	137.4	00.1	24.9	139.8	-08.0	24.9	41.064	-42.346
X1563	25.588	16.298	Rhyolite	8/8	163.5	-32.0	7.8	178.8	-24.3	7.8	51.670	14.412
X1564	25.597	16.239	Basalt	8/8	327.9	21.5	9.0	331.8	-00.5	9.0	52.813	-35.187
X1566	25.596	16.24	Volcaniclastic breccia (Basalt)	14/14	129.1	-40.5	36.1	141.1	-37.5	36.1	30.033	-26.387
X1567	25.596	16.24	Basalt	8/8	139.5	03.5	5.9	140.1	-15.7	5.9	38.681	-38.219
VERGENOEG mean				8 sites	346.3	22.8	23.1	355.4	21.1	22.7		
NAUS+HEUW+VERG gm				18 sites	9.4	59.7	19.3	352.1	23.4	10.7		

Figure X1401. Panel (a) shows the view of a representative sample in an orthographic projection in geographic coordinates. Blue=horizontal projection, red=vertical projection. Each pair of points represents a measurement step (natural remanent magnetization NRM, liquid nitrogen LN2, or thermal degrees C). Panel (b) shows the same sample in an equal-area projection in geographic coordinates. Blue=lower hemisphere, red=upper hemisphere. Panels (c) and (d) show equal-area projections of the site mean in geographic and tilt-corrected coordinates, respectively. Each point is a ChRM of a sample within the site. Blue=lower hemisphere, red=upper hemisphere. The circle represents the Fisher alpha 95-error of the site mean. Lighter colored points represent sample ChRMs that were not selected into the mean.

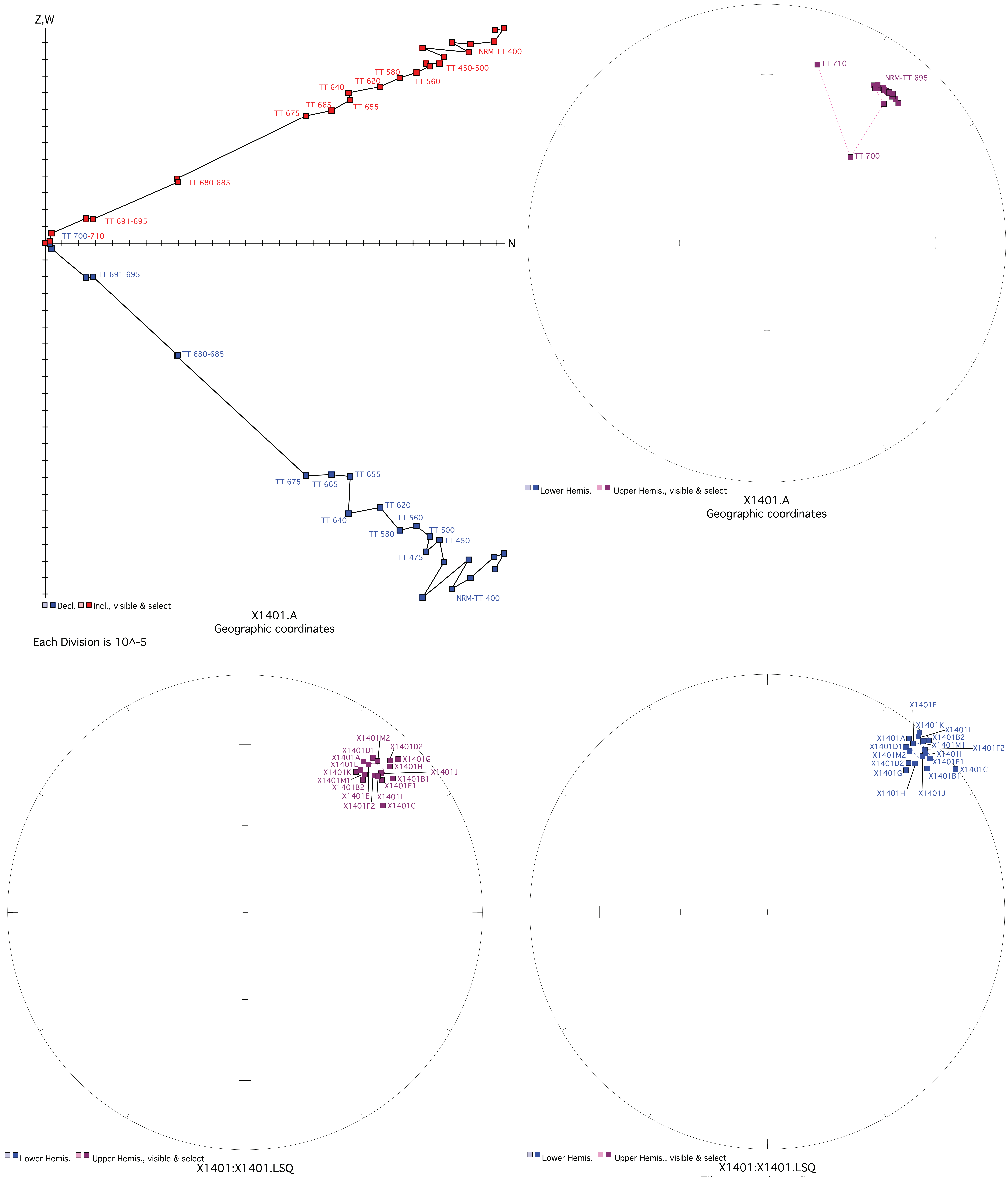

Fisher mean geog. decl.: 42.9, incl.: -19.8 a95 2.7, N: 17

Fisher mean strat. decl.: 43.7, incl.: 7.4 a95 2.6, N: 17

Figure X1402. Panel (a) shows the view of a representative sample in an orthographic projection in geographic coordinates. Blue=horizontal projection, red=vertical projection. Each pair of points represents a measurement step (natural remanent magnetization NRM, liquid nitrogen LN2, or thermal degrees C). Panel (b) shows the same sample in an equal-area projection in geographic coordinates. Blue=lower hemisphere, red=upper hemisphere. Panels (c) and (d) show equal-area projections of the site mean in geographic and tilt-corrected coordinates, respectively. Each point is a ChRM of a sample within the site. Blue=lower hemisphere, red=upper hemisphere. The circle represents the Fisher alpha 95-error of the site mean. Lighter colored points represent sample ChRMs that were not selected into the mean.

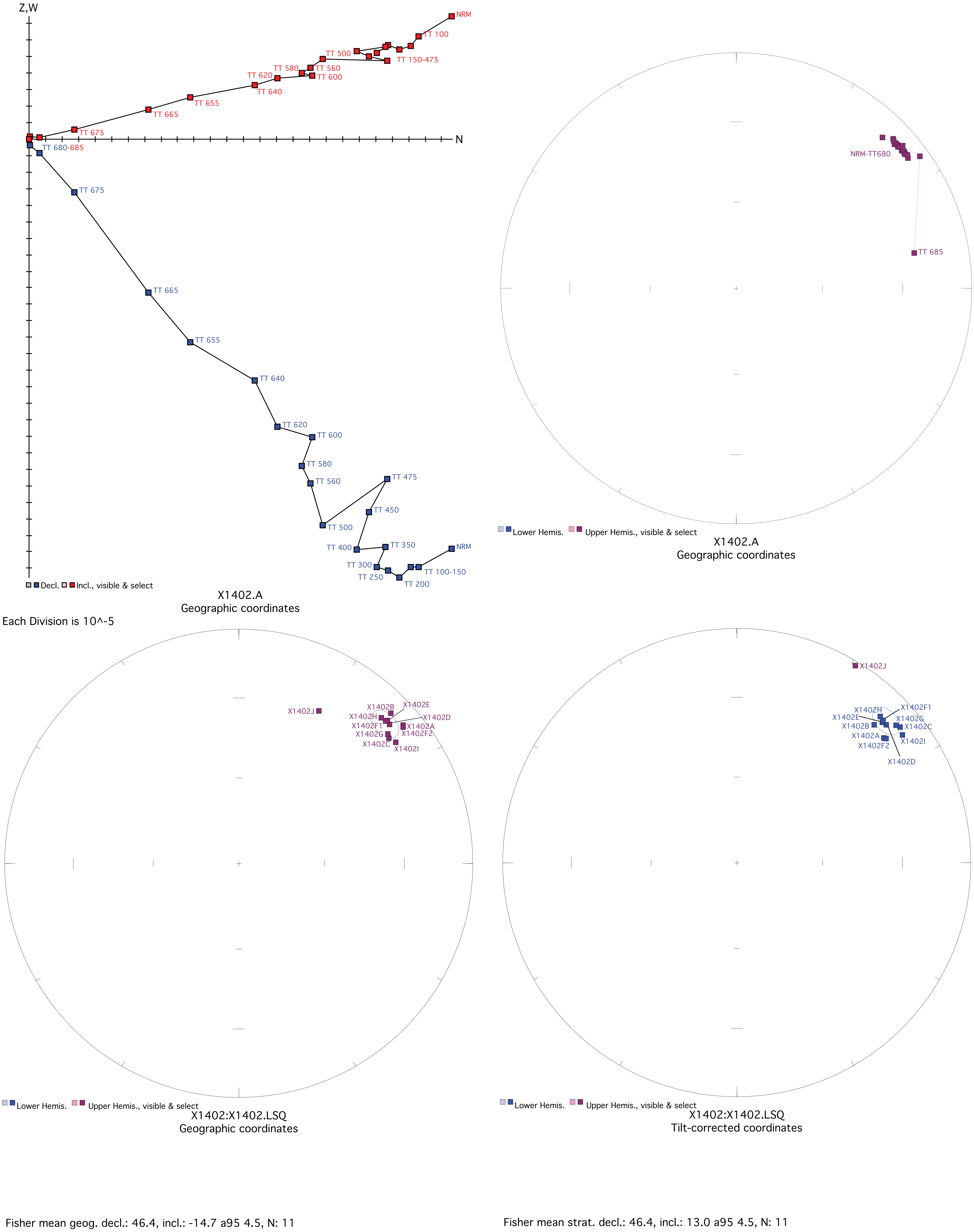

Figure X1403. Panel (a) shows the view of a representative sample in an orthographic projection in geographic coordinates. Blue=horizontal projection, red=vertical projection. Each pair of points represents a measurement step (natural remanent magnetization NRM, liquid nitrogen LN2, or thermal degrees C). Panel (b) shows the same sample in an equal-area projection in geographic coordinates. Blue=lower hemisphere, red=upper hemisphere. Panels (c) and (d) show equal-area projections of the site mean in geographic and tilt-corrected coordinates, respectively. Each point is a ChRM of a sample within the site. Blue=lower hemisphere, red=upper hemisphere. The circle represents the Fisher alpha 95-error of the site mean. Lighter colored points represent sample ChRMs that were not selected into the mean.

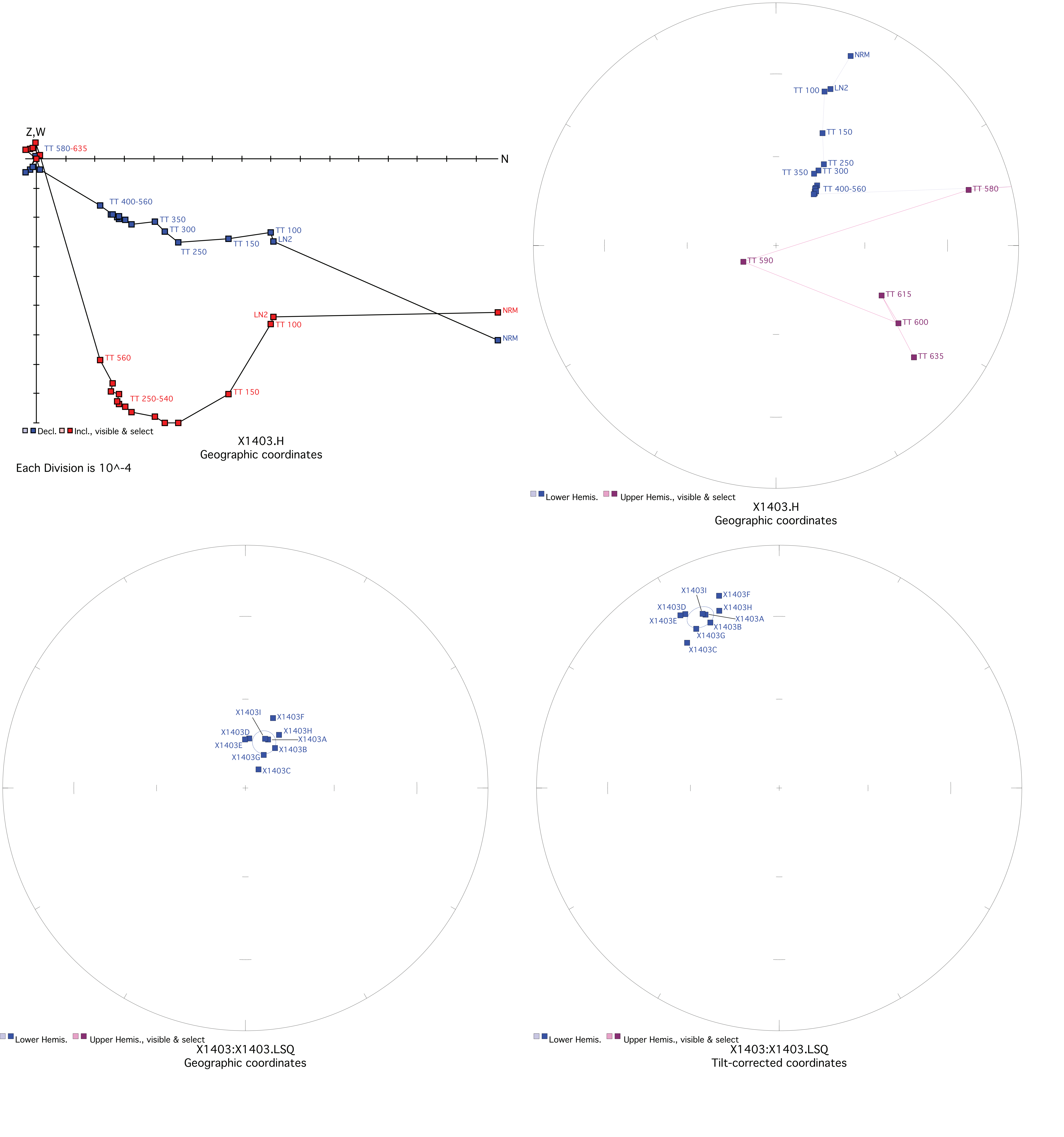

Fisher mean geog. decl.: 22.3, incl.: 73.5 a95 3.9, N: 9

Fisher mean strat. decl.: 335.2, incl.: 23.5 a95 3.9, N: 9

Figure X1419. Panel (a) shows the view of a representative sample in an orthographic projection in geographic coordinates. Blue=horizontal projection, red=vertical projection. Each pair of points represents a measurement step (natural remanent magnetization NRM, liquid nitrogen LN2, or thermal degrees C). Panel (b) shows the same sample in an equal-area projection in geographic coordinates. Blue=lower hemisphere, red=upper hemisphere. Panels (c) and (d) show equal-area projections of the site mean in geographic and tilt-corrected coordinates, respectively. Each point is a ChRM of a sample within the site. Blue=lower hemisphere, red=upper hemisphere. The circle represents the Fisher alpha 95-error of the site mean. Lighter colored points represent sample ChRMs that were not selected into the mean.

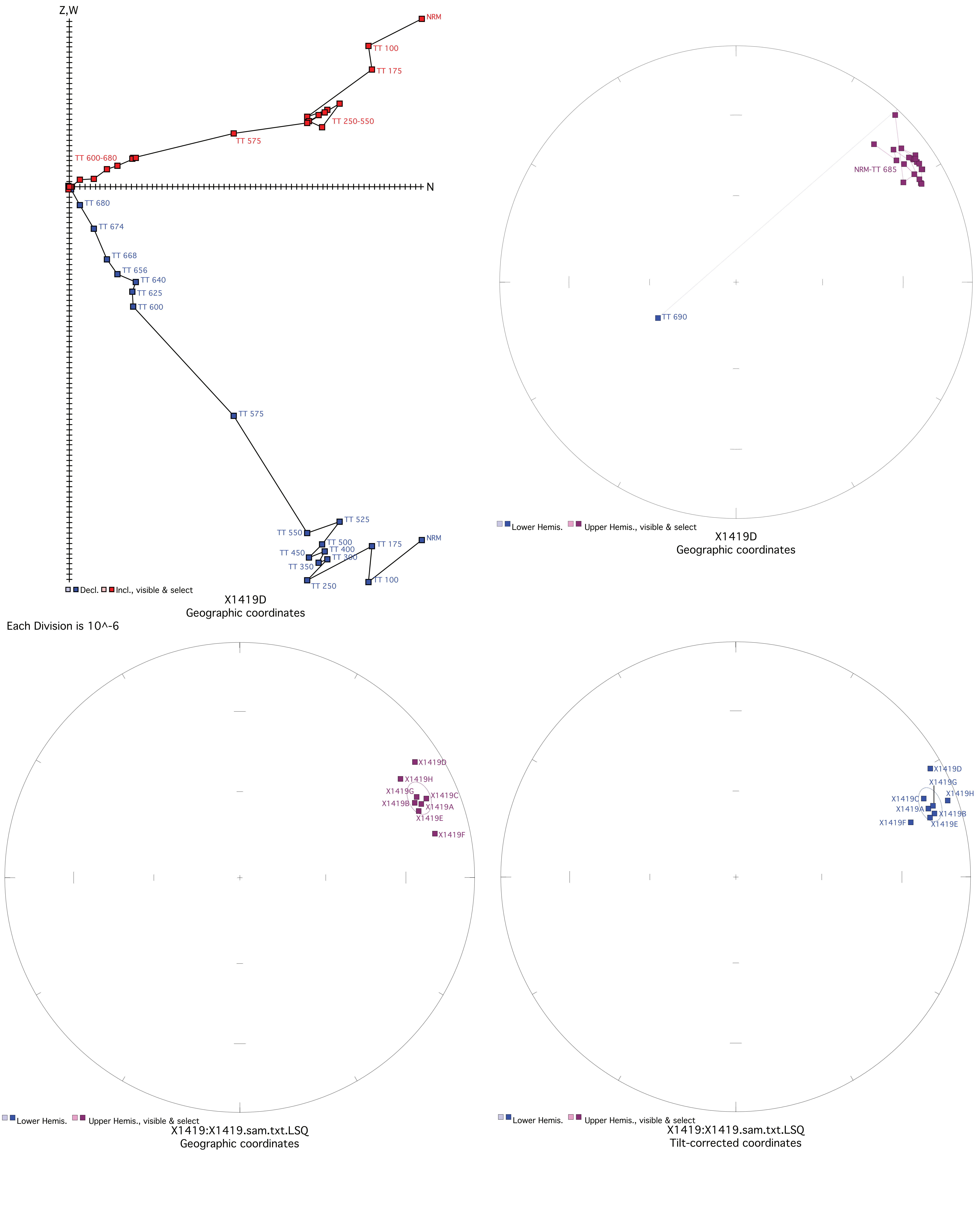

Fisher mean geog. decl.: 66.1, incl.: -17.5 a95 4.7, N: 8

Fisher mean strat. decl.: 69.6, incl.: 12.6 a95 4.7, N: 8

Figure X1420. Panel (a) shows the view of a representative sample in an orthographic projection in geographic coordinates. Blue=horizontal projection, red=vertical projection. Each pair of points represents a measurement step (natural remanent magnetization NRM, liquid nitrogen LN2, or thermal degrees C). Panel (b) shows the same sample in an equal-area projection in geographic coordinates. Blue=lower hemisphere, red=upper hemisphere. Panels (c) and (d) show equal-area projections of the site mean in geographic and tilt-corrected coordinates, respectively. Each point is a ChRM of a sample within the site. Blue=lower hemisphere, red=upper hemisphere. The circle represents the Fisher alpha 95-error of the site mean. Lighter colored points represent sample ChRMs that were not selected into the mean.

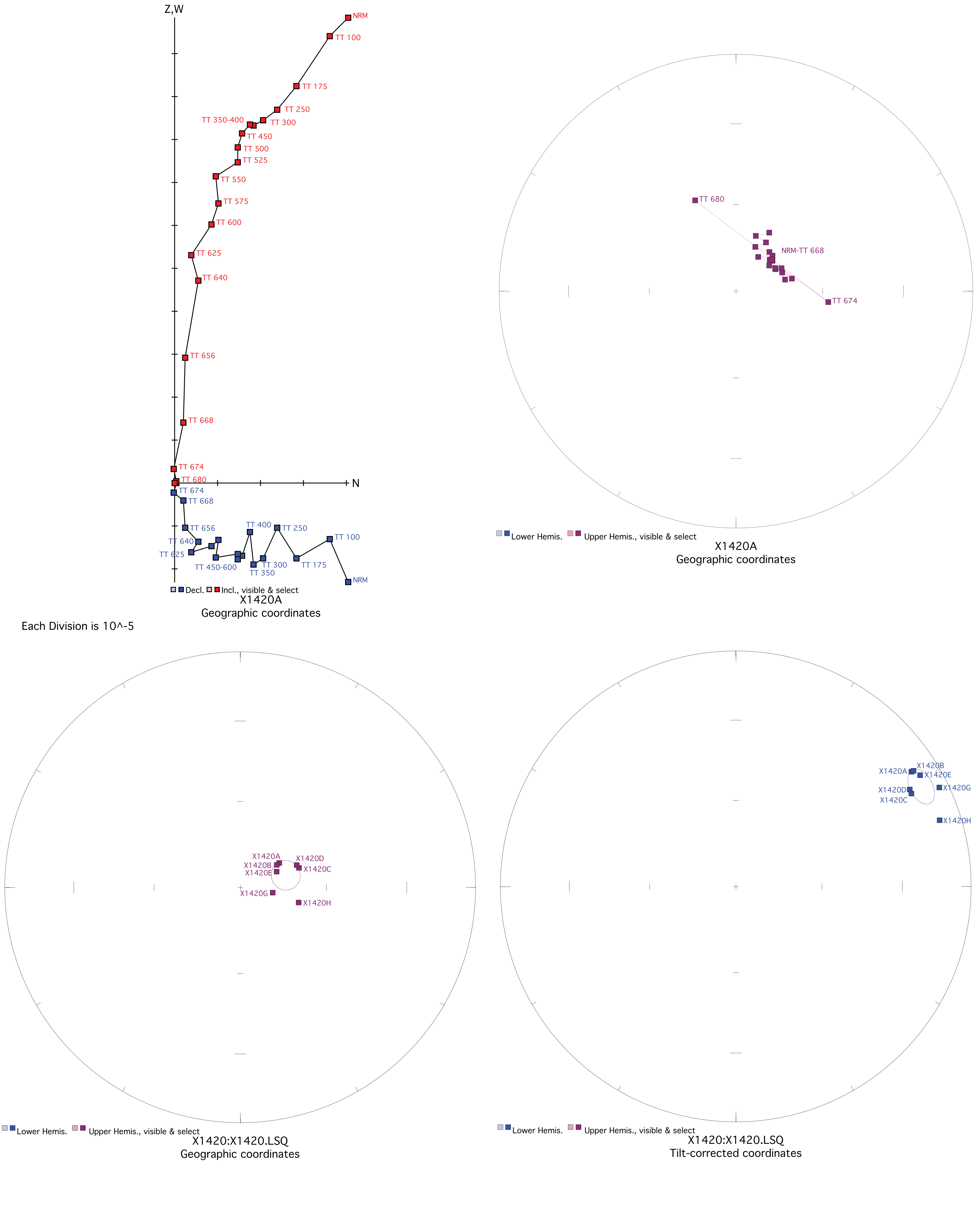

Fisher mean geog. decl.: 75.0, incl.: -73.7 a95 5.0, N: 7

Fisher mean strat. decl.: 61.6, incl.: 11.4 a95 5.0, N: 7

Figure X1421. Panel (a) shows the view of a representative sample in an orthographic projection in geographic coordinates. Blue=horizontal projection, red=vertical projection. Each pair of points represents a measurement step (natural remanent magnetization NRM, liquid nitrogen LN2, or thermal degrees C). Panel (b) shows the same sample in an equal-area projection in geographic coordinates. Blue=lower hemisphere, red=upper hemisphere. Panels (c) and (d) show equal-area projections of the site mean in geographic and tilt-corrected coordinates, respectively. Each point is a ChRM of a sample within the site. Blue=lower hemisphere, red=upper hemisphere. The circle represents the Fisher alpha 95-error of the site mean. Lighter colored points represent sample ChRMs that were not selected into the mean.

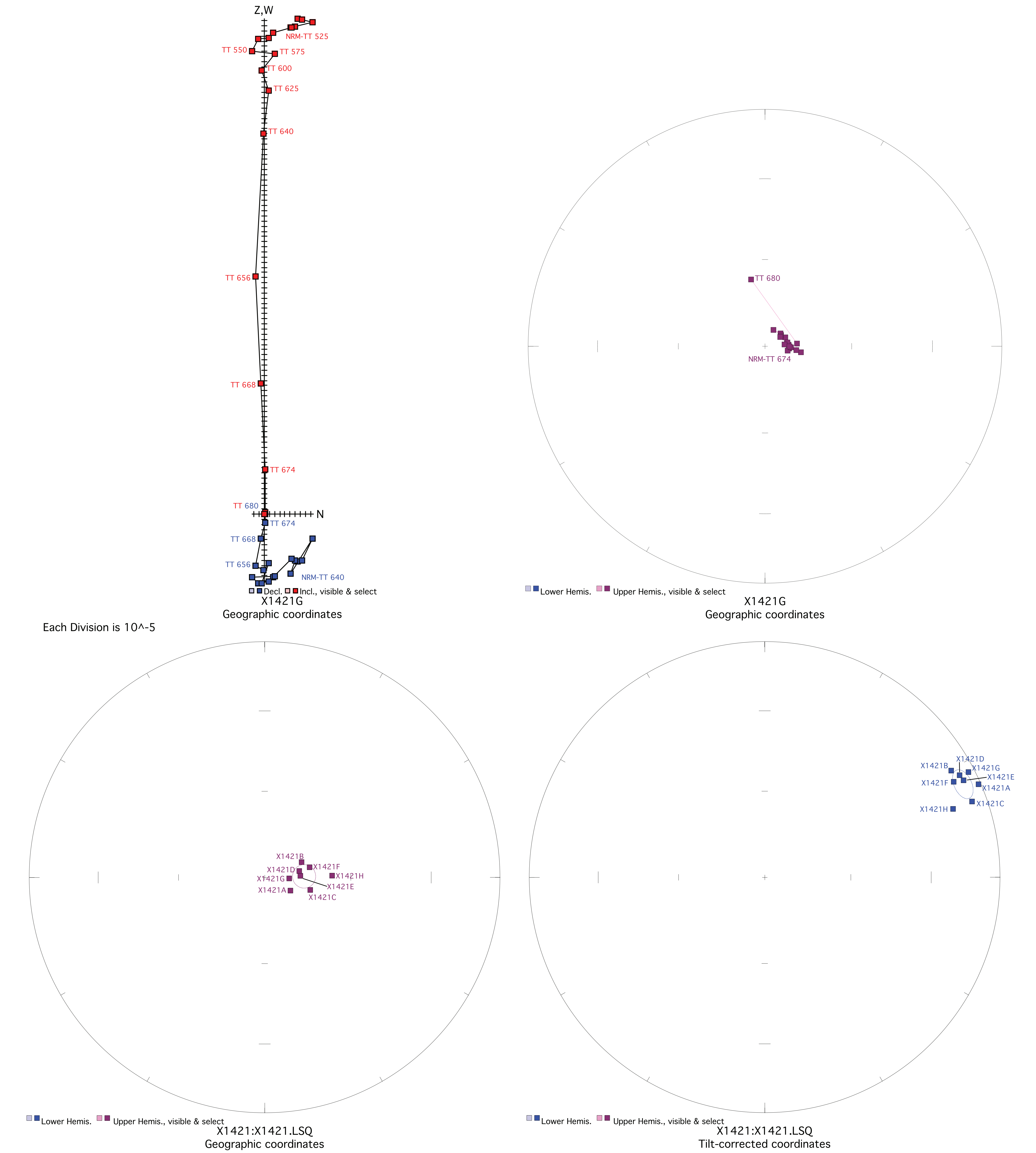

Fisher mean geog. decl.: 88.4, incl.: -76.4 a95 4.0, N: 8

Fisher mean strat. decl.: 64.8, incl.: 7.7 a95 4.0, N: 8

Figure X1416. Panel (a) shows the view of a representative sample in an orthographic projection in geographic coordinates. Blue=horizontal projection, red=vertical projection. Each pair of points represents a measurement step (natural remanent magnetization NRM, liquid nitrogen LN2, or thermal degrees C). Panel (b) shows the same sample in an equal-area projection in geographic coordinates. Blue=lower hemisphere, red=upper hemisphere. Panels (c) and (d) show equal-area projections of the site mean in geographic and tilt-corrected coordinates, respectively. Each point is a ChRM of a sample within the site. Blue=lower hemisphere, red=upper hemisphere. The circle represents the Fisher alpha 95-error of the site mean. Lighter colored points represent sample ChRMs that were not selected into the mean.

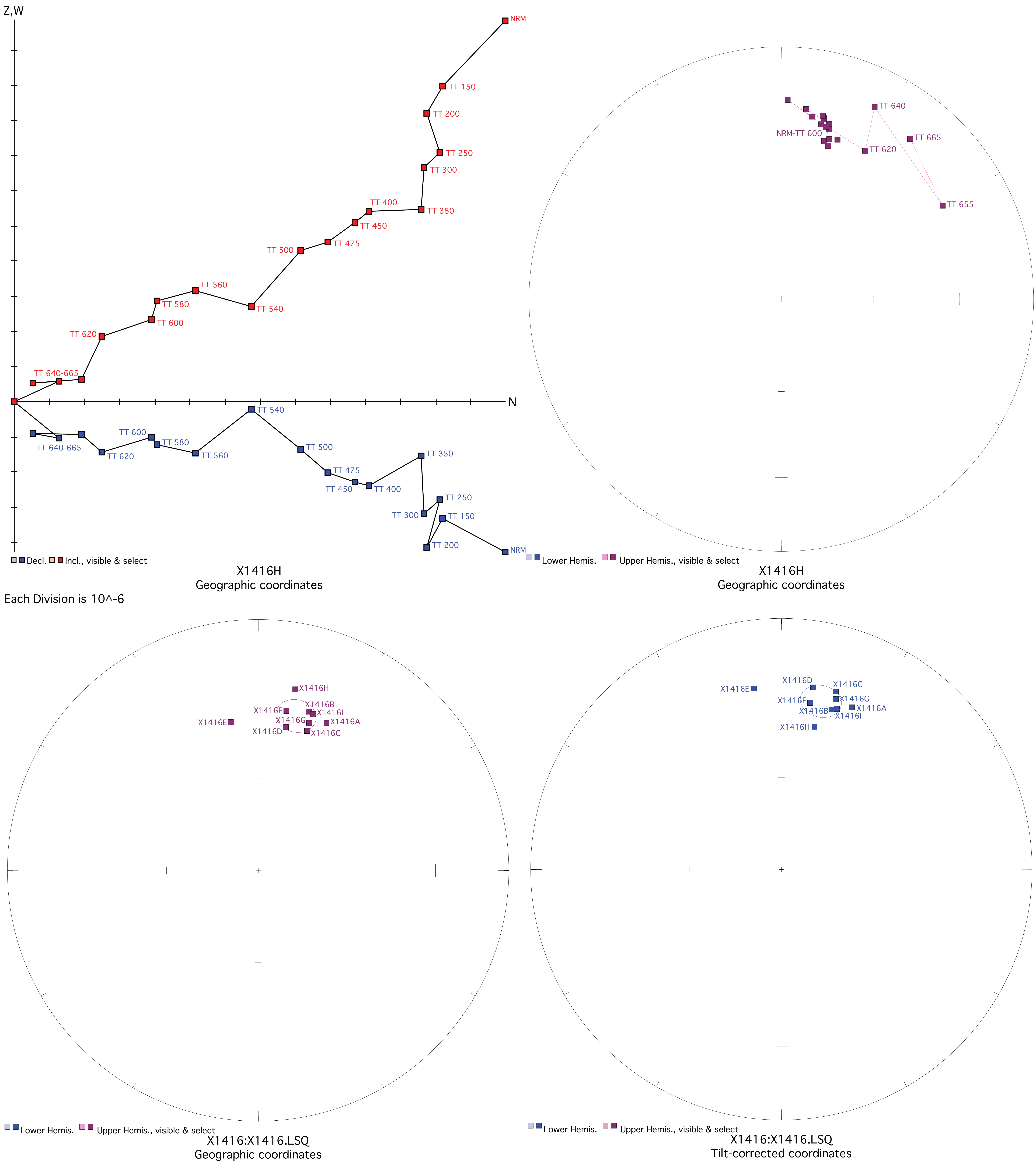

Fisher mean geog. decl.: 13.7, incl.: -36.6 a95 5.9, N: 9

Fisher mean strat. decl.: 13.2, incl.: 31.7 a95 5.9, N: 9

Figure X1413. Panel (a) shows the view of a representative sample in an orthographic projection in geographic coordinates. Blue=horizontal projection, red=vertical projection. Each pair of points represents a measurement step (natural remanent magnetization NRM, liquid nitrogen LN2, or thermal degrees C). Panel (b) shows the same sample in an equal-area projection in geographic coordinates. Blue=lower hemisphere, red=upper hemisphere. Panels (c) and (d) show equal-area projections of the site mean in geographic and tilt-corrected coordinates, respectively. Each point is a ChRM of a sample within the site. Blue=lower hemisphere, red=upper hemisphere. The circle represents the Fisher alpha 95-error of the site mean. Lighter colored points represent sample ChRMs that were not selected into the mean.

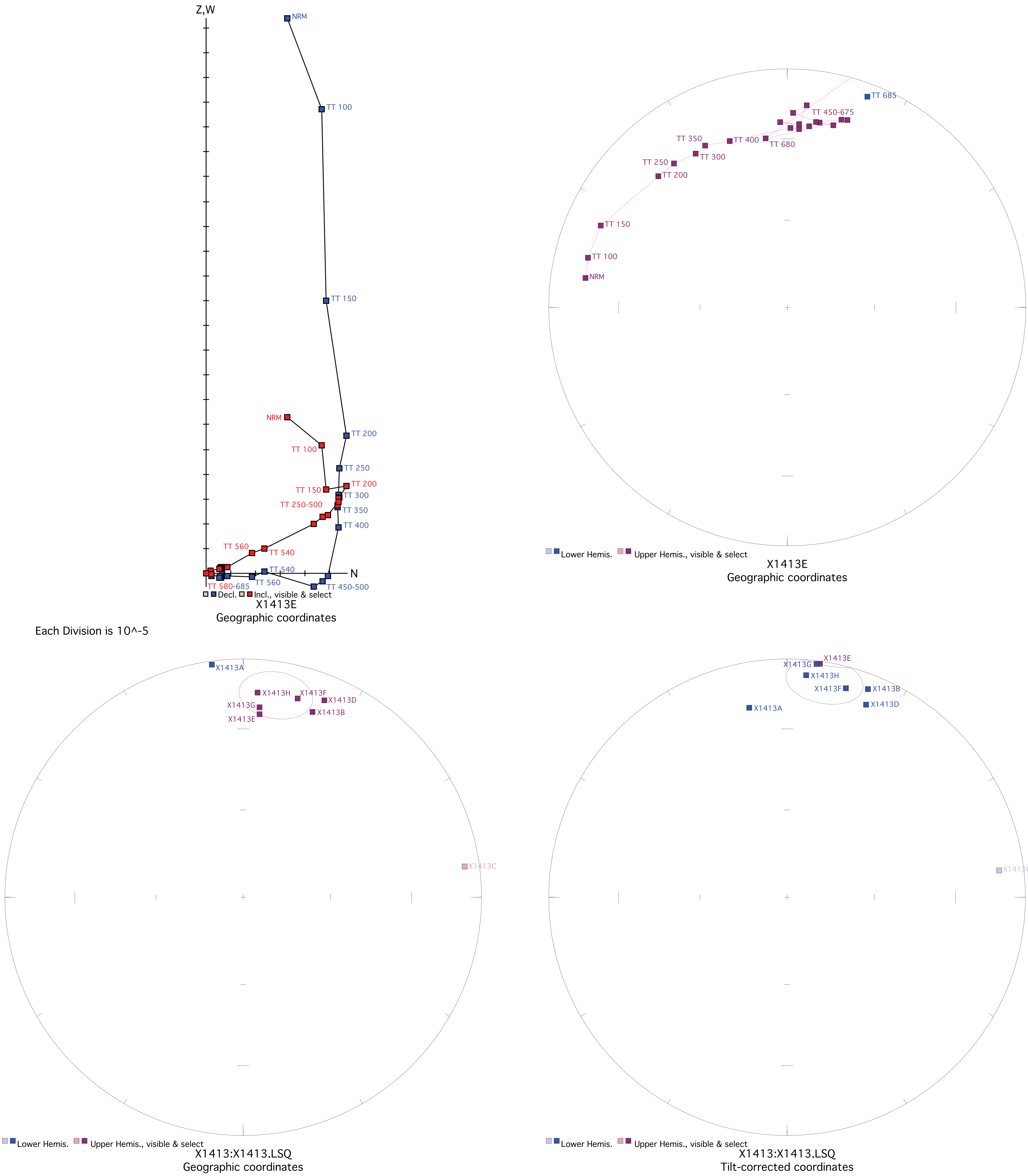

Fisher mean geog. decl.: 9.2, incl.: -14.9 a95 10.0, N: 7

Fisher mean strat. decl.: 9.9, incl.: 8.4 a95 10.0, N: 7

Figure X1414. Panel (a) shows the view of a representative sample in an orthographic projection in geographic coordinates. Blue=horizontal projection, red=vertical projection. Each pair of points represents a measurement step (natural remanent magnetization NRM, liquid nitrogen LN2, or thermal degrees C). Panel (b) shows the same sample in an equal-area projection in geographic coordinates. Blue=lower hemisphere, red=upper hemisphere. Panels (c) and (d) show equal-area projections of the site mean in geographic and tilt-corrected coordinates, respectively. Each point is a ChRM of a sample within the site. Blue=lower hemisphere, red=upper hemisphere. The circle represents the Fisher alpha 95-error of the site mean. Lighter colored points represent sample ChRMs that were not selected into the mean.

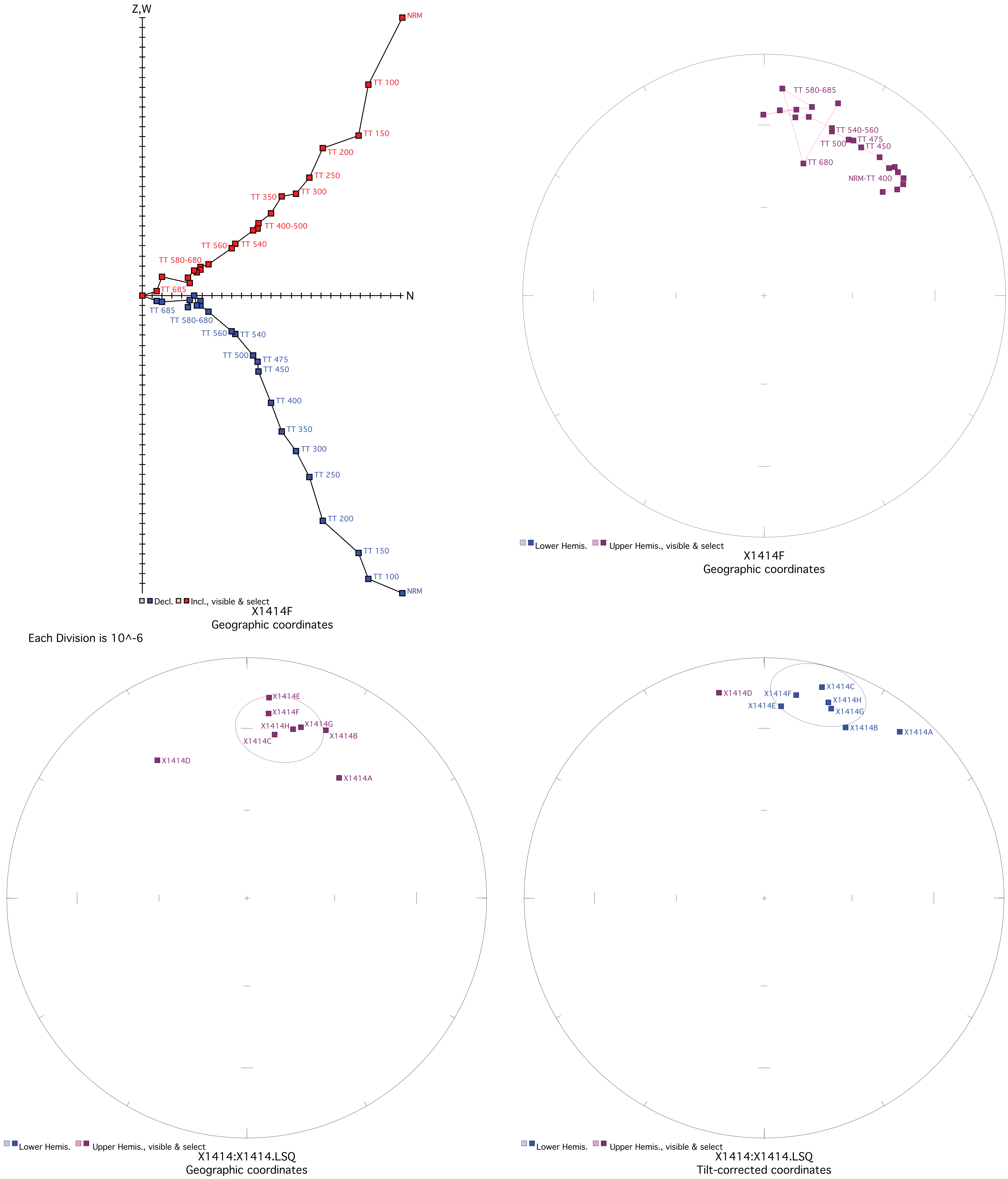

Fisher mean geog. decl.: 10.9, incl.: -28.7 a95 12.9, N: 8

Fisher mean strat. decl.: 15.0, incl.: 12.9 a95 12.9, N: 8

Figure X1415. Panel (a) shows the view of a representative sample in an orthographic projection in geographic coordinates. Blue=horizontal projection, red=vertical projection. Each pair of points represents a measurement step (natural remanent magnetization NRM, liquid nitrogen LN2, or thermal degrees C). Panel (b) shows the same sample in an equal-area projection in geographic coordinates. Blue=lower hemisphere, red=upper hemisphere. Panels (c) and (d) show equal-area projections of the site mean in geographic and tilt-corrected coordinates, respectively. Each point is a ChRM of a sample within the site. Blue=lower hemisphere, red=upper hemisphere. The circle represents the Fisher alpha 95-error of the site mean. Lighter colored points represent sample ChRMs that were not selected into the mean.

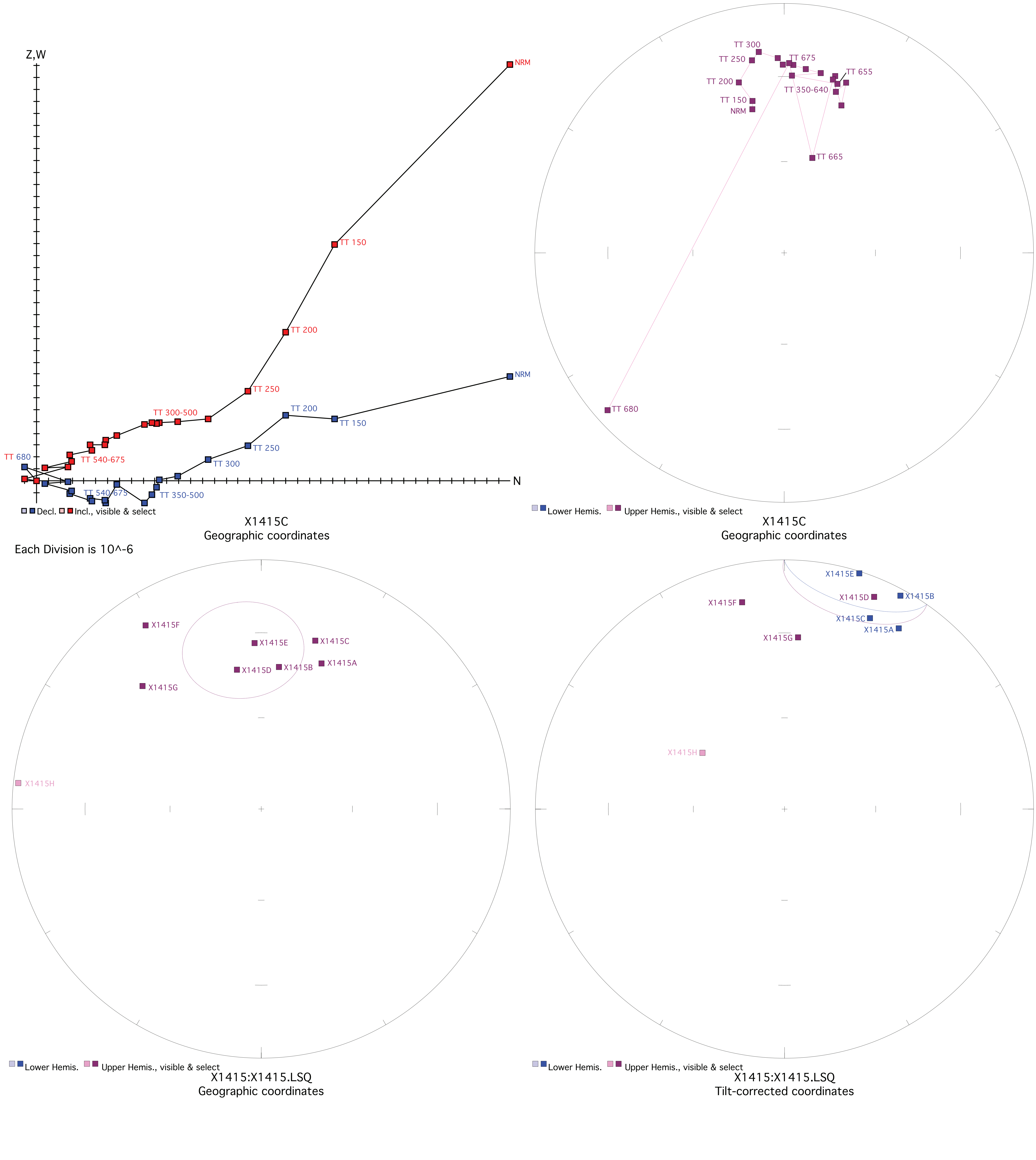

Fisher mean geog. decl.: 353.5, incl.: -35.3 a95 17.7, N: 7

Fisher mean strat. decl.: 17.4, incl.: -2.9 a95 17.7, N: 7

Figure X1417. Panel (a) shows the view of a representative sample in an orthographic projection in geographic coordinates. Blue=horizontal projection, red=vertical projection. Each pair of points represents a measurement step (natural remanent magnetization NRM, liquid nitrogen LN2, or thermal degrees C). Panel (b) shows the same sample in an equal-area projection in geographic coordinates. Blue=lower hemisphere, red=upper hemisphere. Panels (c) and (d) show equal-area projections of the site mean in geographic and tilt-corrected coordinates, respectively. Each point is a ChRM of a sample within the site. Blue=lower hemisphere, red=upper hemisphere. The circle represents the Fisher alpha 95-error of the site mean. Lighter colored points represent sample ChRMs that were not selected into the mean.

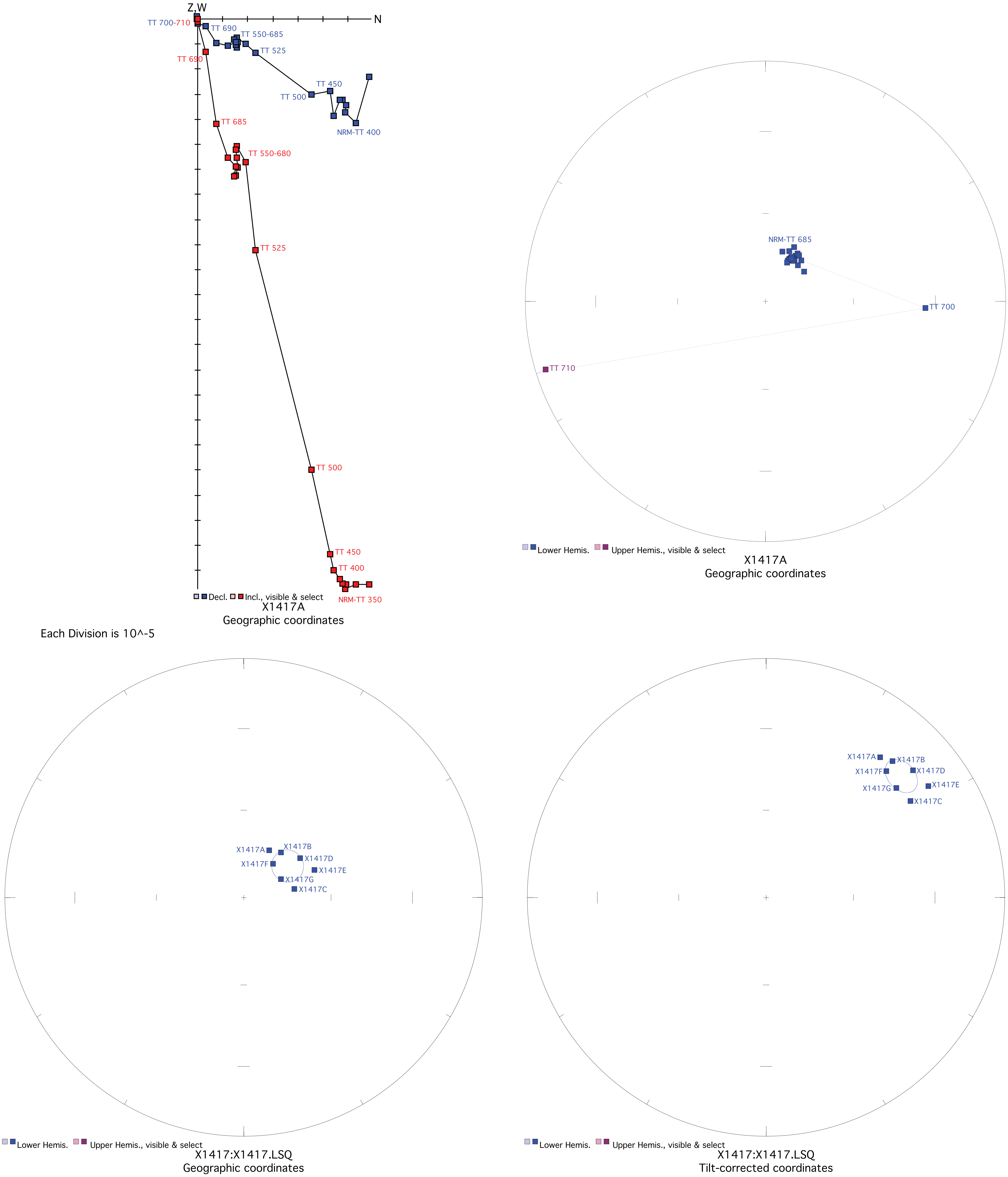

Fisher mean geog. decl.: 54.3, incl.: 71.5 a95 5.4, N: 7

Fisher mean strat. decl.: 48.0, incl.: 24.7 a95 5.4, N: 7

Figure X1418. Panel (a) shows the view of a representative sample in an orthographic projection in geographic coordinates. Blue=horizontal projection, red=vertical projection. Each pair of points represents a measurement step (natural remanent magnetization NRM, liquid nitrogen LN2, or thermal degrees C). Panel (b) shows the same sample in an equal-area projection in geographic coordinates. Blue=lower hemisphere, red=upper hemisphere. Panels (c) and (d) show equal-area projections of the site mean in geographic and tilt-corrected coordinates, respectively. Each point is a ChRM of a sample within the site. Blue=lower hemisphere, red=upper hemisphere. The circle represents the Fisher alpha 95-error of the site mean. Lighter colored points represent sample ChRMs that were not selected into the mean.

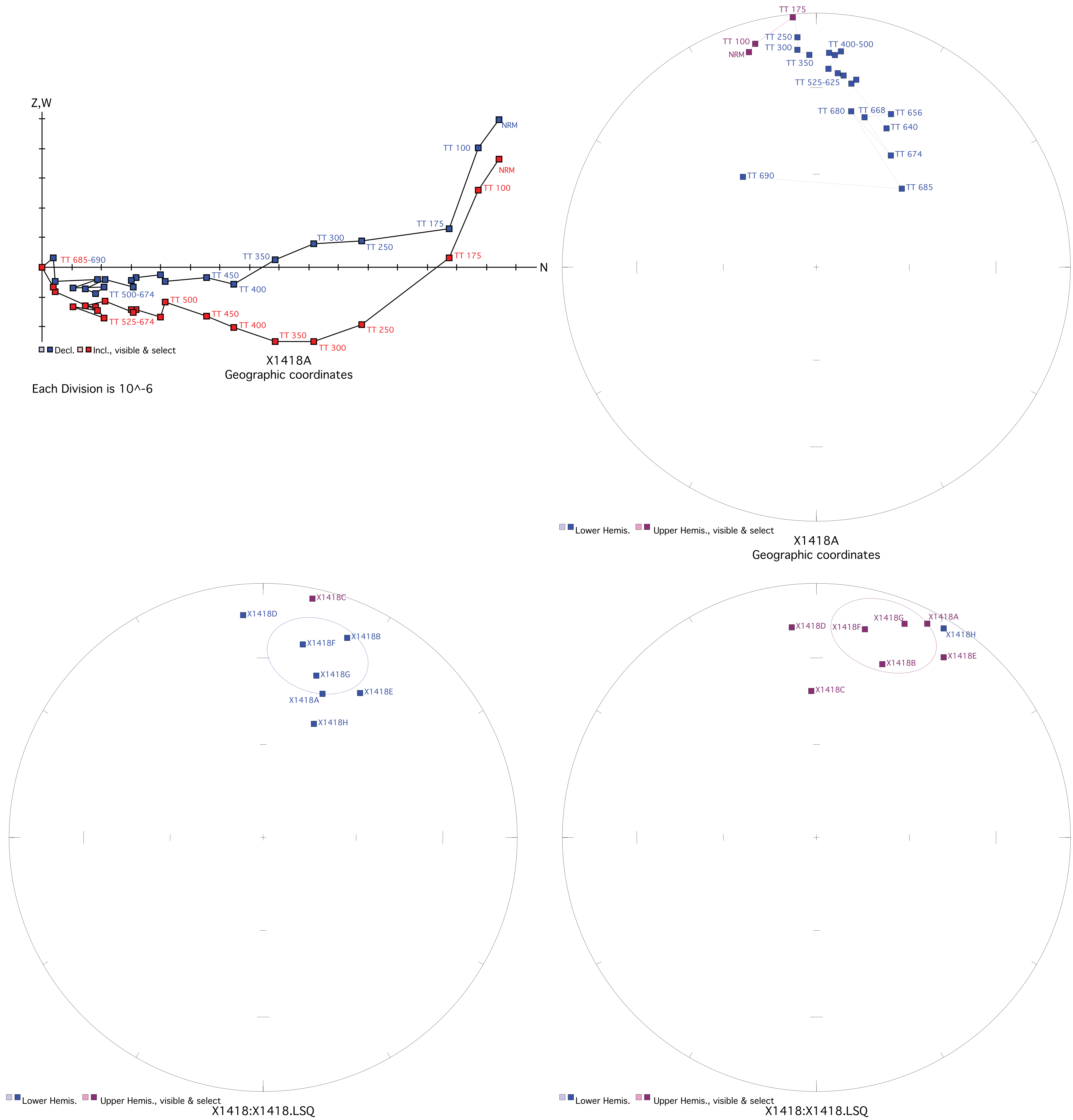

Fisher mean geog. decl.: 16.7, incl.: 25.7 a95 13.9, N: 8

Fisher mean strat. decl.: 18.5, incl.: -16.7 a95 14.0, N: 8

Figure X1422. Panel (a) shows the view of a representative sample in an orthographic projection in geographic coordinates. Blue=horizontal projection, red=vertical projection. Each pair of points represents a measurement step (natural remanent magnetization NRM, liquid nitrogen LN2, or thermal degrees C). Panel (b) shows the same sample in an equal-area projection in geographic coordinates. Blue=lower hemisphere, red=upper hemisphere. Panels (c) and (d) show equal-area projections of the site mean in geographic and tilt-corrected coordinates, respectively. Each point is a ChRM of a sample within the site. Blue=lower hemisphere, red=upper hemisphere. The circle represents the Fisher alpha 95-error of the site mean. Lighter colored points represent sample ChRMs that were not selected into the mean.

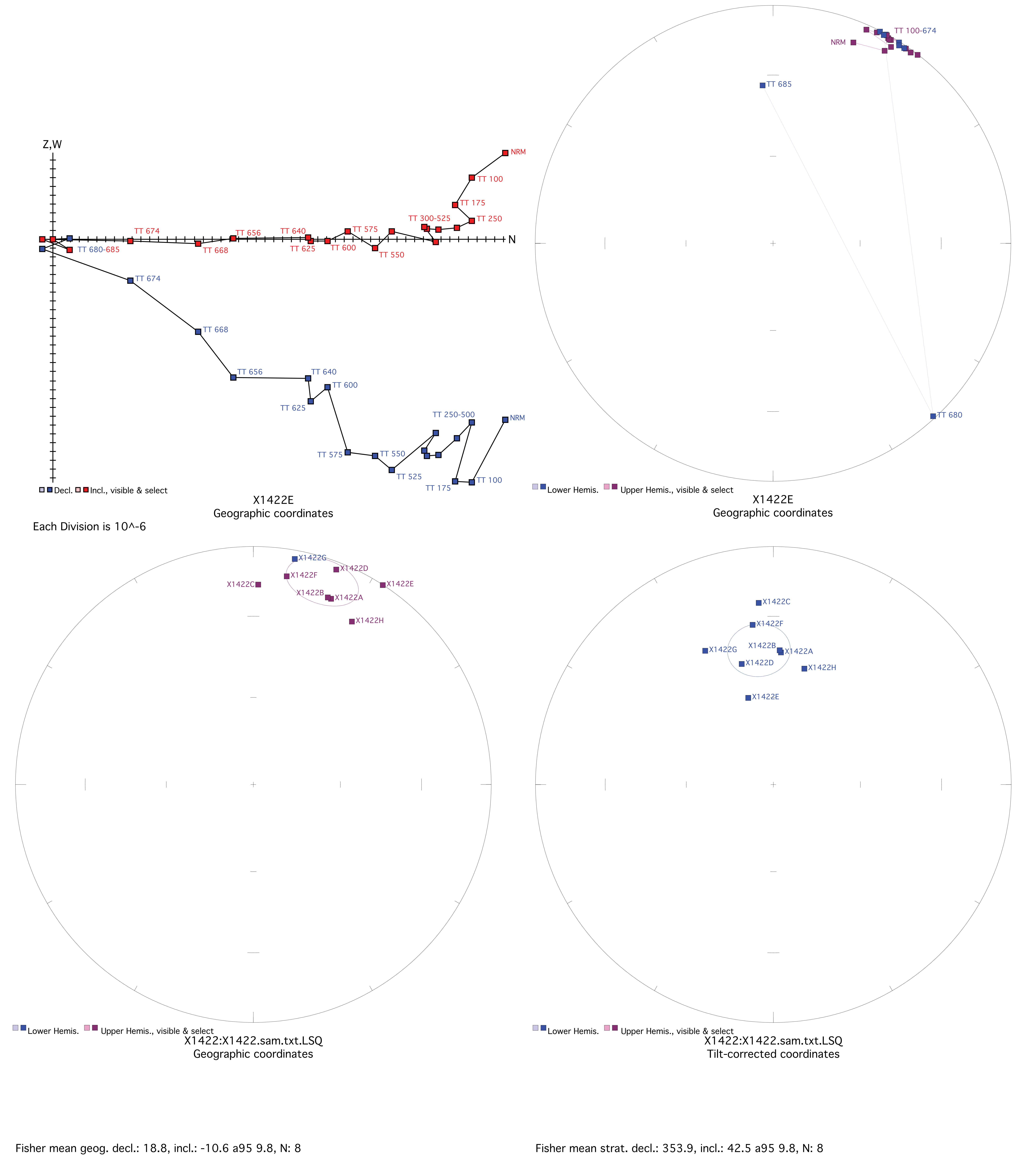

Figure X1512. Panel (a) shows the view of a representative sample in an orthographic projection in geographic coordinates. Blue=horizontal projection, red=vertical projection. Each pair of points represents a measurement step (natural remanent magnetization NRM, liquid nitrogen LN2, or thermal degrees C). Panel (b) shows the same sample in an equal-area projection in geographic coordinates. Blue=lower hemisphere, red=upper hemisphere. Panels (c) and (d) show equal-area projections of the site mean in geographic and tilt-corrected coordinates, respectively. Each point is a ChRM of a sample within the site. Blue=lower hemisphere, red=upper hemisphere. The circle represents the Fisher alpha 95-error of the site mean. Lighter colored points represent sample ChRMs that were not selected into the mean.

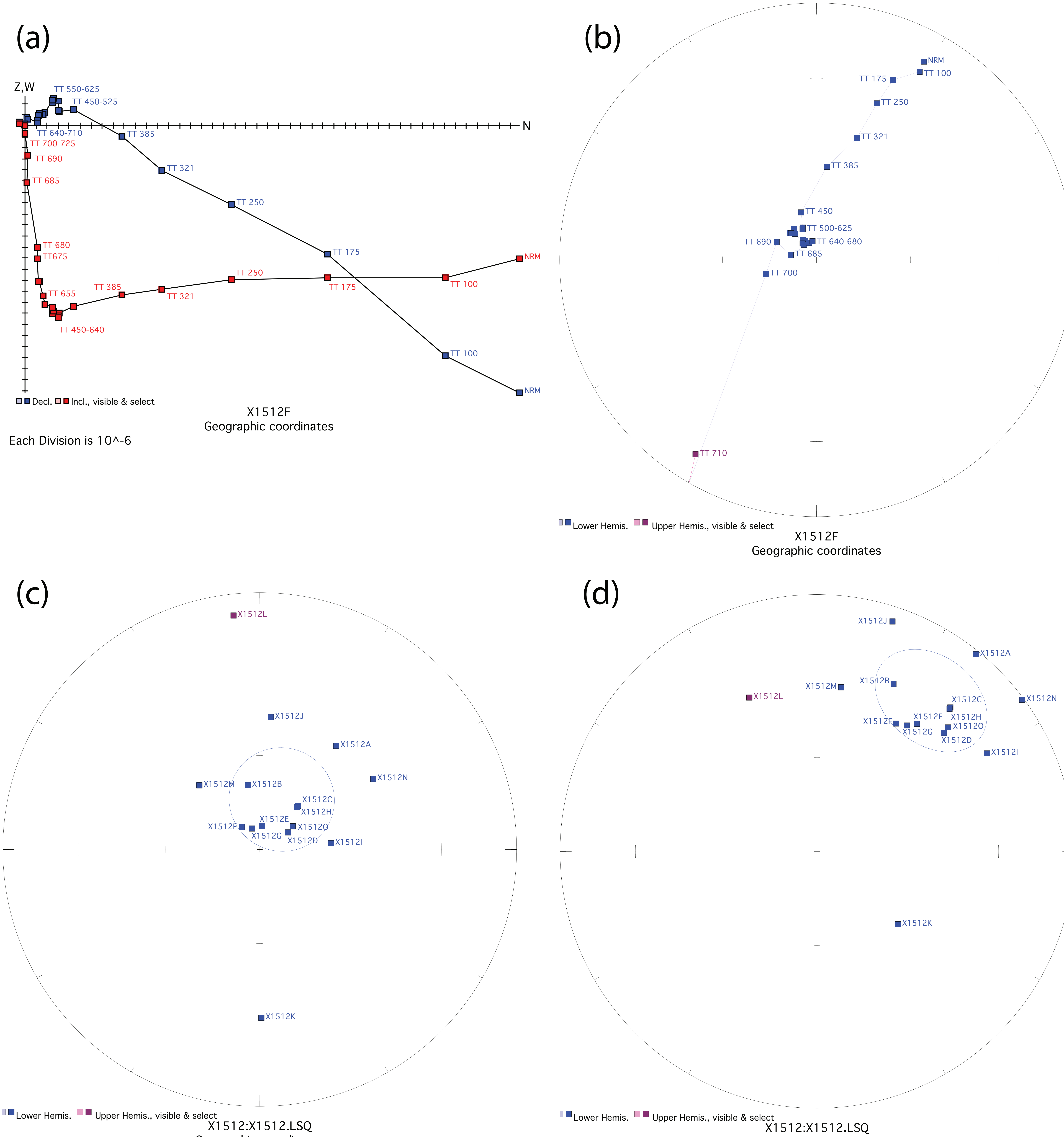

Fisher mean geog. decl.: 23.8, incl.: 72.5 a95 16.5, N: 15

Fisher mean strat. decl.: 37.1, incl.: 26.4 a95 16.5, N: 15

Figure X1513. Panel (a) shows the view of a representative sample in an orthographic projection in geographic coordinates. Blue=horizontal projection, red=vertical projection. Each pair of points represents a measurement step (natural remanent magnetization NRM, liquid nitrogen LN2, or thermal degrees C). Panel (b) shows the same sample in an equal-area projection in geographic coordinates. Blue=lower hemisphere, red=upper hemisphere. Panels (c) and (d) show equal-area projections of the site mean in geographic and tilt-corrected coordinates, respectively. Each point is a ChRM of a sample within the site. Blue=lower hemisphere, red=upper hemisphere. The circle represents the Fisher alpha 95-error of the site mean. Lighter colored points represent sample ChRMs that were not selected into the mean.

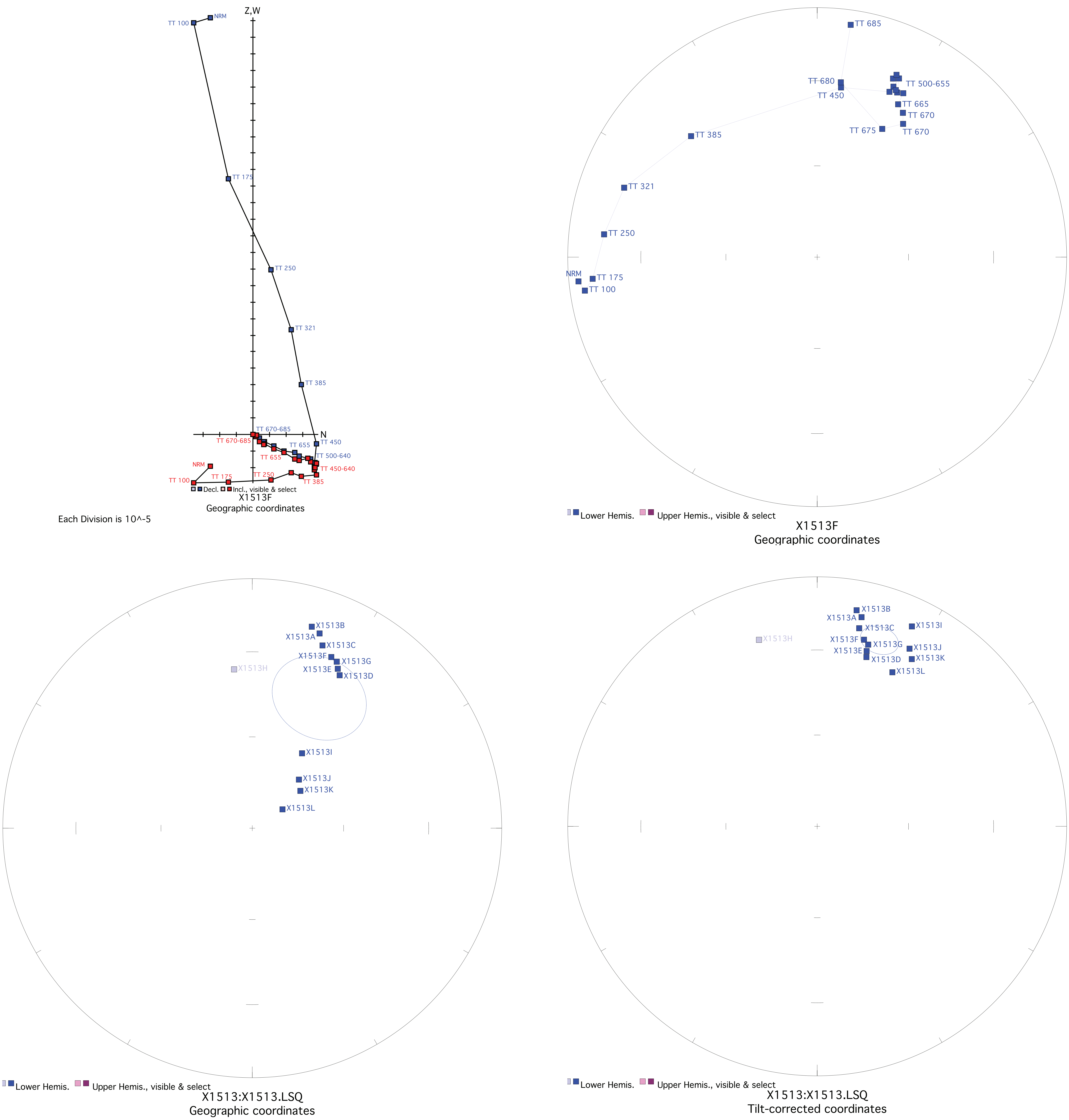

Fisher mean geog. decl.: 27.3, incl.: 40.5 a95 14.4, N: 11

Fisher mean strat. decl.: 18.5, incl.: 22.4 a95 5.3, N: 11

Figure X1514. Panel (a) shows the view of a representative sample in an orthographic projection in geographic coordinates. Blue=horizontal projection, red=vertical projection. Each pair of points represents a measurement step (natural remanent magnetization NRM, liquid nitrogen LN2, or thermal degrees C). Panel (b) shows the same sample in an equal-area projection in geographic coordinates. Blue=lower hemisphere, red=upper hemisphere. Panels (c) and (d) show equal-area projections of the site mean in geographic and tilt-corrected coordinates, respectively. Each point is a ChRM of a sample within the site. Blue=lower hemisphere, red=upper hemisphere. The circle represents the Fisher alpha 95-error of the site mean. Lighter colored points represent sample ChRMs that were not selected into the mean.

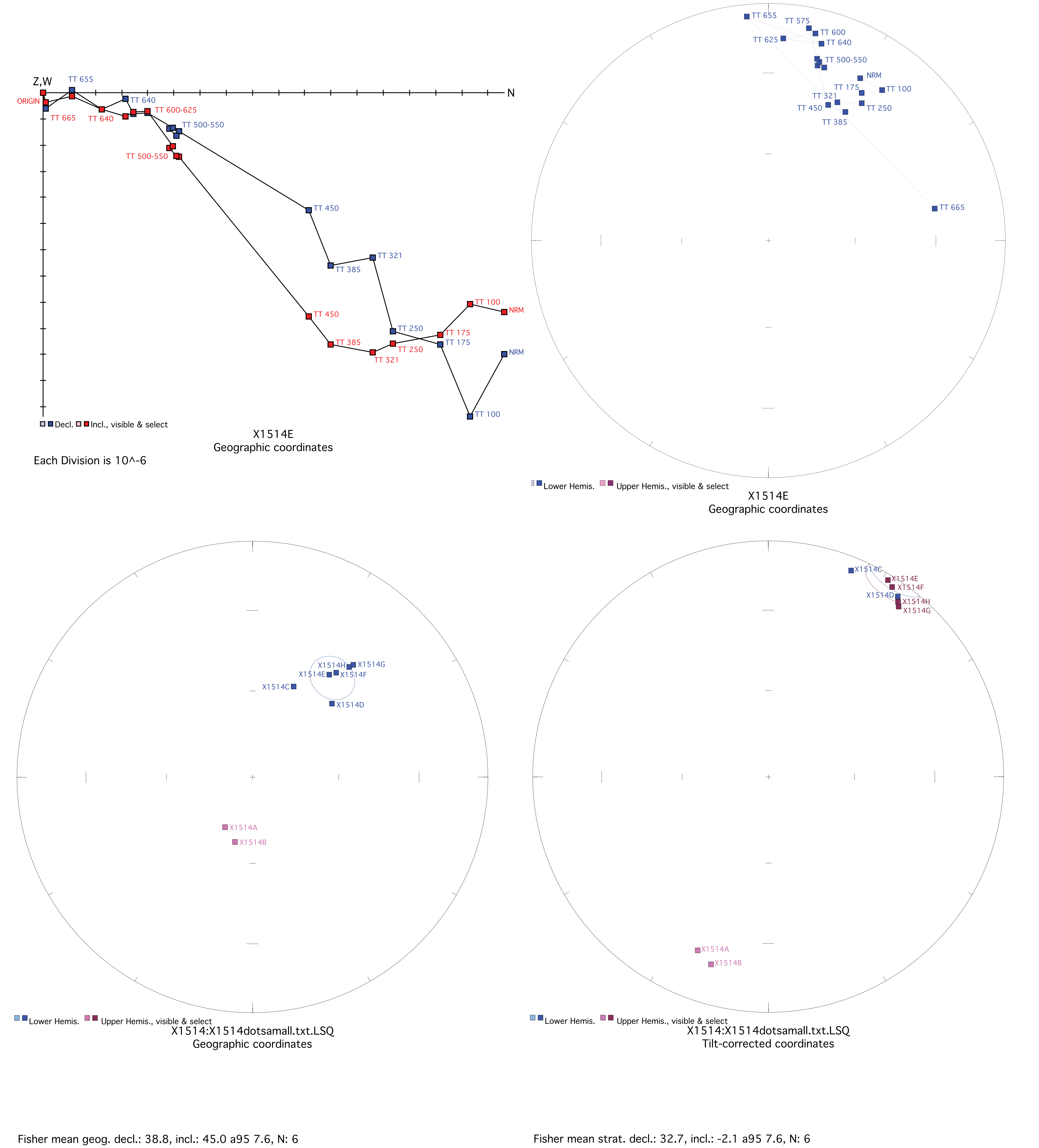

Figure X1515. Panel (a) shows the view of a representative sample in an orthographic projection in geographic coordinates. Blue=horizontal projection, red=vertical projection. Each pair of points represents a measurement step (natural remanent magnetization NRM, liquid nitrogen LN2, or thermal degrees C). Panel (b) shows the same sample in an equal-area projection in geographic coordinates. Blue=lower hemisphere, red=upper hemisphere. Panels (c) and (d) show equal-area projections of the site mean in geographic and tilt-corrected coordinates, respectively. Each point is a ChRM of a sample within the site. Blue=lower hemisphere, red=upper hemisphere. The circle represents the Fisher alpha 95-error of the site mean. Lighter colored points represent sample ChRMs that were not selected into the mean.

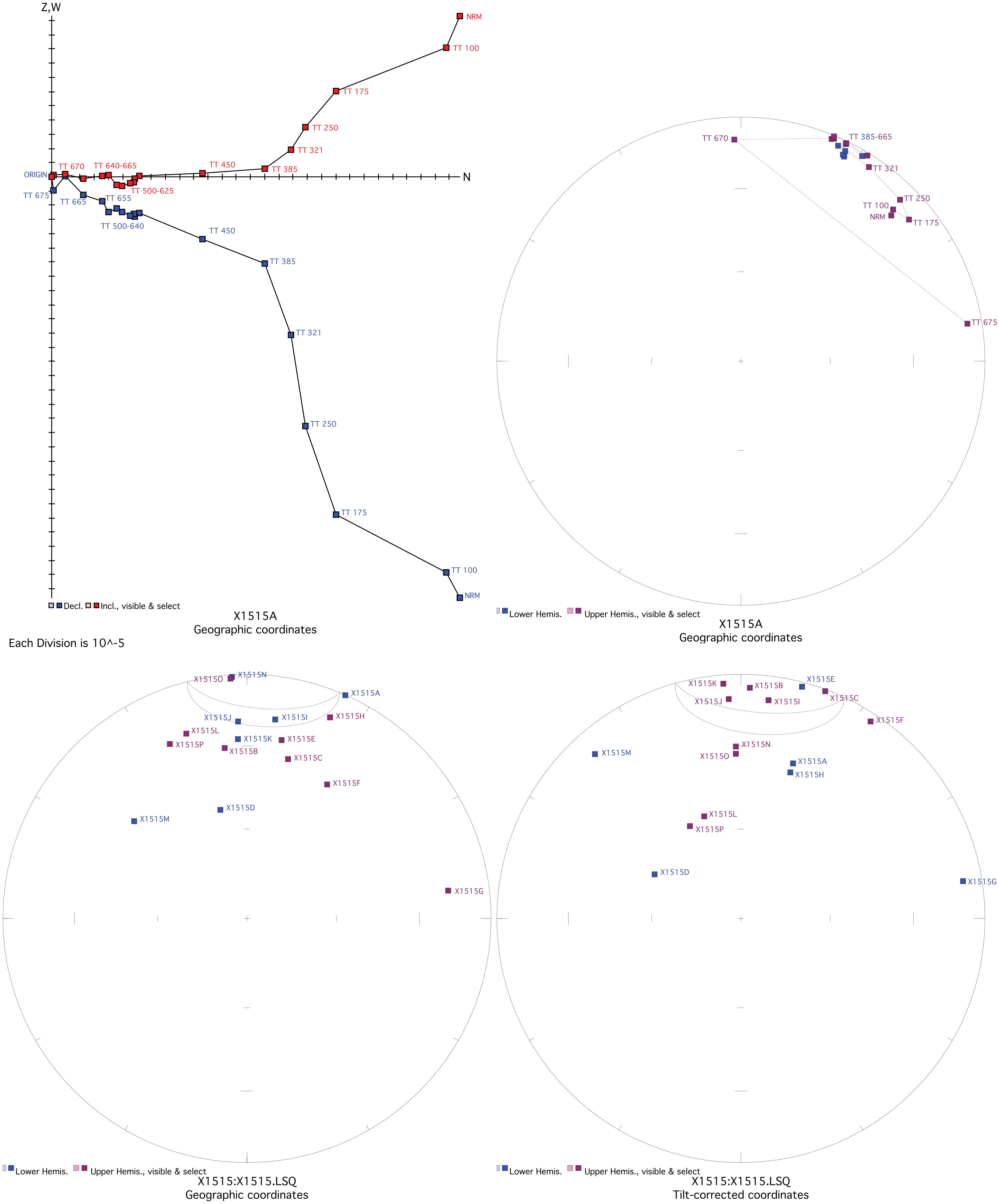

Fisher mean geog. decl.: 4.1, incl.: -3.7 a95 18.5, N: 16

Fisher mean strat. decl.: 4.8, incl.: -4.4 a95 20.8, N: 16

Figure X1516. Panel (a) shows the view of a representative sample in an orthographic projection in geographic coordinates. Blue=horizontal projection, red=vertical projection. Each pair of points represents a measurement step (natural remanent magnetization NRM, liquid nitrogen LN2, or thermal degrees C). Panel (b) shows the same sample in an equal-area projection in geographic coordinates. Blue=lower hemisphere, red=upper hemisphere. Panels (c) and (d) show equal-area projections of the site mean in geographic and tilt-corrected coordinates, respectively. Each point is a ChRM of a sample within the site. Blue=lower hemisphere, red=upper hemisphere. The circle represents the Fisher alpha 95-error of the site mean. Lighter colored points represent sample ChRMs that were not selected into the mean.

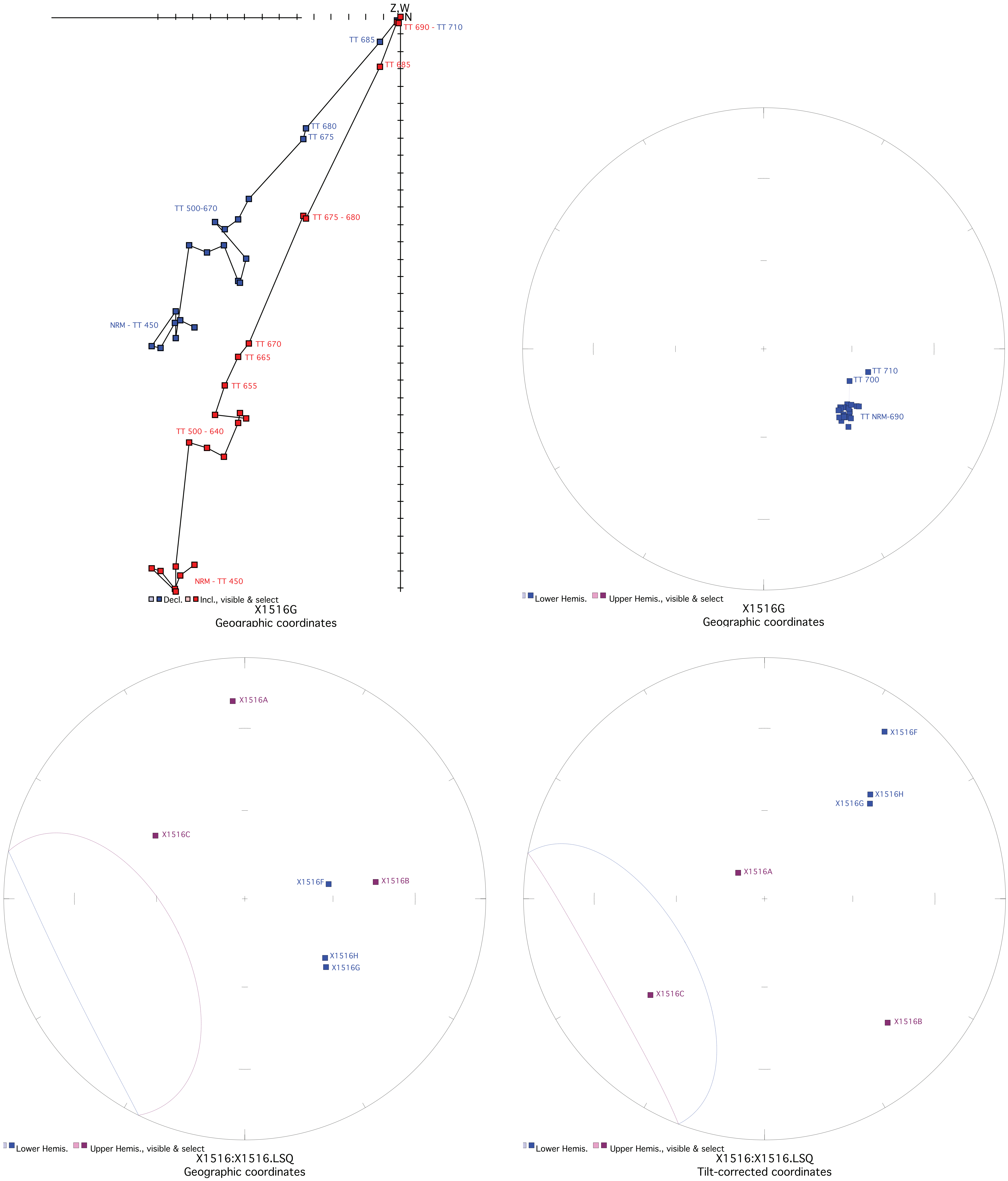

Fisher mean geog. decl.: 63.8, incl.: 22.0 a95 137.3, N: 6

Fisher mean strat. decl.: 60.9, incl.: -16.5 a95 137.3, N: 6

Figure X1546. Panel (a) shows the view of a representative sample in an orthographic projection in geographic coordinates. Blue=horizontal projection, red=vertical projection. Each pair of points represents a measurement step (natural remanent magnetization NRM, liquid nitrogen LN2, or thermal degrees C). Panel (b) shows the same sample in an equal-area projection in geographic coordinates. Blue=lower hemisphere, red=upper hemisphere. Panels (c) and (d) show equal-area projections of the site mean in geographic and tilt-corrected coordinates, respectively. Each point is a ChRM of a sample within the site. Blue=lower hemisphere, red=upper hemisphere. The circle represents the Fisher alpha 95-error of the site mean. Lighter colored points represent sample ChRMs that were not selected into the mean.

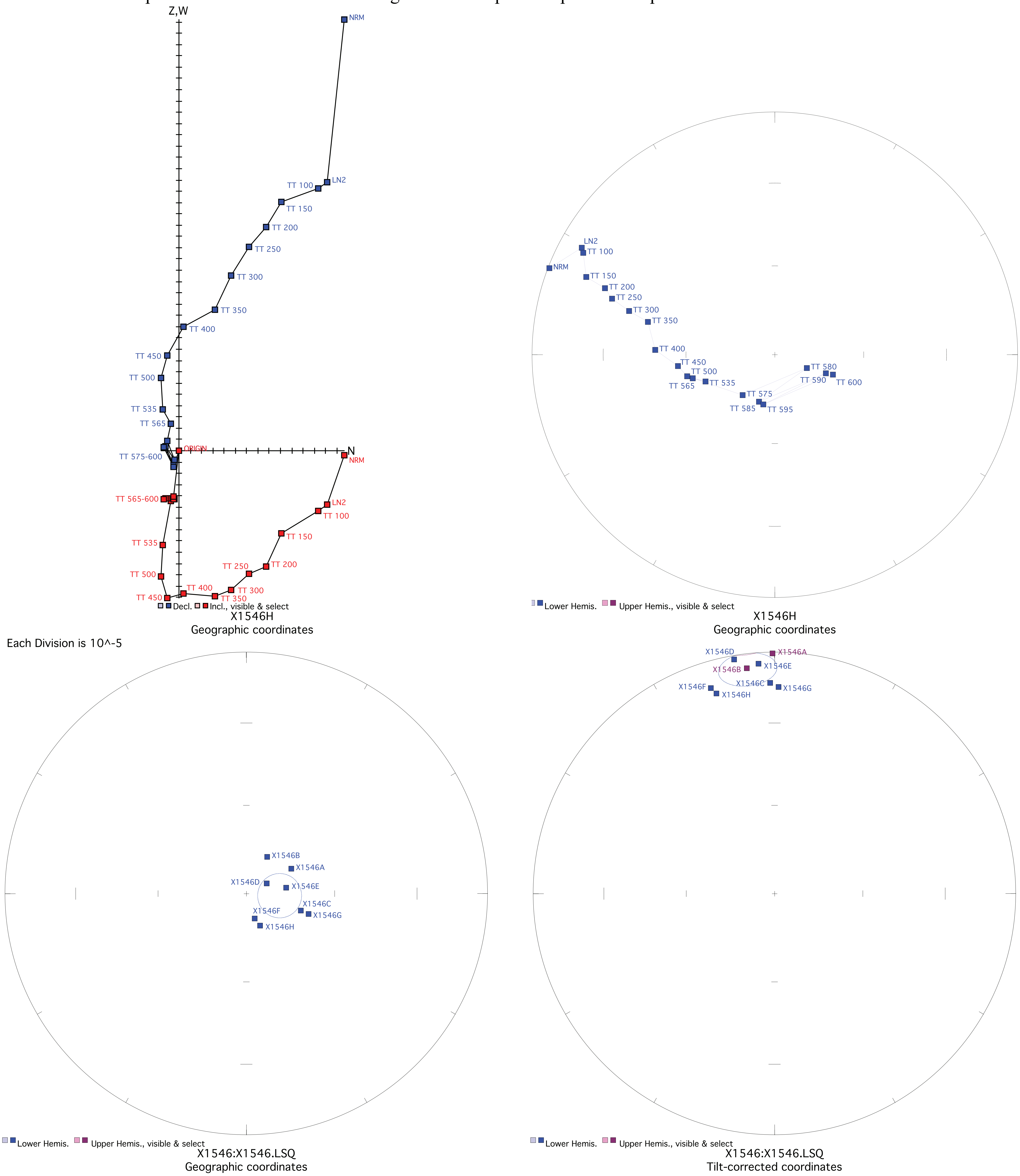

Fisher mean geog. decl.: 93.6, incl.: 78.8 a95 7.4, N: 8

Fisher mean strat. decl.: 353.2, incl.: 7.0 a95 7.4, N: 8

Figure X1403. Panel (a) shows the view of a representative sample in an orthographic projection in geographic coordinates. Blue=horizontal projection, red=vertical projection. Each pair of points represents a measurement step (natural remanent magnetization NRM, liquid nitrogen LN2, or thermal degrees C). Panel (b) shows the same sample in an equal-area projection in geographic coordinates. Blue=lower hemisphere, red=upper hemisphere. Panels (c) and (d) show equal-area projections of the site mean in geographic and tilt-corrected coordinates, respectively. Each point is a ChRM of a sample within the site. Blue=lower hemisphere, red=upper hemisphere. The circle represents the Fisher alpha 95-error of the site mean. Lighter colored points represent sample ChRMs that were not selected into the mean.

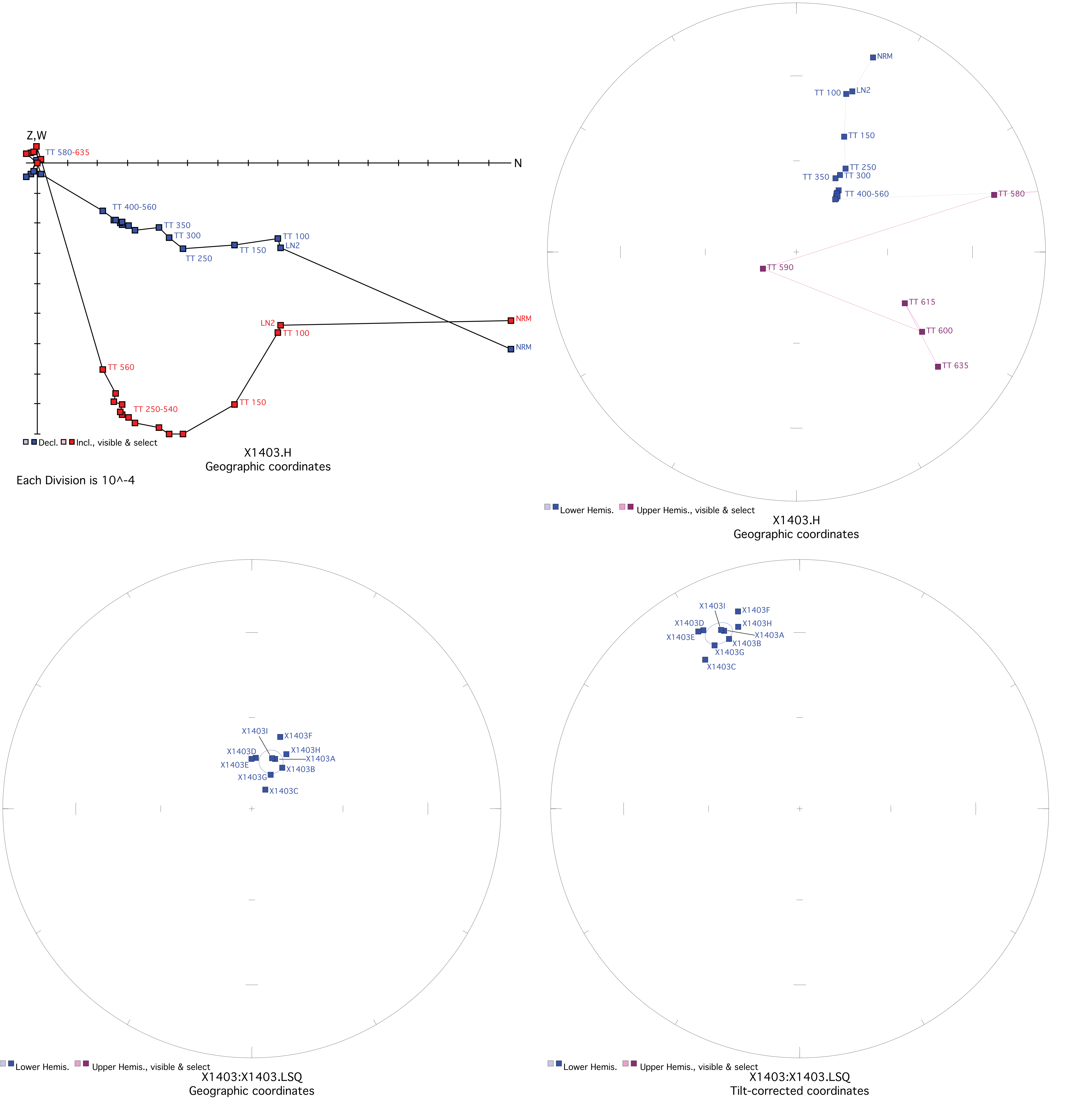

Fisher mean geog. decl.: 22.3, incl.: 73.5 a95 3.9, N: 9

Fisher mean strat. decl.: 335.2, incl.: 23.5 a95 3.9, N: 9

Figure X1404. Panel (a) shows the view of a representative sample in an orthographic projection in geographic coordinates. Blue=horizontal projection, red=vertical projection. Each pair of points represents a measurement step (natural remanent magnetization NRM, liquid nitrogen LN2, or thermal degrees C). Panel (b) shows the same sample in an equal-area projection in geographic coordinates. Blue=lower hemisphere, red=upper hemisphere. Panels (c) and (d) show equal-area projections of the site mean in geographic and tilt-corrected coordinates, respectively. Each point is a ChRM of a sample within the site. Blue=lower hemisphere, red=upper hemisphere. The circle represents the Fisher alpha 95-error of the site mean. Lighter colored points represent sample ChRMs that were not selected into the mean.

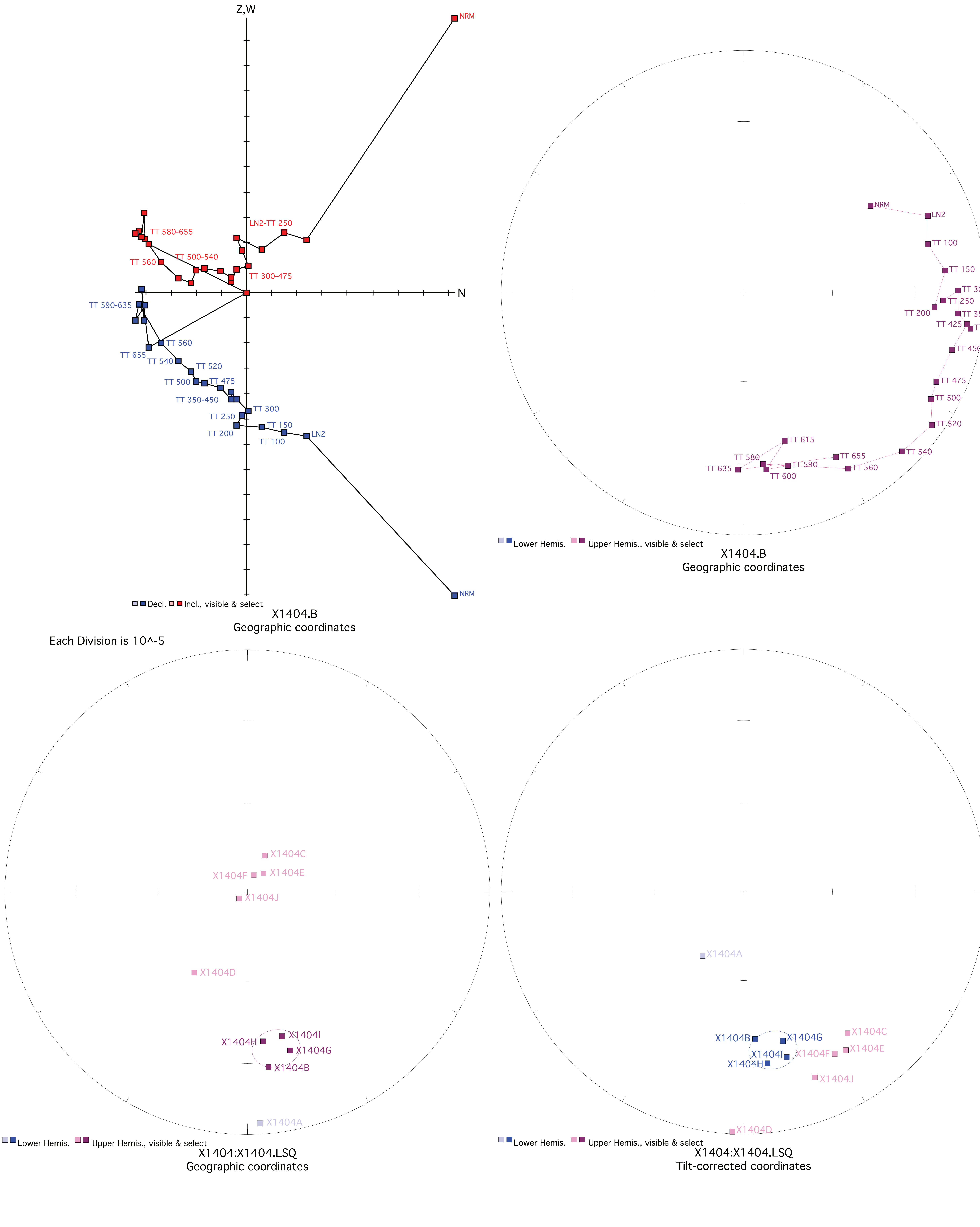

Fisher mean geog. decl.: 169.7, incl.: -34.5 a95 7.1, N: 4

Fisher mean strat. decl.: 169.5, incl.: 33.8 a95 7.1, N: 4

Figure X1405. Panel (a) shows the view of a representative sample in an orthographic projection in geographic coordinates. Blue=horizontal projection, red=vertical projection. Each pair of points represents a measurement step (natural remanent magnetization NRM, liquid nitrogen LN2, or thermal degrees C). Panel (b) shows the same sample in an equal-area projection in geographic coordinates. Blue=lower hemisphere, red=upper hemisphere. Panels (c) and (d) show equal-area projections of the site mean in geographic and tilt-corrected coordinates, respectively. Each point is a ChRM of a sample within the site. Blue=lower hemisphere, red=upper hemisphere. The circle represents the Fisher alpha 95-error of the site mean. Lighter colored points represent sample ChRMs that were not selected into the mean.

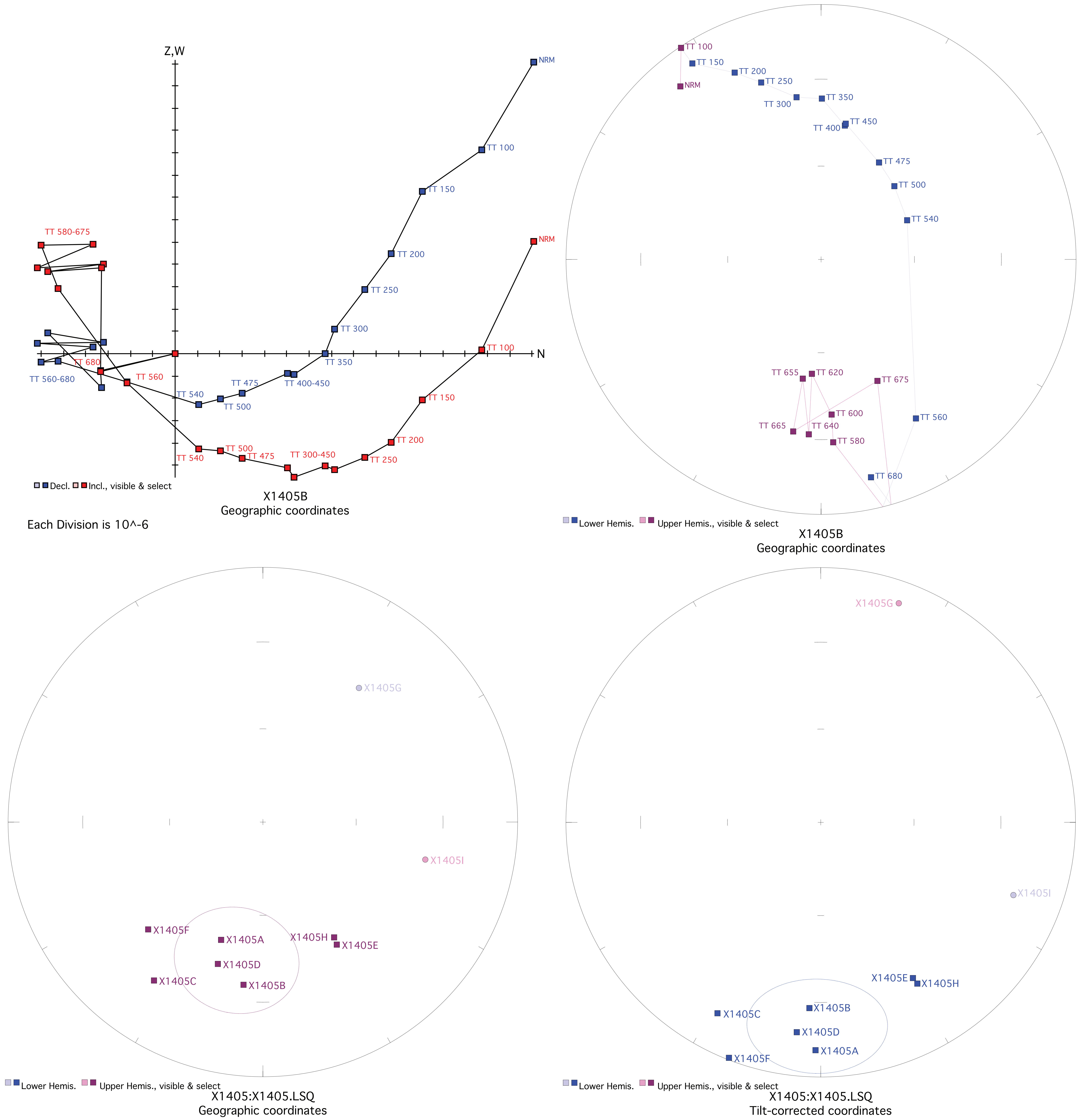

Fisher mean geog. decl.: 190.8, incl.: -43.4 a95 18.4, N: 7

Fisher mean strat. decl.: 181.0, incl.: 20.0 a95 18.4, N: 7

Figure X1406. Panel (a) shows the view of a representative sample in an orthographic projection in geographic coordinates. Blue=horizontal projection, red=vertical projection. Each pair of points represents a measurement step (natural remanent magnetization NRM, liquid nitrogen LN2, or thermal degrees C). Panel (b) shows the same sample in an equal-area projection in geographic coordinates. Blue=lower hemisphere, red=upper hemisphere. Panels (c) and (d) show equal-area projections of the site mean in geographic and tilt-corrected coordinates, respectively. Each point is a ChRM of a sample within the site. Blue=lower hemisphere, red=upper hemisphere. The circle represents the Fisher alpha 95-error of the site mean. Lighter colored points represent sample ChRMs that were not selected into the mean.

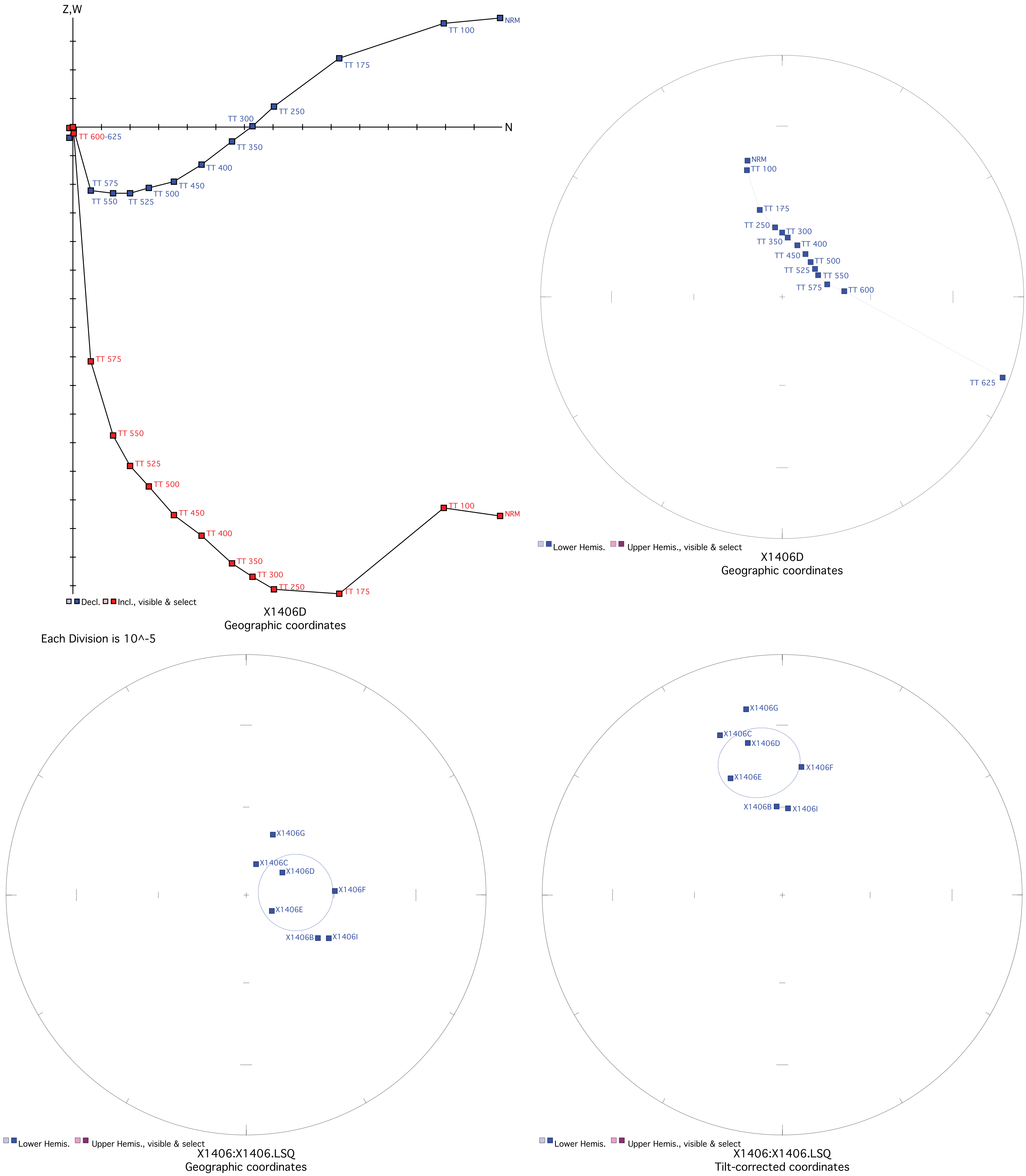

Fisher mean geog. decl.: 87.1, incl.: 73.1 a95 12.8, N: 7

Fisher mean strat. decl.: 350.0, incl.: 43.1 a95 12.8, N: 7

Figure X1407. Panel (a) shows the view of a representative sample in an orthographic projection in geographic coordinates. Blue=horizontal projection, red=vertical projection. Each pair of points represents a measurement step (natural remanent magnetization NRM, liquid nitrogen LN2, or thermal degrees C). Panel (b) shows the same sample in an equal-area projection in geographic coordinates. Blue=lower hemisphere, red=upper hemisphere. Panels (c) and (d) show equal-area projections of the site mean in geographic and tilt-corrected coordinates, respectively. Each point is a ChRM of a sample within the site. Blue=lower hemisphere, red=upper hemisphere. The circle represents the Fisher alpha 95-error of the site mean. Lighter colored points represent sample ChRMs that were not selected into the mean.

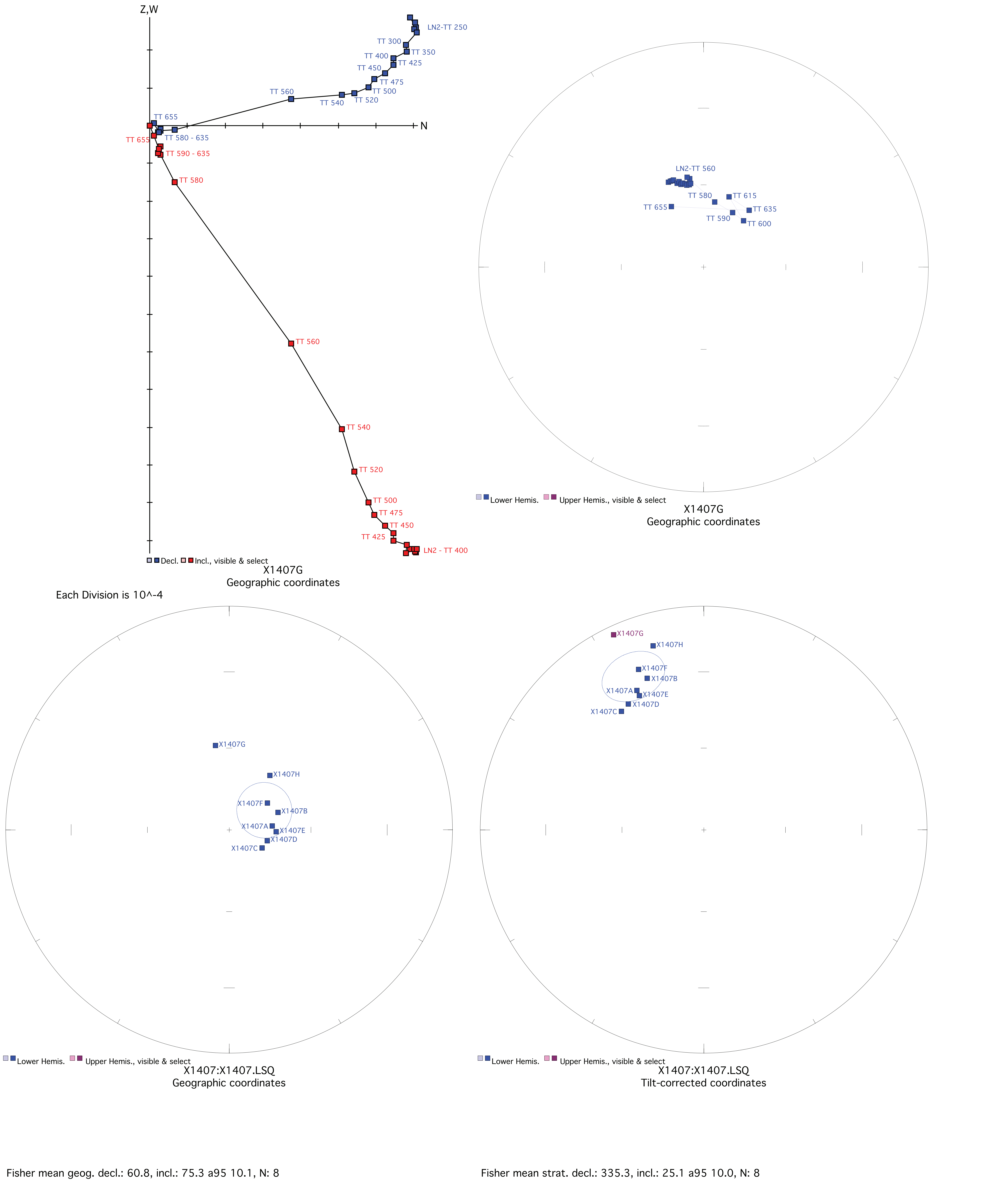

Figure X1408. Panel (a) shows the view of a representative sample in an orthographic projection in geographic coordinates. Blue=horizontal projection, red=vertical projection. Each pair of points represents a measurement step (natural remanent magnetization NRM, liquid nitrogen LN2, or thermal degrees C). Panel (b) shows the same sample in an equal-area projection in geographic coordinates. Blue=lower hemisphere, red=upper hemisphere. Panels (c) and (d) show equal-area projections of the site mean in geographic and tilt-corrected coordinates, respectively. Each point is a ChRM of a sample within the site. Blue=lower hemisphere, red=upper hemisphere. The circle represents the Fisher alpha 95-error of the site mean. Lighter colored points represent sample ChRMs that were not selected into the mean.

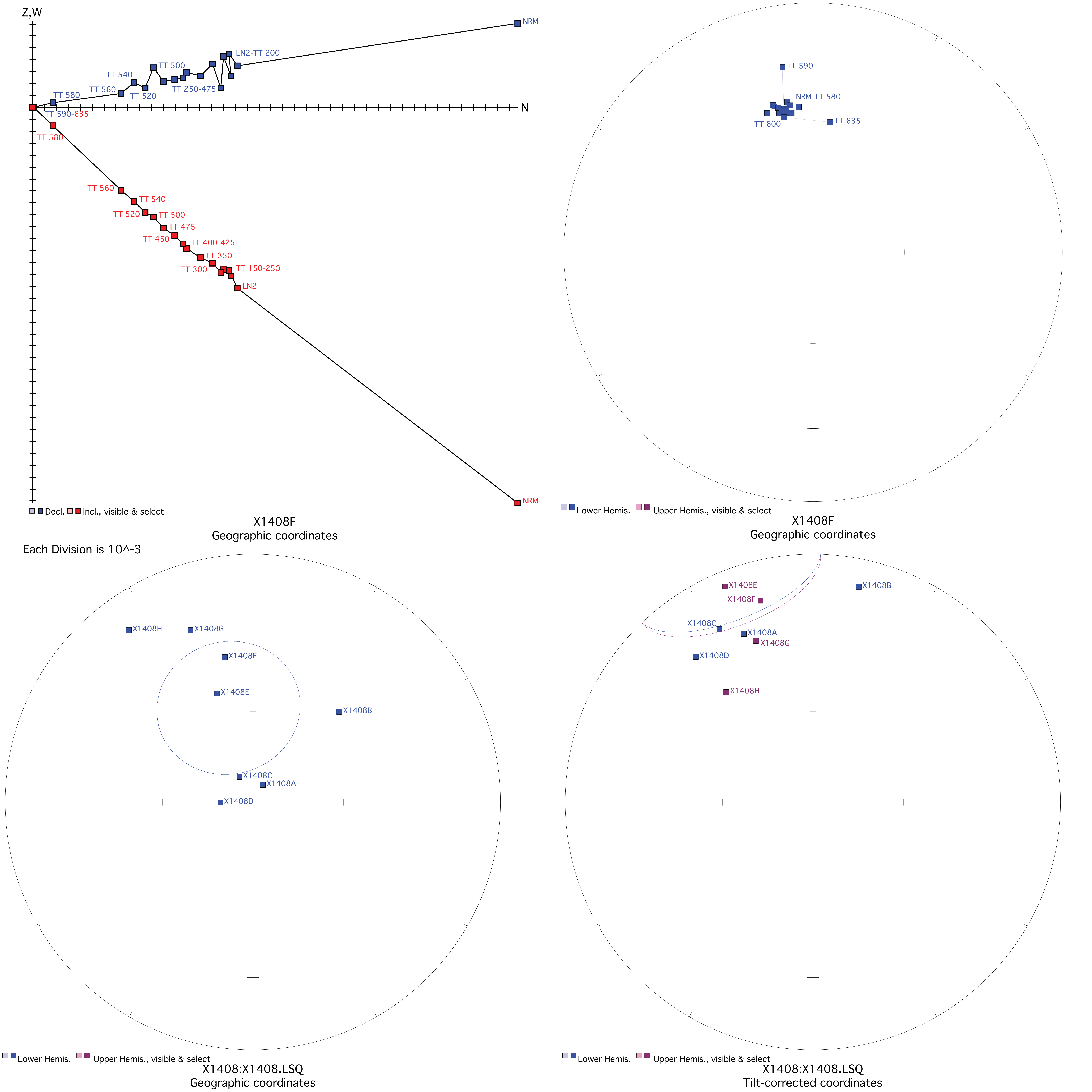

Fisher mean geog. decl.: 345.5, incl.: 57.0 a95 22.7, N: 8

Fisher mean strat. decl.: 339.1, incl.: -1.2 a95 22.7, N: 8

Figure X1410. Panel (a) shows the view of a representative sample in an orthographic projection in geographic coordinates. Blue=horizontal projection, red=vertical projection. Each pair of points represents a measurement step (natural remanent magnetization NRM, liquid nitrogen LN2, or thermal degrees C). Panel (b) shows the same sample in an equal-area projection in geographic coordinates. Blue=lower hemisphere, red=upper hemisphere. Panels (c) and (d) show equal-area projections of the site mean in geographic and tilt-corrected coordinates, respectively. Each point is a ChRM of a sample within the site. Blue=lower hemisphere, red=upper hemisphere. The circle represents the Fisher alpha 95-error of the site mean. Lighter colored points represent sample ChRMs that were not selected into the mean.

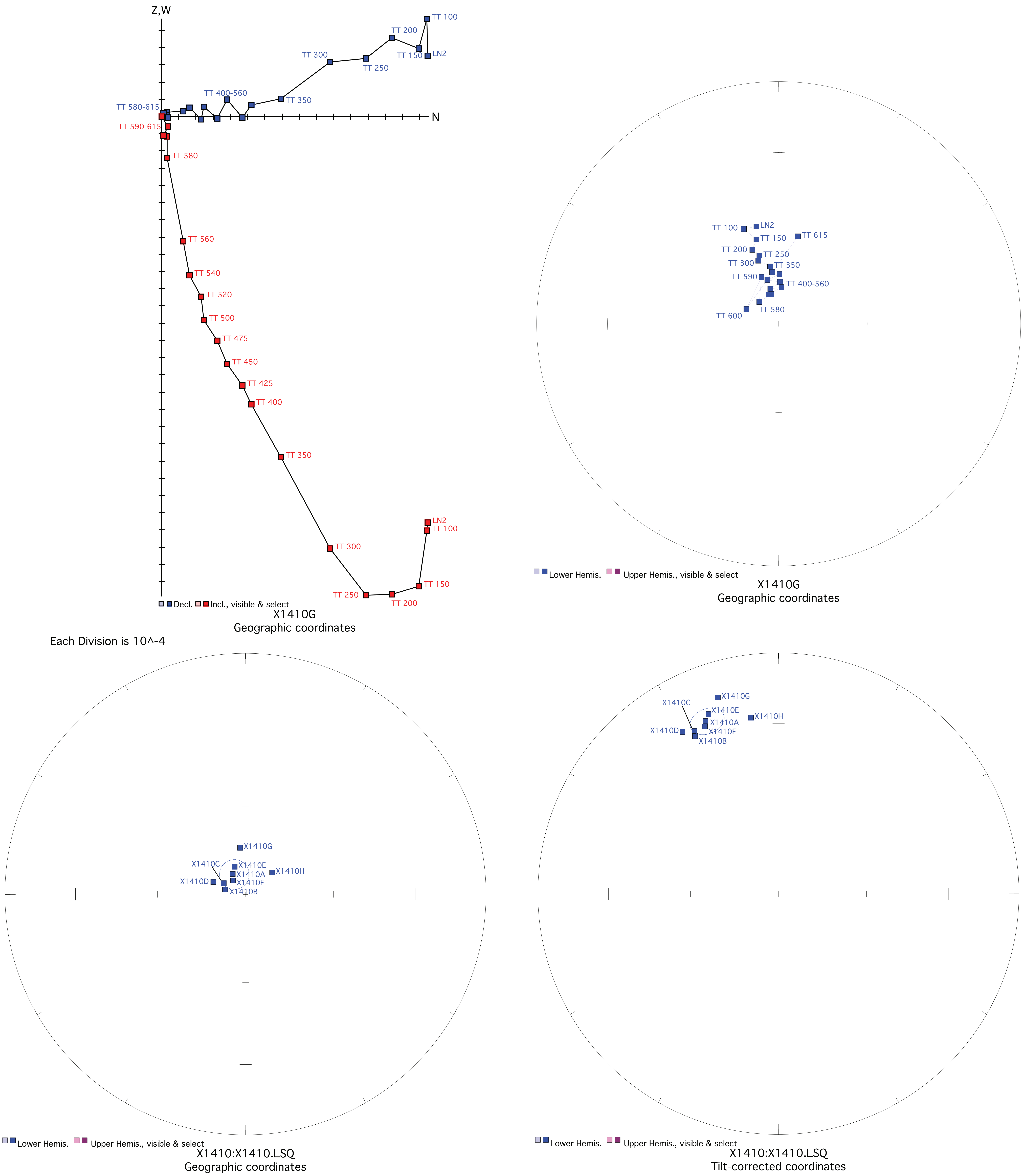

Fisher mean geog. decl.: 330.5, incl.: 82.3 a95 5.0, N: 8

Fisher mean strat. decl.: 337.5, incl.: 23.4 a95 5.0, N: 8

Figure X1412. Panel (a) shows the view of a representative sample in an orthographic projection in geographic coordinates. Blue=horizontal projection, red=vertical projection. Each pair of points represents a measurement step (natural remanent magnetization NRM, liquid nitrogen LN2, or thermal degrees C). Panel (b) shows the same sample in an equal-area projection in geographic coordinates. Blue=lower hemisphere, red=upper hemisphere. Panels (c) and (d) show equal-area projections of the site mean in geographic and tilt-corrected coordinates, respectively. Each point is a ChRM of a sample within the site. Blue=lower hemisphere, red=upper hemisphere. The circle represents the Fisher alpha 95-error of the site mean. Lighter colored points represent sample ChRMs that were not selected into the mean.

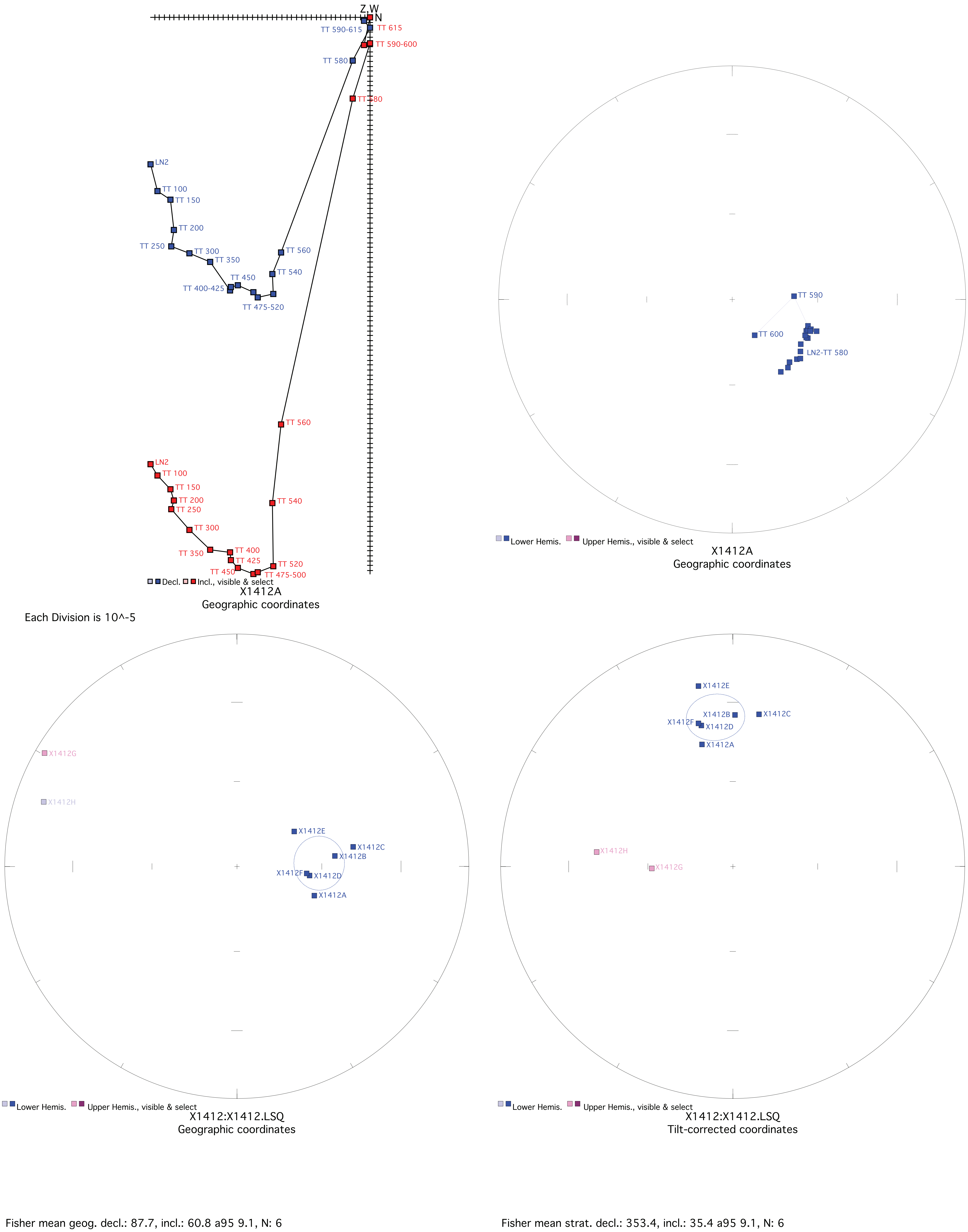

Figure X1547. Panel (a) shows the view of a representative sample in an orthographic projection in geographic coordinates. Blue=horizontal projection, red=vertical projection. Each pair of points represents a measurement step (natural remanent magnetization NRM, liquid nitrogen LN2, or thermal degrees C). Panel (b) shows the same sample in an equal-area projection in geographic coordinates. Blue=lower hemisphere, red=upper hemisphere. Panels (c) and (d) show equal-area projections of the site mean in geographic and tilt-corrected coordinates, respectively. Each point is a ChRM of a sample within the site. Blue=lower hemisphere, red=upper hemisphere. The circle represents the Fisher alpha 95-error of the site mean. Lighter colored points represent sample ChRMs that were not selected into the mean.

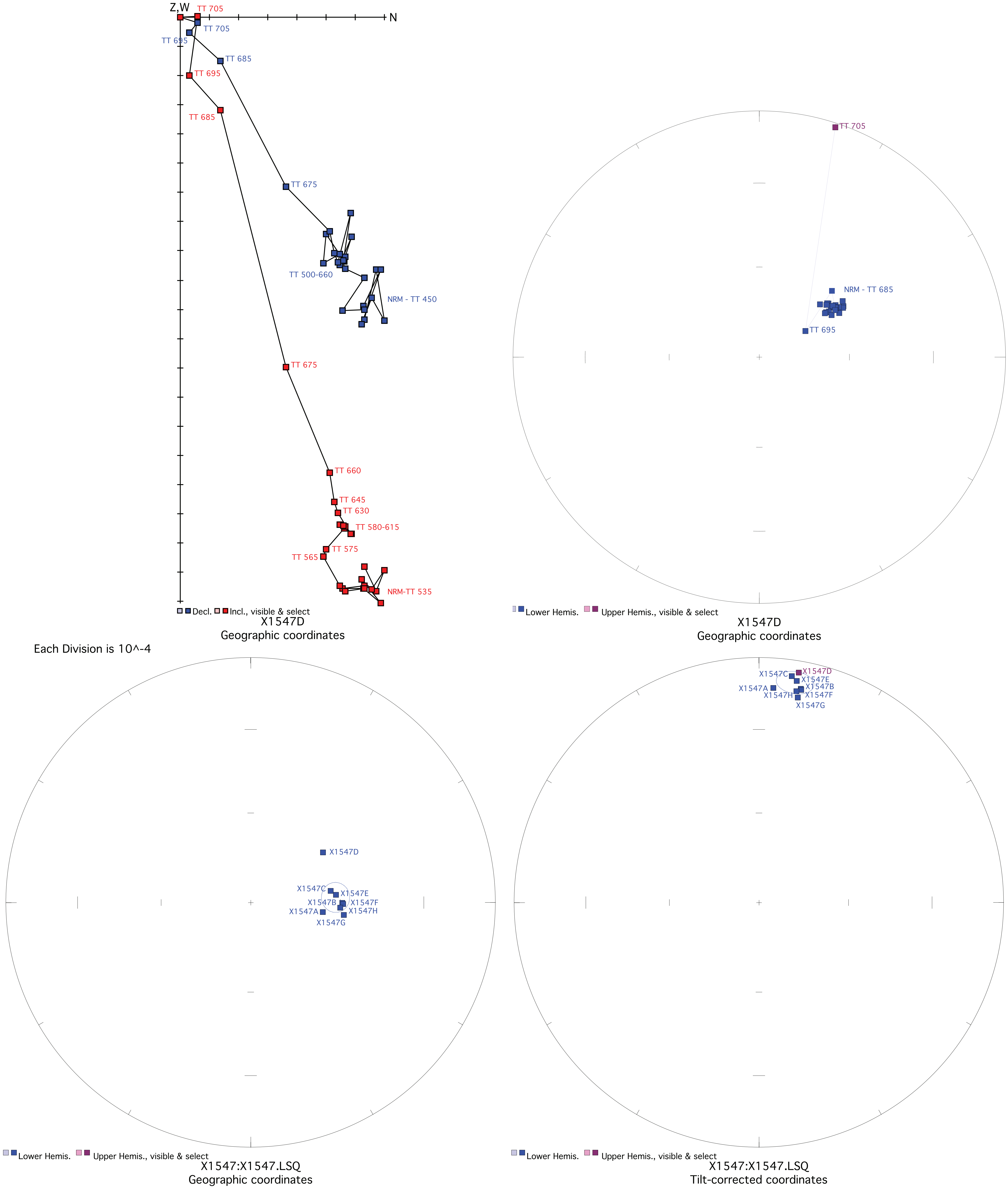

Fisher mean geog. decl.: 86.5, incl.: 61.6 a95 4.8, N: 8

Fisher mean strat. decl.: 9.3, incl.: 9.7 a95 4.8, N: 8

Figure X1548. Panel (a) shows the view of a representative sample in an orthographic projection in geographic coordinates. Blue=horizontal projection, red=vertical projection. Each pair of points represents a measurement step (natural remanent magnetization NRM, liquid nitrogen LN2, or thermal degrees C). Panel (b) shows the same sample in an equal-area projection in geographic coordinates. Blue=lower hemisphere, red=upper hemisphere. Panels (c) and (d) show equal-area projections of the site mean in geographic and tilt-corrected coordinates, respectively. Each point is a ChRM of a sample within the site. Blue=lower hemisphere, red=upper hemisphere. The circle represents the Fisher alpha 95-error of the site mean. Lighter colored points represent sample ChRMs that were not selected into the mean.

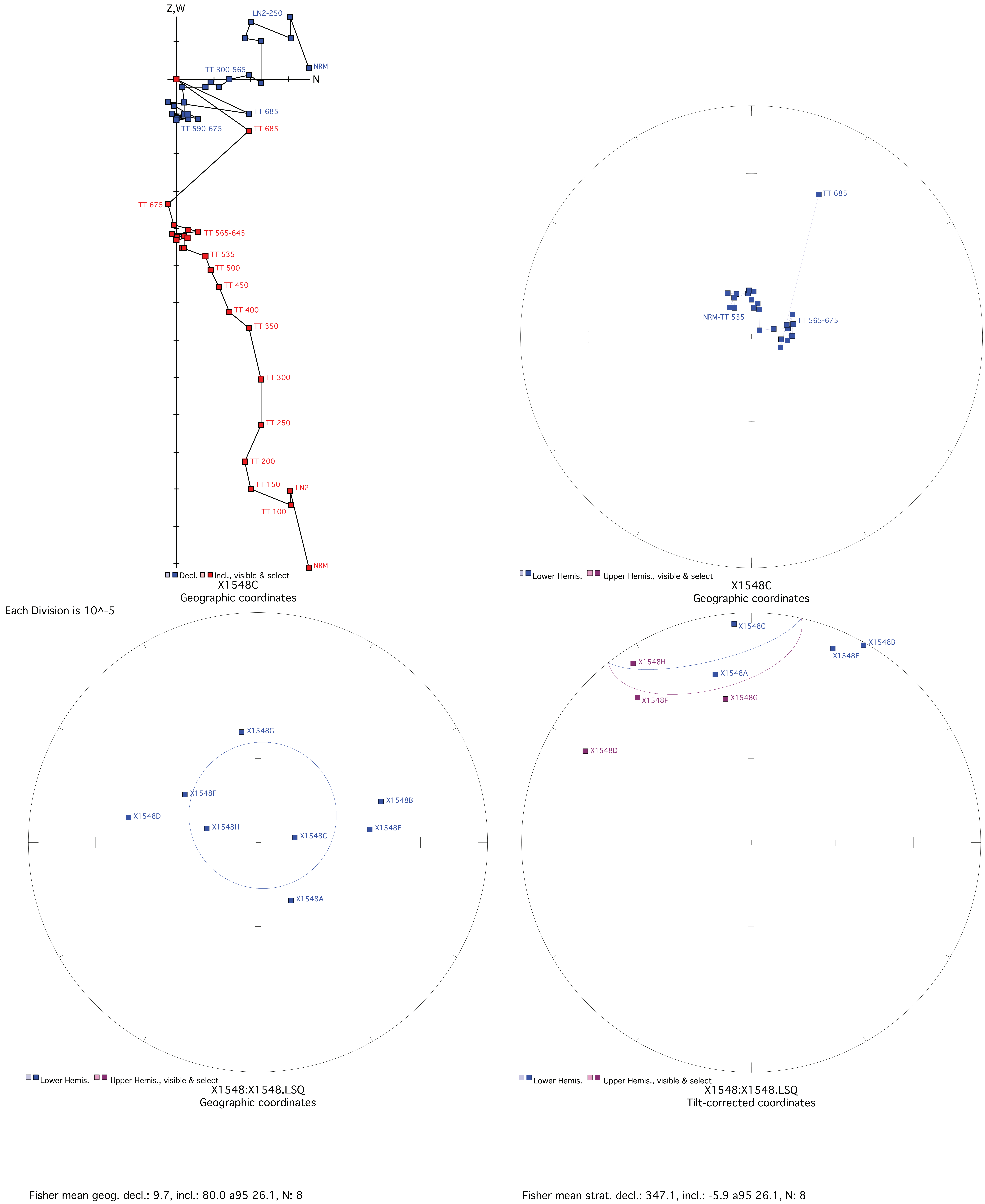

Figure X1549. Panel (a) shows the view of a representative sample in an orthographic projection in geographic coordinates. Blue=horizontal projection, red=vertical projection. Each pair of points represents a measurement step (natural remanent magnetization NRM, liquid nitrogen LN2, or thermal degrees C). Panel (b) shows the same sample in an equal-area projection in geographic coordinates. Blue=lower hemisphere, red=upper hemisphere. Panels (c) and (d) show equal-area projections of the site mean in geographic and tilt-corrected coordinates, respectively. Each point is a ChRM of a sample within the site. Blue=lower hemisphere, red=upper hemisphere. The circle represents the Fisher alpha 95-error of the site mean. Lighter colored points represent sample ChRMs that were not selected into the mean.

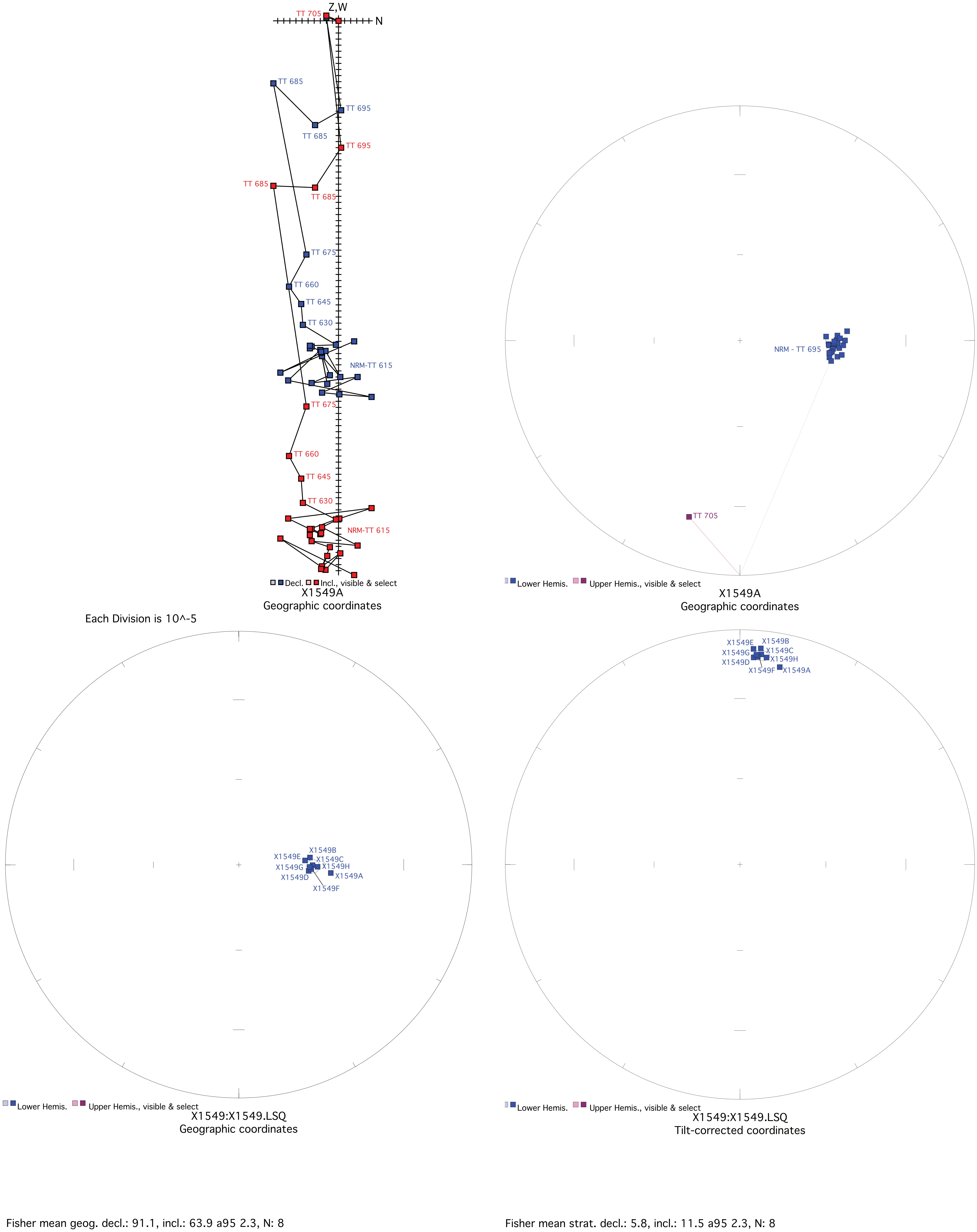

Figure X1550. Panel (a) shows the view of a representative sample in an orthographic projection in geographic coordinates. Blue=horizontal projection, red=vertical projection. Each pair of points represents a measurement step (natural remanent magnetization NRM, liquid nitrogen LN2, or thermal degrees C). Panel (b) shows the same sample in an equal-area projection in geographic coordinates. Blue=lower hemisphere, red=upper hemisphere. Panels (c) and (d) show equal-area projections of the site mean in geographic and tilt-corrected coordinates, respectively. Each point is a ChRM of a sample within the site. Blue=lower hemisphere, red=upper hemisphere. The circle represents the Fisher alpha 95-error of the site mean. Lighter colored points represent sample ChRMs that were not selected into the mean.

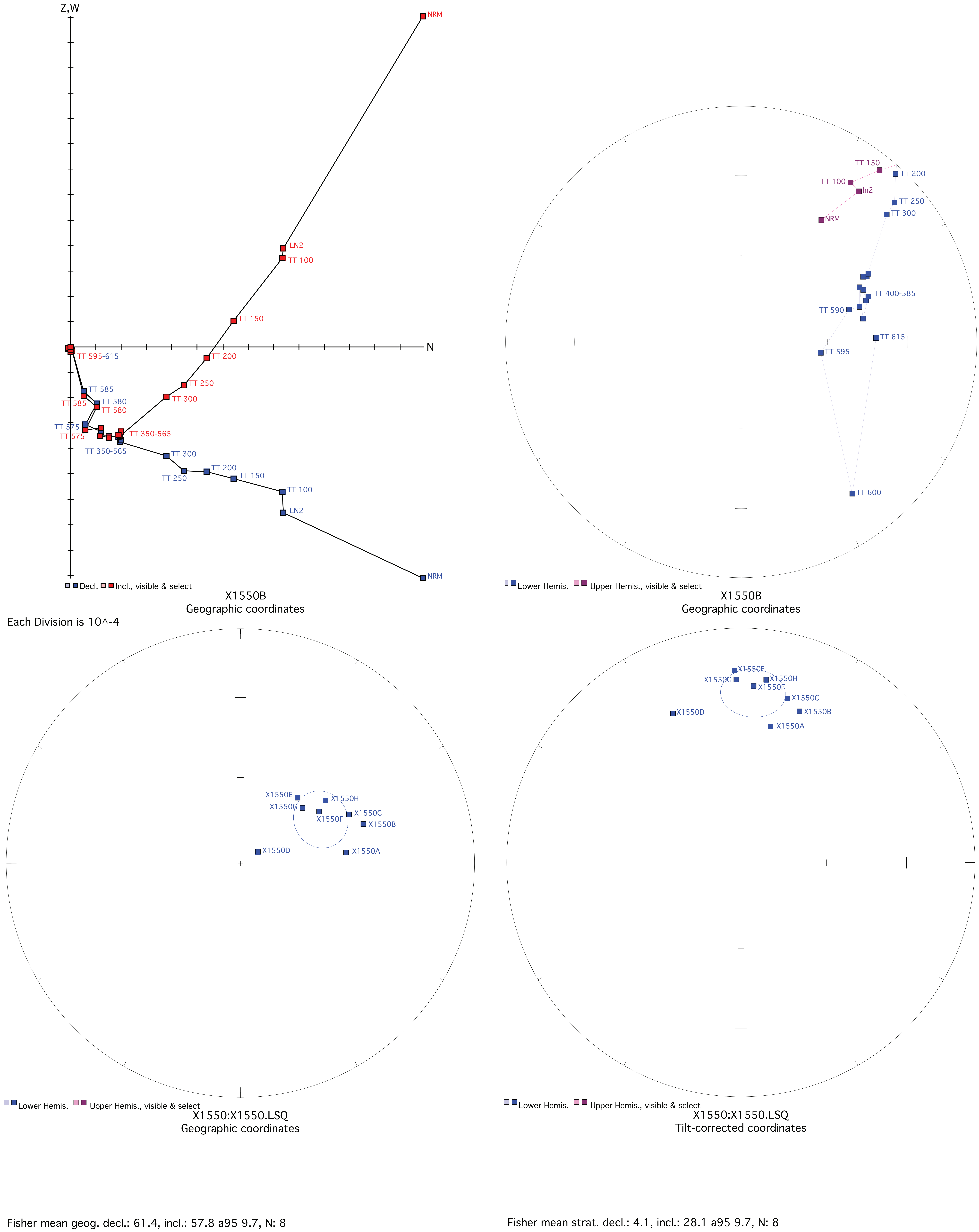

Figure X1551. Panel (a) shows the view of a representative sample in an orthographic projection in geographic coordinates. Blue=horizontal projection, red=vertical projection. Each pair of points represents a measurement step (natural remanent magnetization NRM, liquid nitrogen LN2, or thermal degrees C). Panel (b) shows the same sample in an equal-area projection in geographic coordinates. Blue=lower hemisphere, red=upper hemisphere. Panels (c) and (d) show equal-area projections of the site mean in geographic and tilt-corrected coordinates, respectively. Each point is a ChRM of a sample within the site. Blue=lower hemisphere, red=upper hemisphere. The circle represents the Fisher alpha 95-error of the site mean. Lighter colored points represent sample ChRMs that were not selected into the mean.

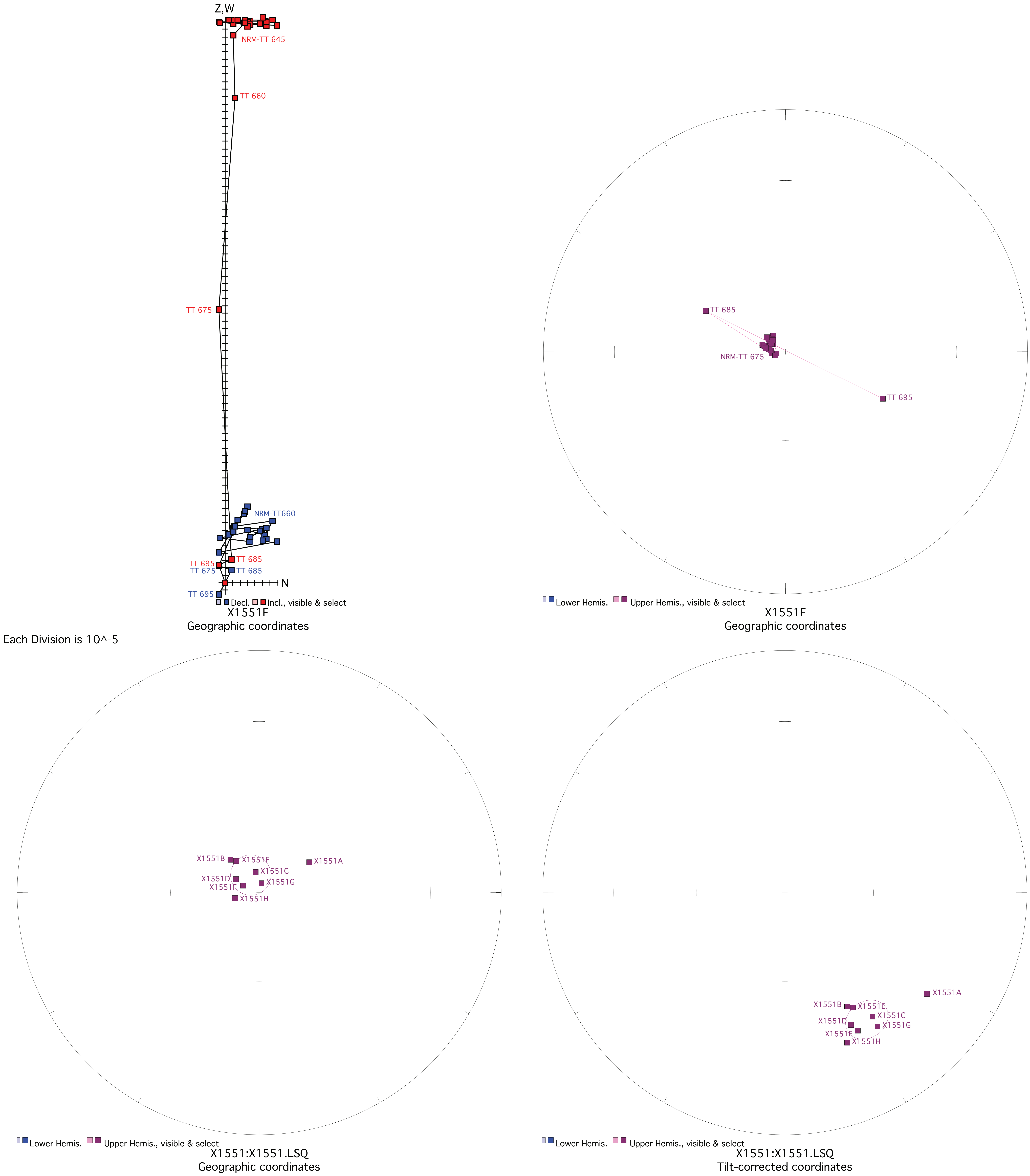

Fisher mean geog. decl.: 334.2, incl.: -83.5 a95 6.8, N: 8

Fisher mean strat. decl.: 147.1, incl.: -37.5 a95 6.8, N: 8

Figure X1552. Panel (a) shows the view of a representative sample in an orthographic projection in geographic coordinates. Blue=horizontal projection, red=vertical projection. Each pair of points represents a measurement step (natural remanent magnetization NRM, liquid nitrogen LN2, or thermal degrees C). Panel (b) shows the same sample in an equal-area projection in geographic coordinates. Blue=lower hemisphere, red=upper hemisphere. Panels (c) and (d) show equal-area projections of the site mean in geographic and tilt-corrected coordinates, respectively. Each point is a ChRM of a sample within the site. Blue=lower hemisphere, red=upper hemisphere. The circle represents the Fisher alpha 95-error of the site mean. Lighter colored points represent sample ChRMs that were not selected into the mean.

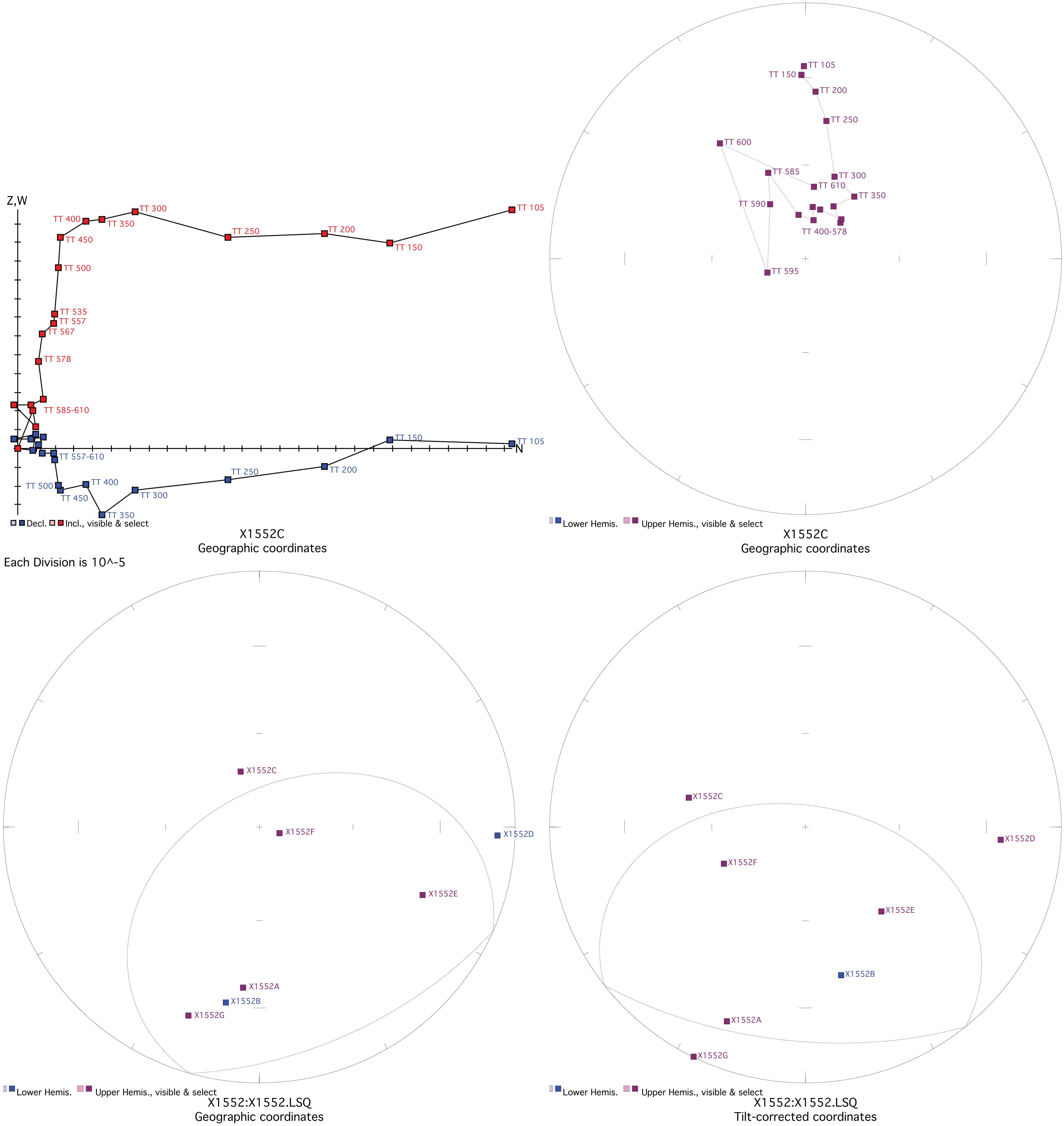

Fisher mean geog. decl.: 154.8, incl.: -44.3 a95 57.2, N: 7

Fisher mean strat. decl.: 186.6, incl.: -39.7 a95 57.2, N: 7

Figure X1553. Panel (a) shows the view of a representative sample in an orthographic projection in geographic coordinates. Blue=horizontal projection, red=vertical projection. Each pair of points represents a measurement step (natural remanent magnetization NRM, liquid nitrogen LN2, or thermal degrees C). Panel (b) shows the same sample in an equal-area projection in geographic coordinates. Blue=lower hemisphere, red=upper hemisphere. Panels (c) and (d) show equal-area projections of the site mean in geographic and tilt-corrected coordinates, respectively. Each point is a ChRM of a sample within the site. Blue=lower hemisphere, red=upper hemisphere. The circle represents the Fisher alpha 95-error of the site mean. Lighter colored points represent sample ChRMs that were not selected into the mean.

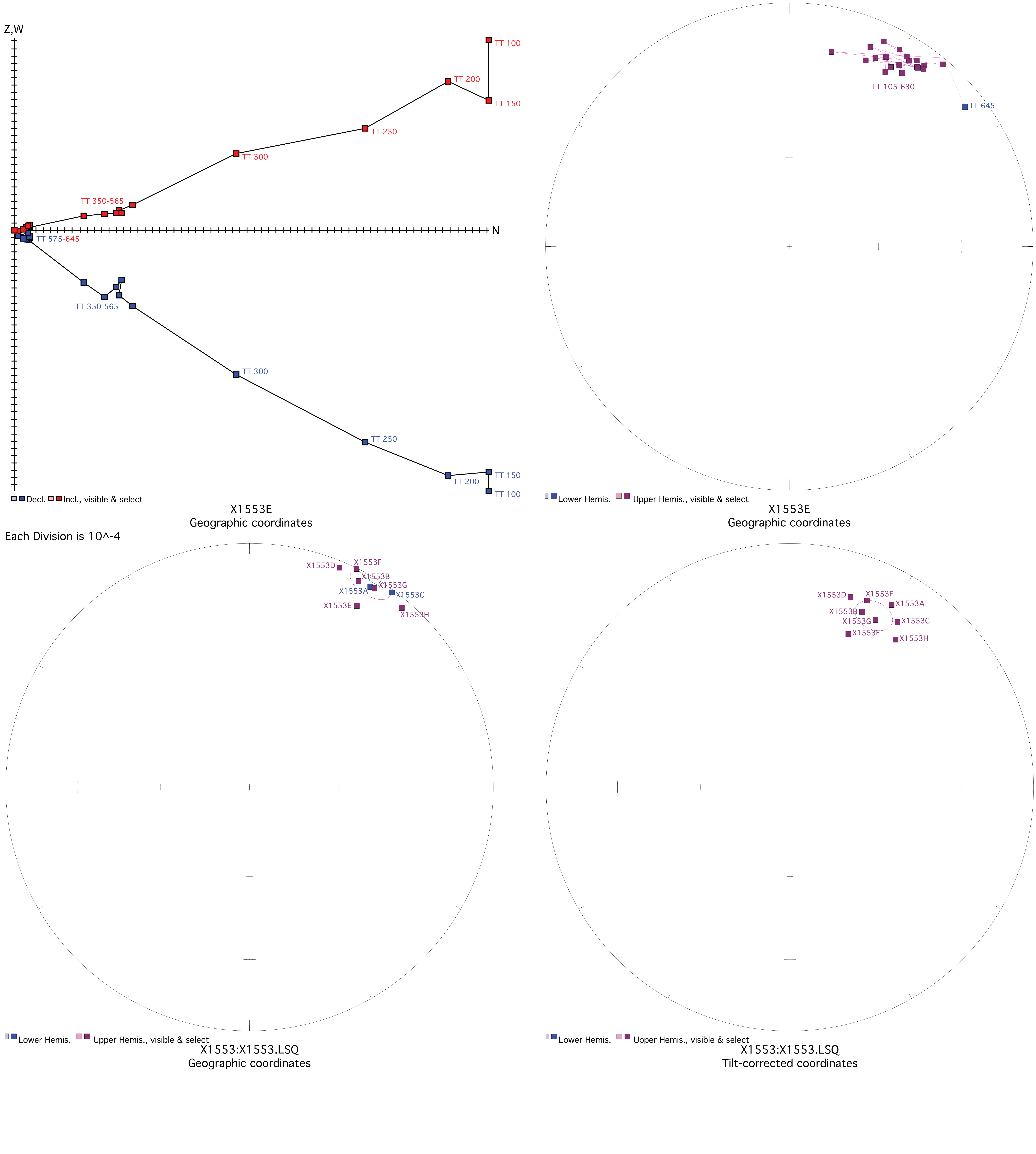

Figure X1554. Panel (a) shows the view of a representative sample in an orthographic projection in geographic coordinates. Blue=horizontal projection, red=vertical projection. Each pair of points represents a measurement step (natural remanent magnetization NRM, liquid nitrogen LN2, or thermal degrees C). Panel (b) shows the same sample in an equal-area projection in geographic coordinates. Blue=lower hemisphere, red=upper hemisphere. Panels (c) and (d) show equal-area projections of the site mean in geographic and tilt-corrected coordinates, respectively. Each point is a ChRM of a sample within the site. Blue=lower hemisphere, red=upper hemisphere. The circle represents the Fisher alpha 95-error of the site mean. Lighter colored points represent sample ChRMs that were not selected into the mean.

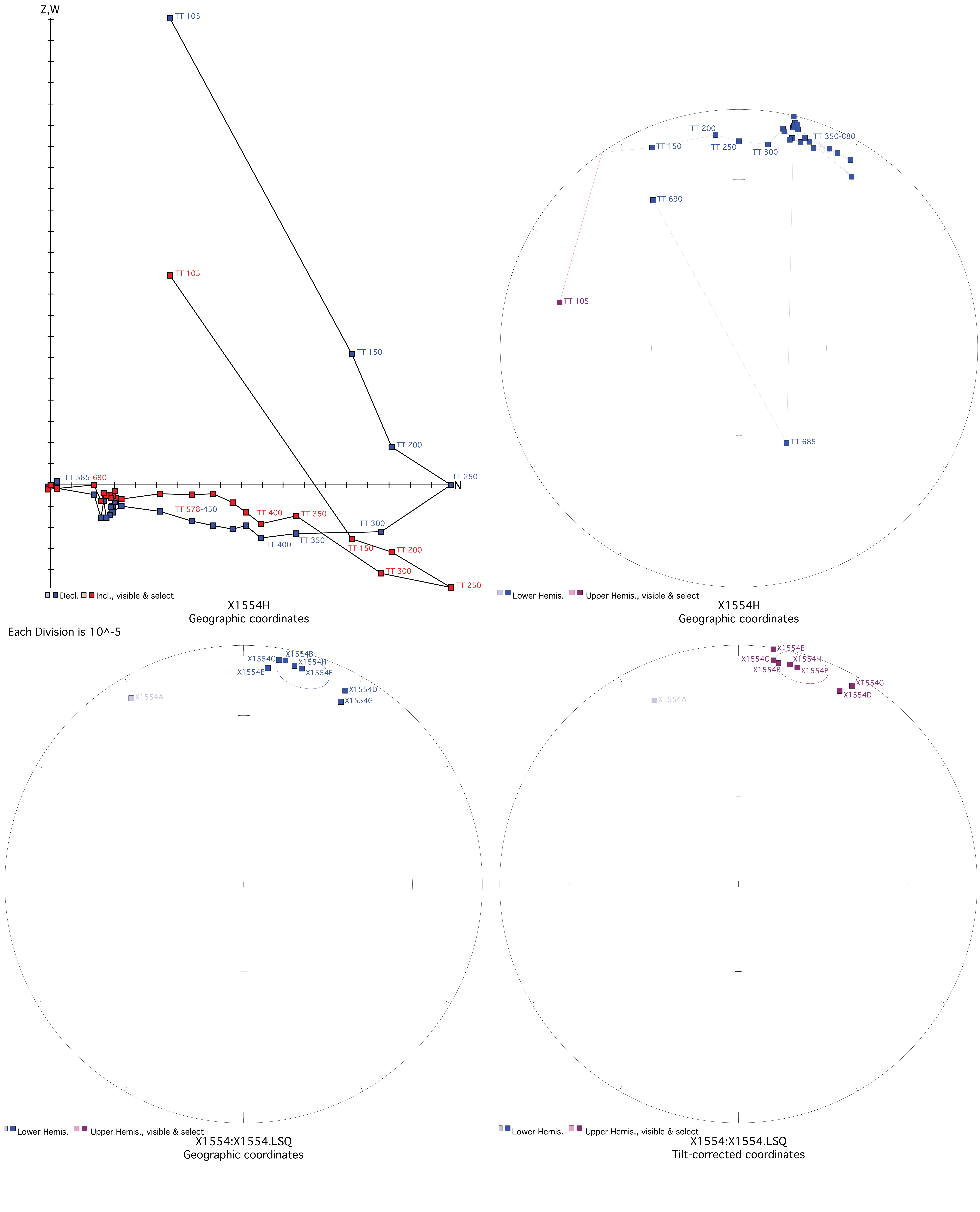

Fisher mean geog. decl.: 15.6, incl.: 8.4 a95 6.9, N: 7

Fisher mean strat. decl.: 16.2, incl.: -5.9 a95 6.9, N: 7

Figure X1555. Panel (a) shows the view of a representative sample in an orthographic projection in geographic coordinates. Blue=horizontal projection, red=vertical projection. Each pair of points represents a measurement step (natural remanent magnetization NRM, liquid nitrogen LN2, or thermal degrees C). Panel (b) shows the same sample in an equal-area projection in geographic coordinates. Blue=lower hemisphere, red=upper hemisphere. Panels (c) and (d) show equal-area projections of the site mean in geographic and tilt-corrected coordinates, respectively. Each point is a ChRM of a sample within the site. Blue=lower hemisphere, red=upper hemisphere. The circle represents the Fisher alpha 95-error of the site mean. Lighter colored points represent sample ChRMs that were not selected into the mean.

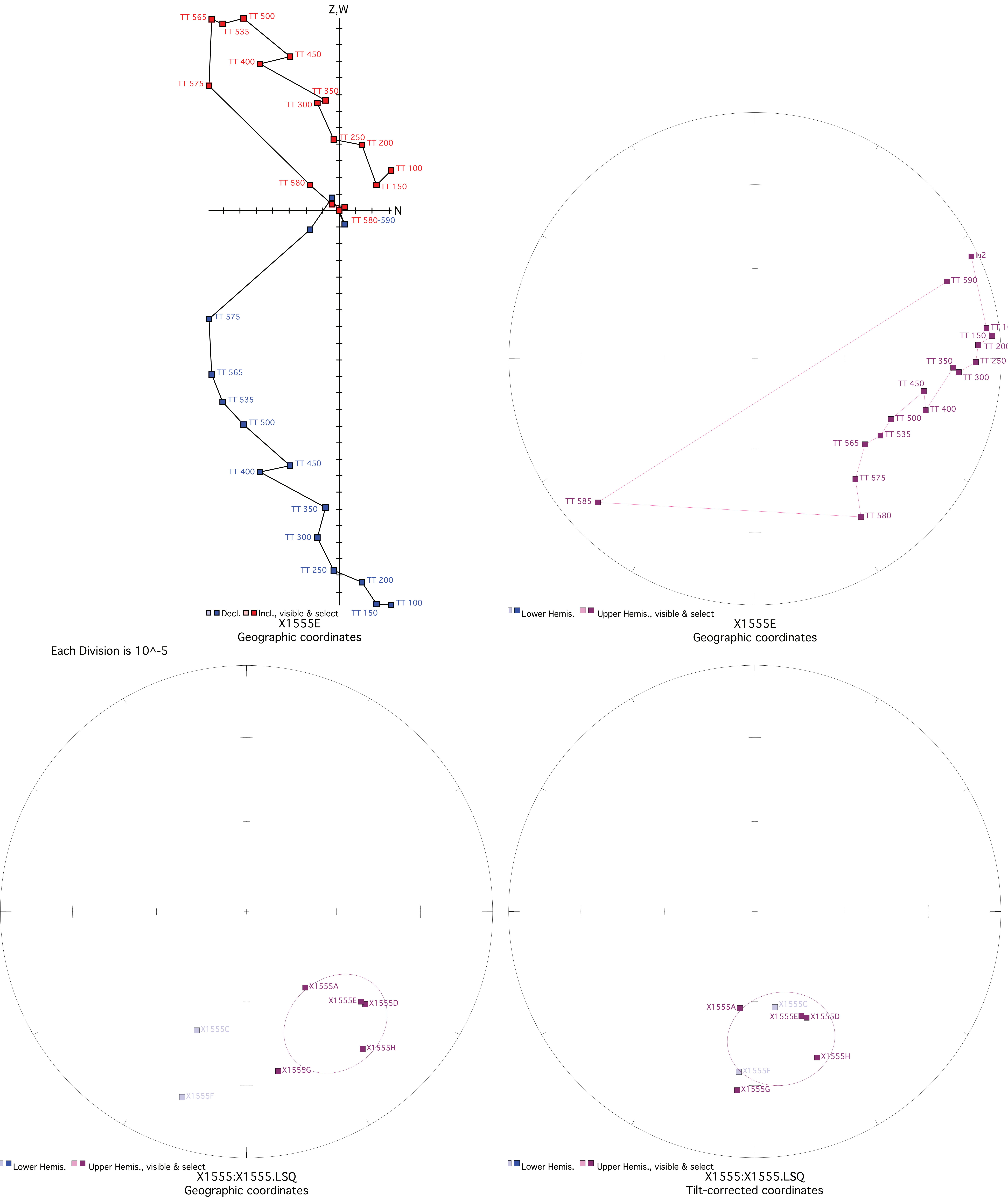

Fisher mean geog. decl.: 141.5, incl.: -40.9 a95 16.6, N: 5

Fisher mean strat. decl.: 168.3, incl.: -45.7 a95 16.6, N: 5

Figure X1556. Panel (a) shows the view of a representative sample in an orthographic projection in geographic coordinates. Blue=horizontal projection, red=vertical projection. Each pair of points represents a measurement step (natural remanent magnetization NRM, liquid nitrogen LN2, or thermal degrees C). Panel (b) shows the same sample in an equal-area projection in geographic coordinates. Blue=lower hemisphere, red=upper hemisphere. Panels (c) and (d) show equal-area projections of the site mean in geographic and tilt-corrected coordinates, respectively. Each point is a ChRM of a sample within the site. Blue=lower hemisphere, red=upper hemisphere. The circle represents the Fisher alpha 95-error of the site mean. Lighter colored points represent sample ChRMs that were not selected into the mean.

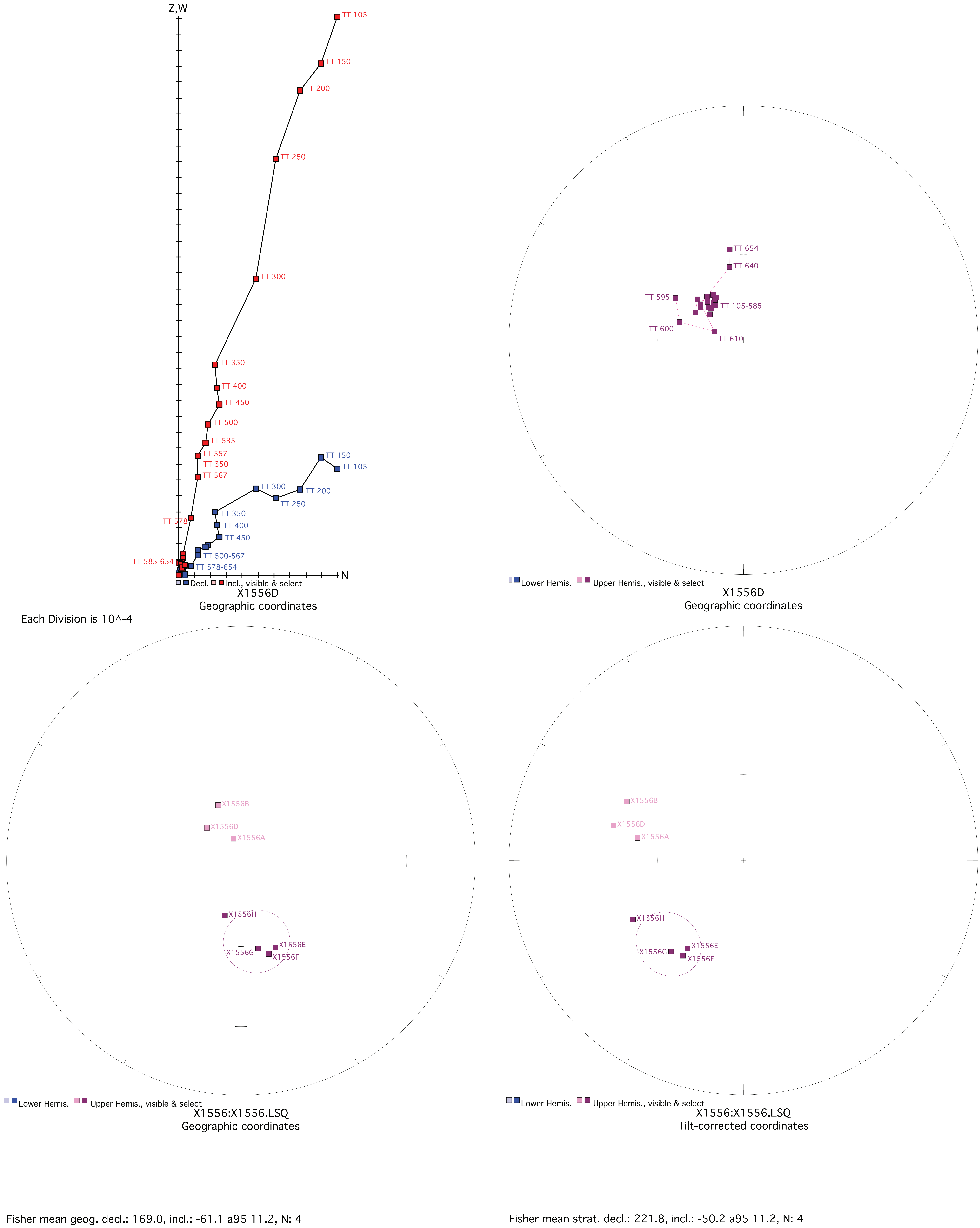

Figure X1558. Panel (a) shows the view of a representative sample in an orthographic projection in geographic coordinates. Blue=horizontal projection, red=vertical projection. Each pair of points represents a measurement step (natural remanent magnetization NRM, liquid nitrogen LN2, or thermal degrees C). Panel (b) shows the same sample in an equal-area projection in geographic coordinates. Blue=lower hemisphere, red=upper hemisphere. Panels (c) and (d) show equal-area projections of the site mean in geographic and tilt-corrected coordinates, respectively. Each point is a ChRM of a sample within the site. Blue=lower hemisphere, red=upper hemisphere. The circle represents the Fisher alpha 95-error of the site mean. Lighter colored points represent sample ChRMs that were not selected into the mean.

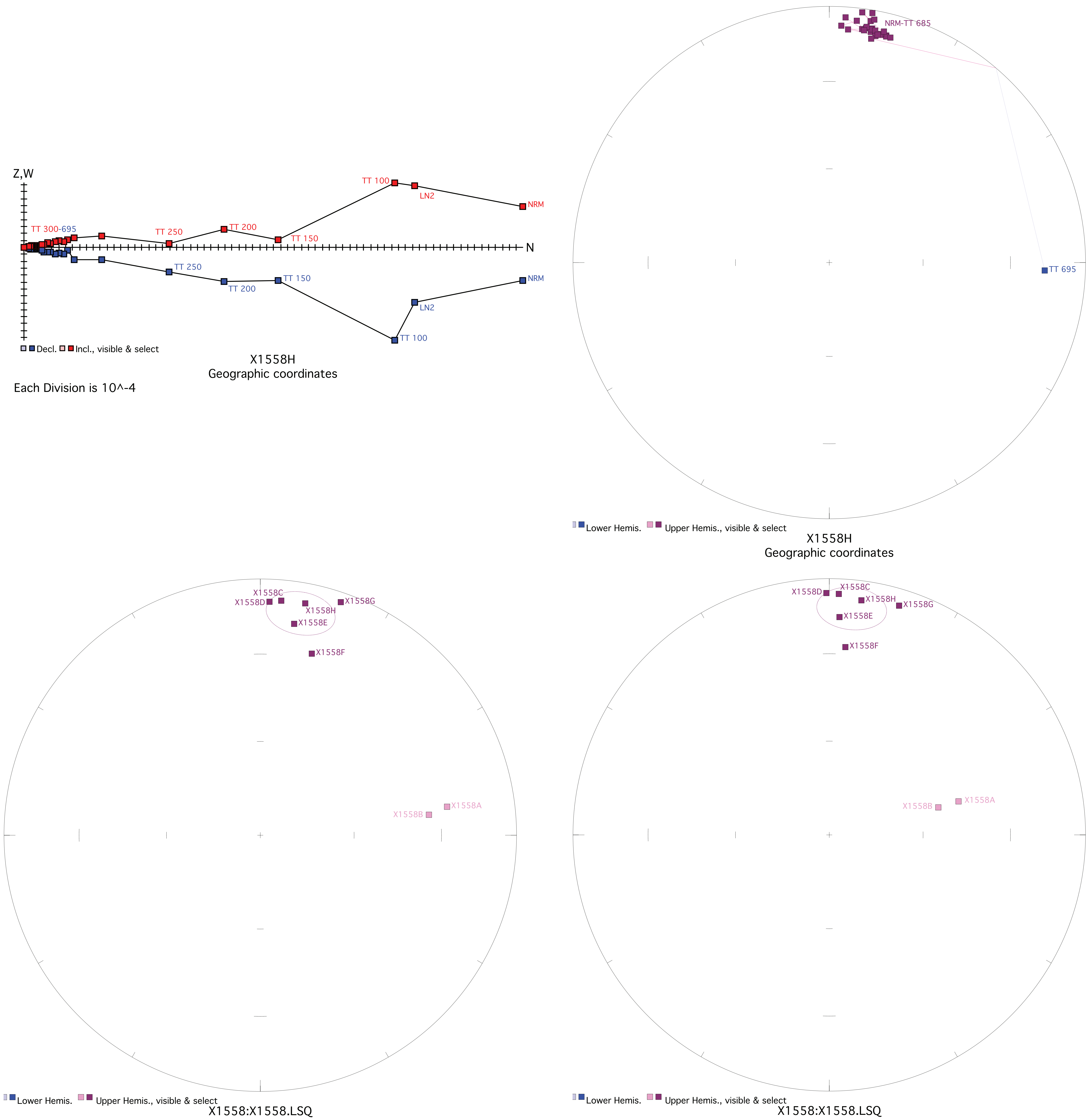

Fisher mean geog. decl.: 10.3, incl.: -12.8 a95 8.6, N: 6

Fisher mean strat. decl.: 5.7, incl.: -12.0 a95 8.6, N: 6

Figure X1559. Panel (a) shows the view of a representative sample in an orthographic projection in geographic coordinates. Blue=horizontal projection, red=vertical projection. Each pair of points represents a measurement step (natural remanent magnetization NRM, liquid nitrogen LN2, or thermal degrees C). Panel (b) shows the same sample in an equal-area projection in geographic coordinates. Blue=lower hemisphere, red=upper hemisphere. Panels (c) and (d) show equal-area projections of the site mean in geographic and tilt-corrected coordinates, respectively. Each point is a ChRM of a sample within the site. Blue=lower hemisphere, red=upper hemisphere. The circle represents the Fisher alpha 95-error of the site mean. Lighter colored points represent sample ChRMs that were not selected into the mean.

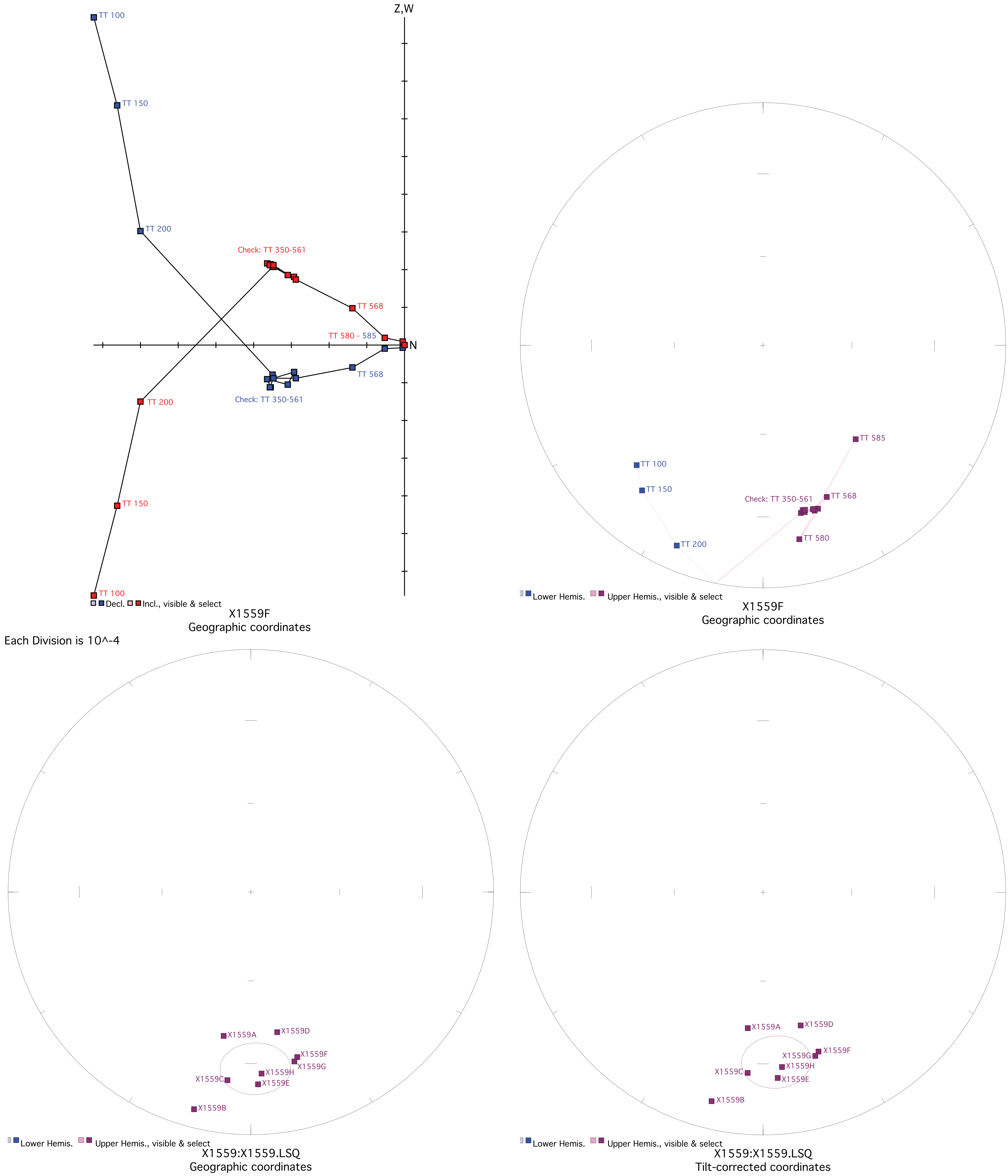

Fisher mean geog. decl.: 178.6, incl.: -27.7 a95 10.1, N: 8

Fisher mean strat. decl.: 175.6, incl.: -30.2 a95 10.1, N: 8

Figure X1560. Panel (a) shows the view of a representative sample in an orthographic projection in geographic coordinates. Blue=horizontal projection, red=vertical projection. Each pair of points represents a measurement step (natural remanent magnetization NRM, liquid nitrogen LN2, or thermal degrees C). Panel (b) shows the same sample in an equal-area projection in geographic coordinates. Blue=lower hemisphere, red=upper hemisphere. Panels (c) and (d) show equal-area projections of the site mean in geographic and tilt-corrected coordinates, respectively. Each point is a ChRM of a sample within the site. Blue=lower hemisphere, red=upper hemisphere. The circle represents the Fisher alpha 95-error of the site mean. Lighter colored points represent sample ChRMs that were not selected into the mean.

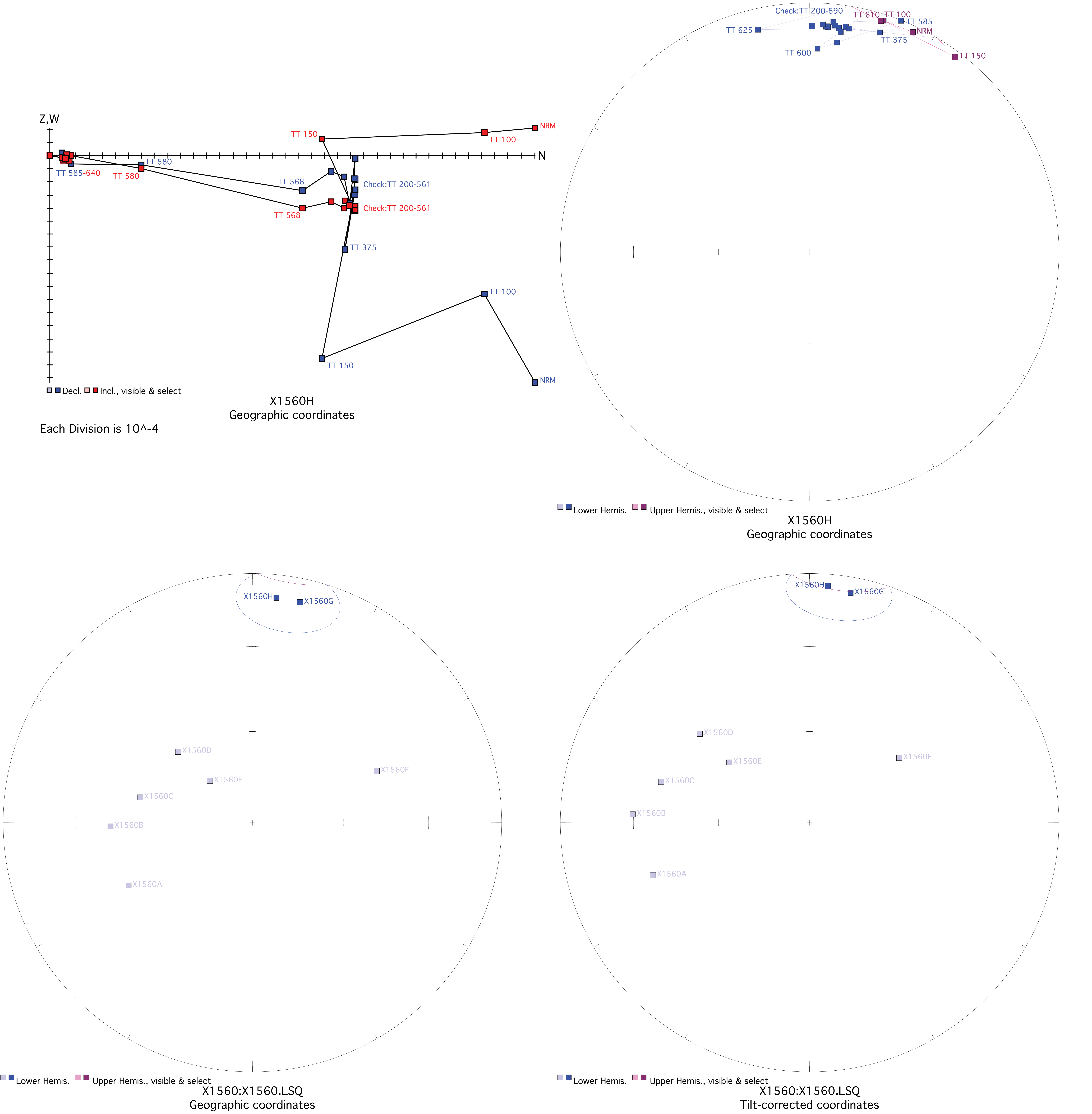

Fisher mean geog. decl.: 9.1, incl.: 10.3 a95 13.1, N: 2

Fisher mean strat. decl.: 7.2, incl.: 6.2 a95 12.9, N: 2

Figure X1561. Panel (a) shows the view of a representative sample in an orthographic projection in geographic coordinates. Blue=horizontal projection, red=vertical projection. Each pair of points represents a measurement step (natural remanent magnetization NRM, liquid nitrogen LN2, or thermal degrees C). Panel (b) shows the same sample in an equal-area projection in geographic coordinates. Blue=lower hemisphere, red=upper hemisphere. Panels (c) and (d) show equal-area projections of the site mean in geographic and tilt-corrected coordinates, respectively. Each point is a ChRM of a sample within the site. Blue=lower hemisphere, red=upper hemisphere. The circle represents the Fisher alpha 95-error of the site mean. Lighter colored points represent sample ChRMs that were not selected into the mean.

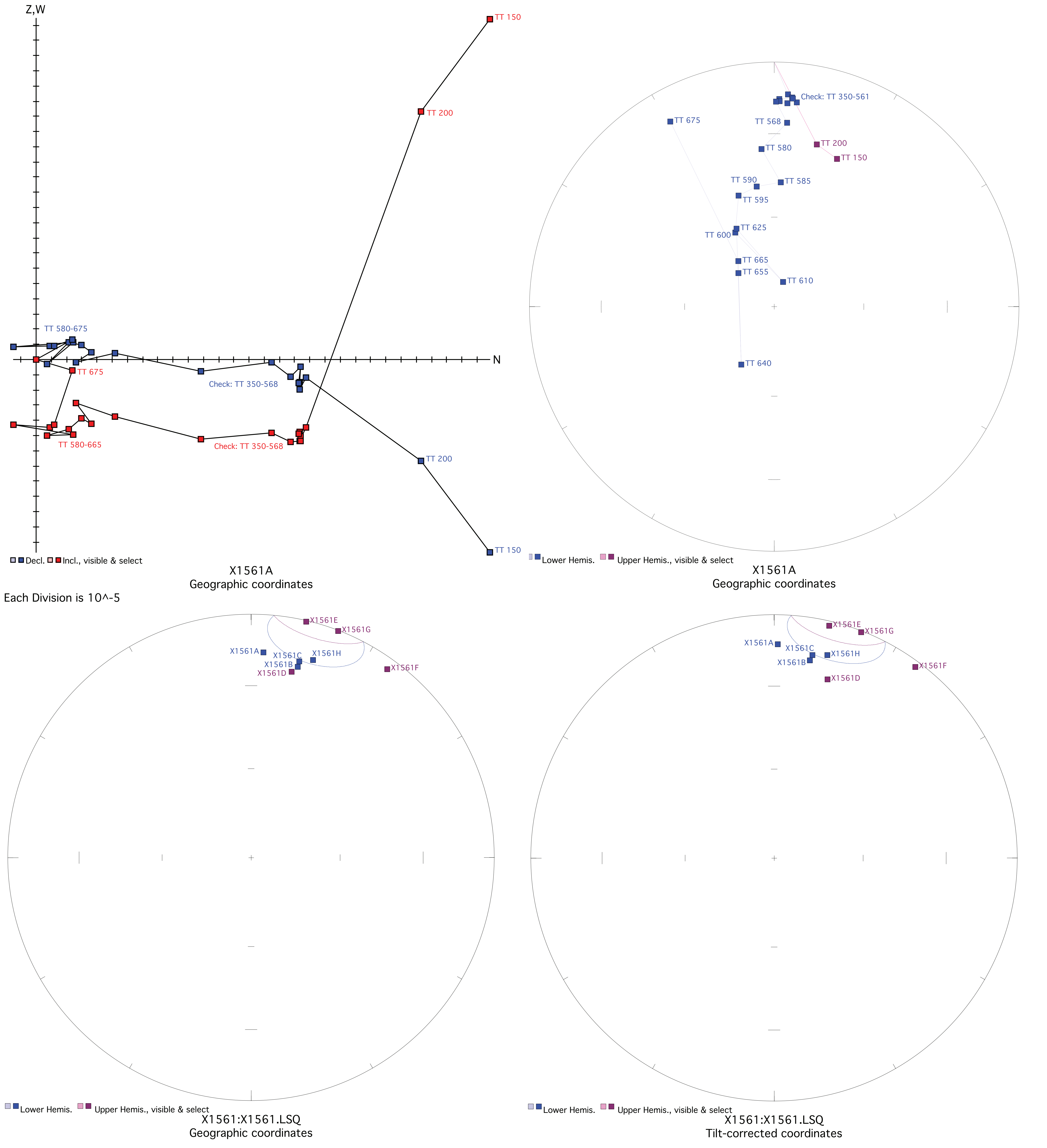

Fisher mean geog. decl.: 16.4, incl.: 5.5 a95 12.3, N: 8

Fisher mean strat. decl.: 15.6, incl.: 4.3 a95 12.3, N: 8

Figure X1562. Panel (a) shows the view of a representative sample in an orthographic projection in geographic coordinates. Blue=horizontal projection, red=vertical projection. Each pair of points represents a measurement step (natural remanent magnetization NRM, liquid nitrogen LN2, or thermal degrees C). Panel (b) shows the same sample in an equal-area projection in geographic coordinates. Blue=lower hemisphere, red=upper hemisphere. Panels (c) and (d) show equal-area projections of the site mean in geographic and tilt-corrected coordinates, respectively. Each point is a ChRM of a sample within the site. Blue=lower hemisphere, red=upper hemisphere. The circle represents the Fisher alpha 95-error of the site mean. Lighter colored points represent sample ChRMs that were not selected into the mean.

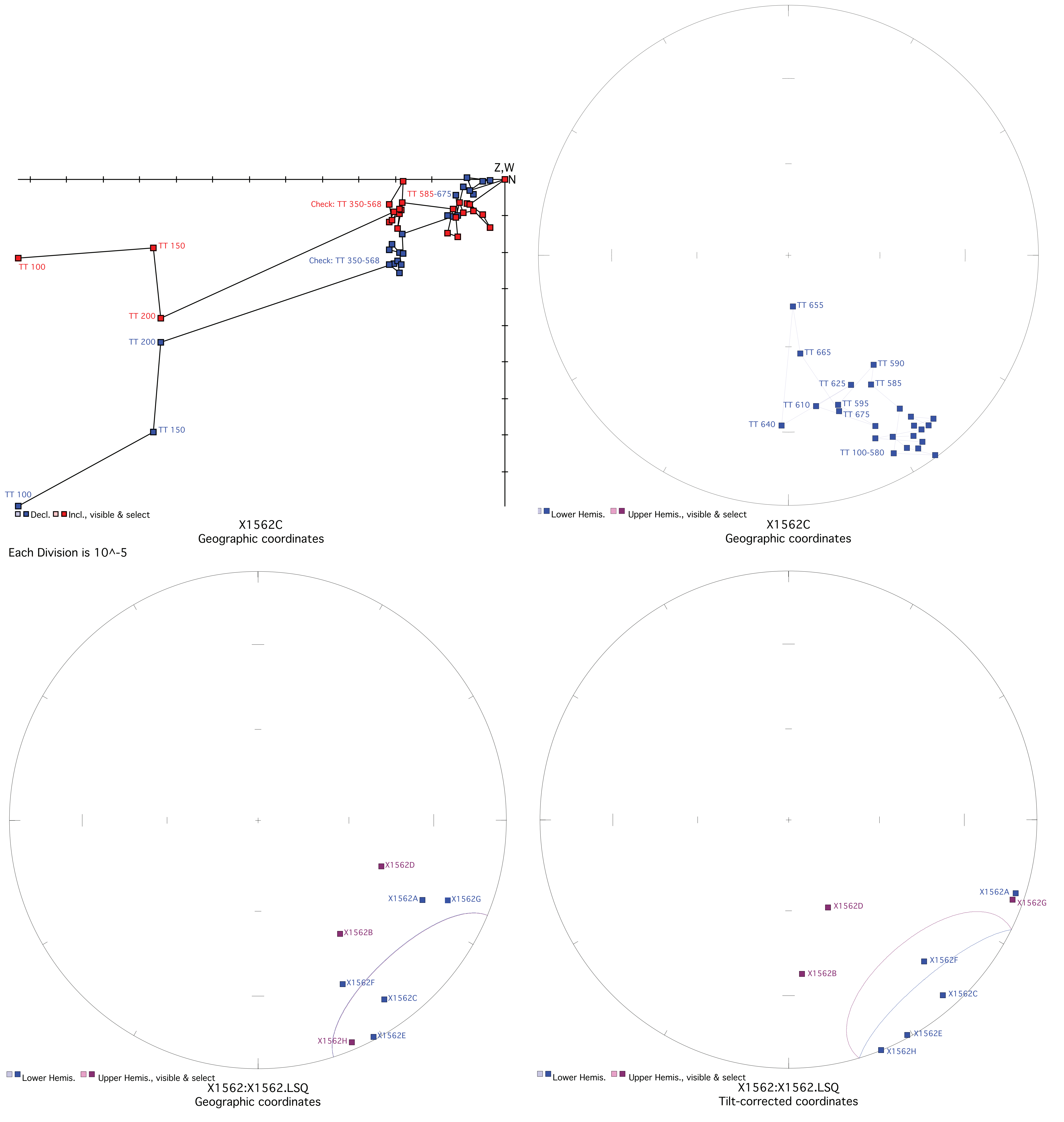

Fisher mean geog. decl.: 137.4, incl.: 0.1 a95 24.9, N: 8

Fisher mean strat. decl.: 139.8, incl.: -8.0 a95 24.9, N: 8

Figure X1563. Panel (a) shows the view of a representative sample in an orthographic projection in geographic coordinates. Blue=horizontal projection, red=vertical projection. Each pair of points represents a measurement step (natural remanent magnetization NRM, liquid nitrogen LN2, or thermal degrees C). Panel (b) shows the same sample in an equal-area projection in geographic coordinates. Blue=lower hemisphere, red=upper hemisphere. Panels (c) and (d) show equal-area projections of the site mean in geographic and tilt-corrected coordinates, respectively. Each point is a ChRM of a sample within the site. Blue=lower hemisphere, red=upper hemisphere. The circle represents the Fisher alpha 95-error of the site mean. Lighter colored points represent sample ChRMs that were not selected into the mean.

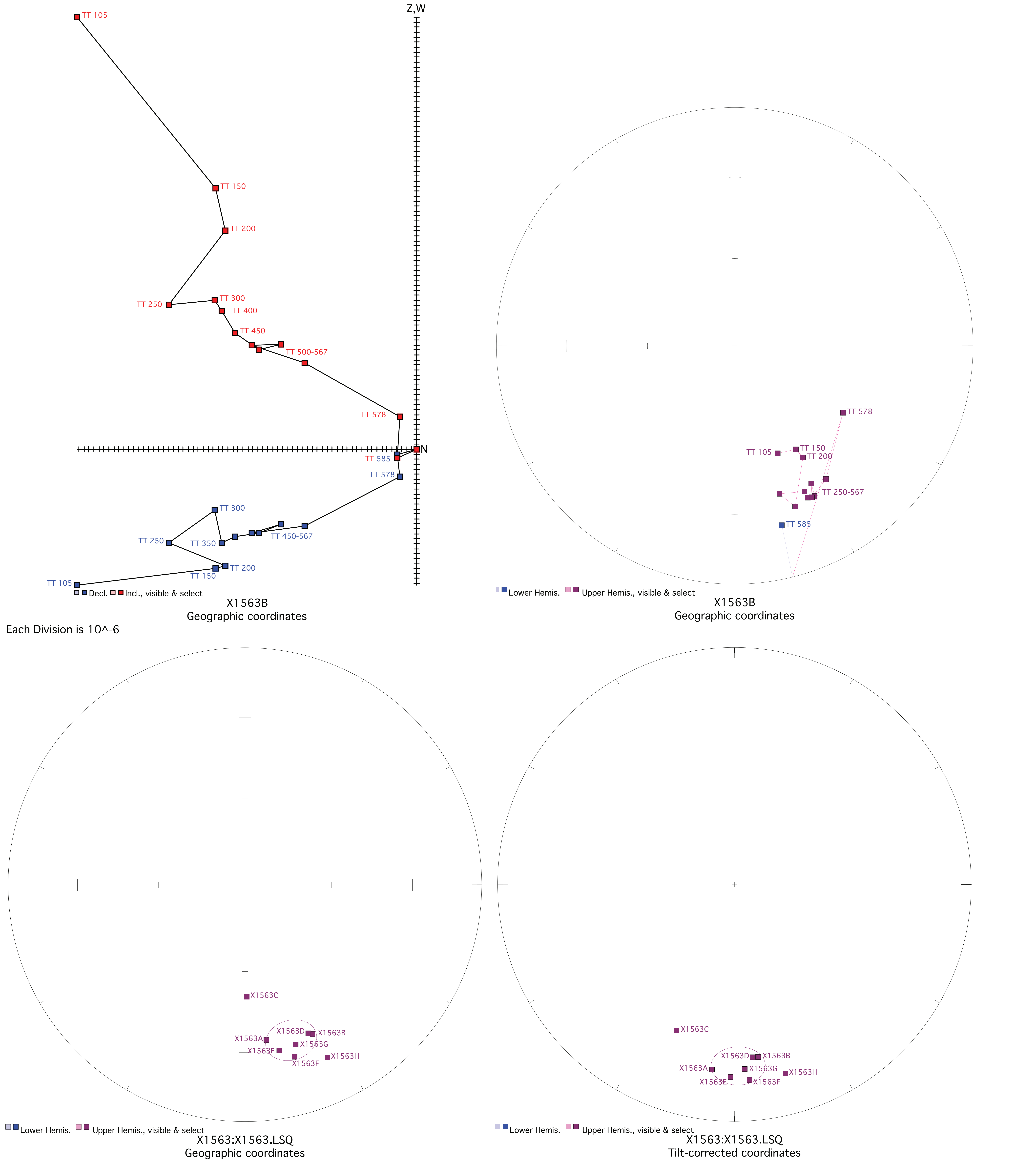

Fisher mean geog. decl.: 163.5, incl.: -32.0 a95 7.8, N: 8

Fisher mean strat. decl.: 178.8, incl.: -24.3 a95 7.8, N: 8

Figure X1564. Panel (a) shows the view of a representative sample in an orthographic projection in geographic coordinates. Blue=horizontal projection, red=vertical projection. Each pair of points represents a measurement step (natural remanent magnetization NRM, liquid nitrogen LN2, or thermal degrees C). Panel (b) shows the same sample in an equal-area projection in geographic coordinates. Blue=lower hemisphere, red=upper hemisphere. Panels (c) and (d) show equal-area projections of the site mean in geographic and tilt-corrected coordinates, respectively. Each point is a ChRM of a sample within the site. Blue=lower hemisphere, red=upper hemisphere. The circle represents the Fisher alpha 95-error of the site mean. Lighter colored points represent sample ChRMs that were not selected into the mean.

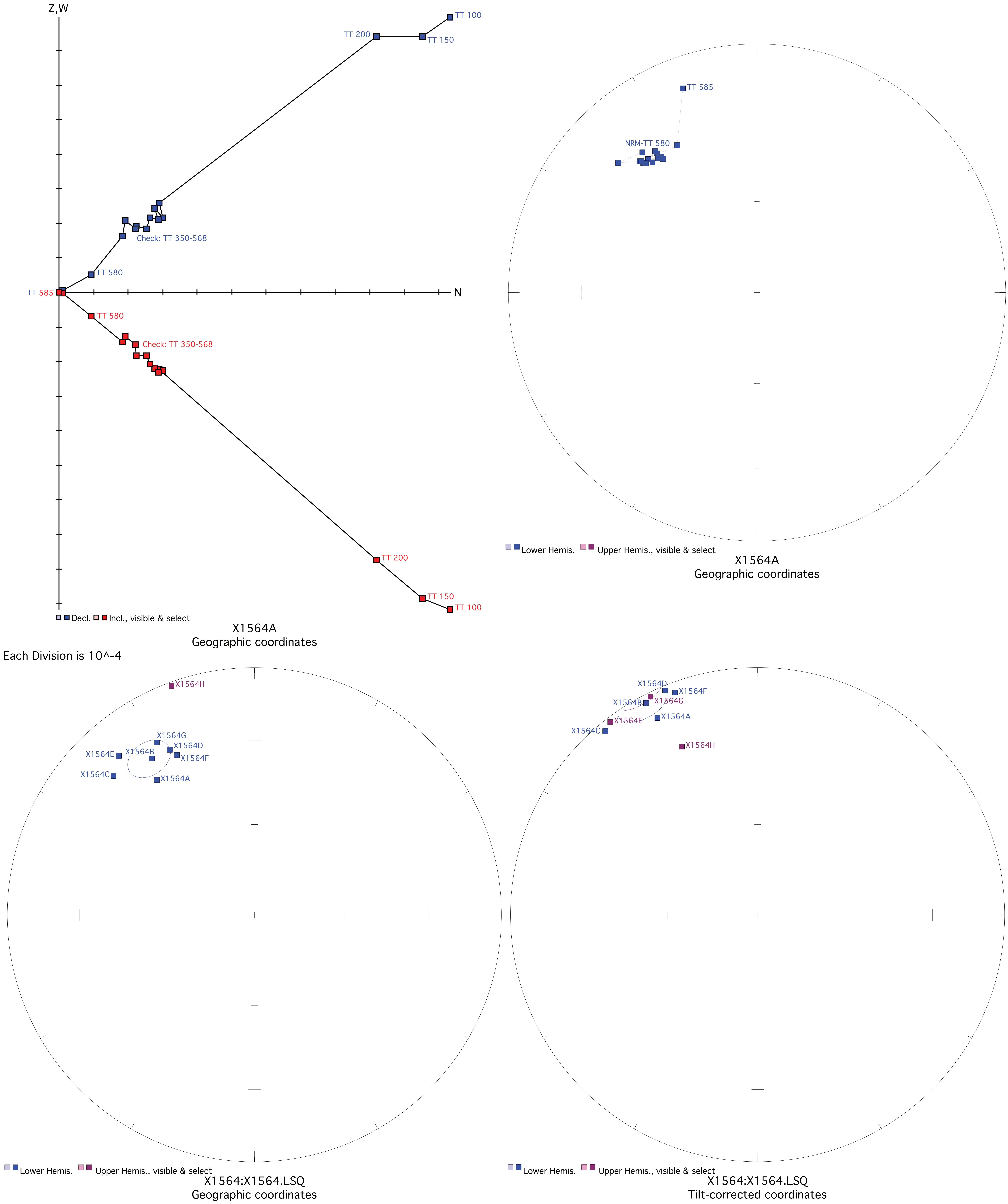

Fisher mean geog. decl.: 326.0, incl.: 24.6 a95 6.4, N: 7

Fisher mean strat. decl.: 331.3, incl.: 3.1 a95 6.4, N: 7

Figure X1565. Panel (a) shows the view of a representative sample in an orthographic projection in geographic coordinates. Blue=horizontal projection, red=vertical projection. Each pair of points represents a measurement step (natural remanent magnetization NRM, liquid nitrogen LN2, or thermal degrees C). Panel (b) shows the same sample in an equal-area projection in geographic coordinates. Blue=lower hemisphere, red=upper hemisphere. Panels (c) and (d) show equal-area projections of the site mean in geographic and tilt-corrected coordinates, respectively. Each point is a ChRM of a sample within the site. Blue=lower hemisphere, red=upper hemisphere. The circle represents the Fisher alpha 95-error of the site mean. Lighter colored points represent sample ChRMs that were not selected into the mean.

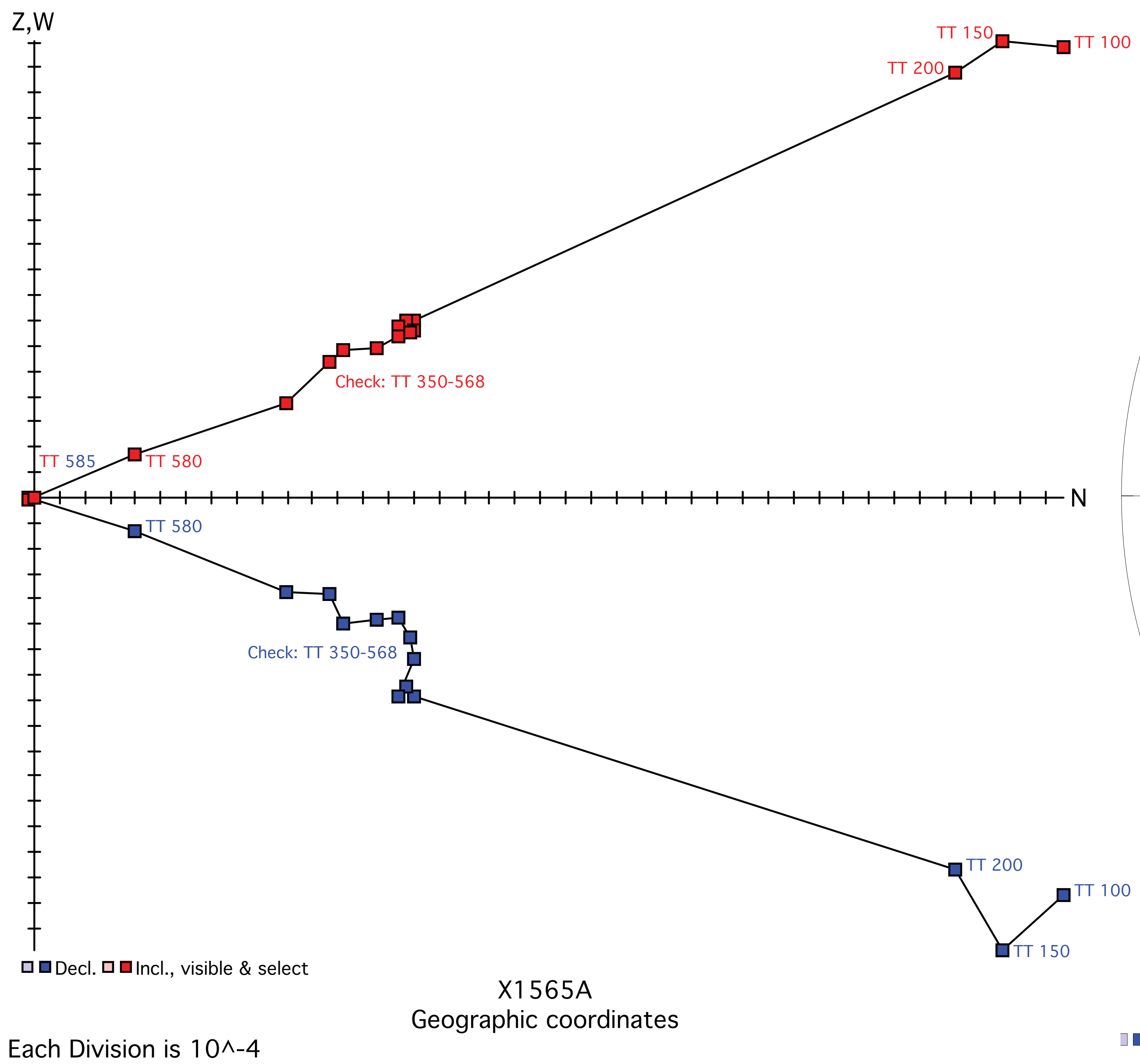

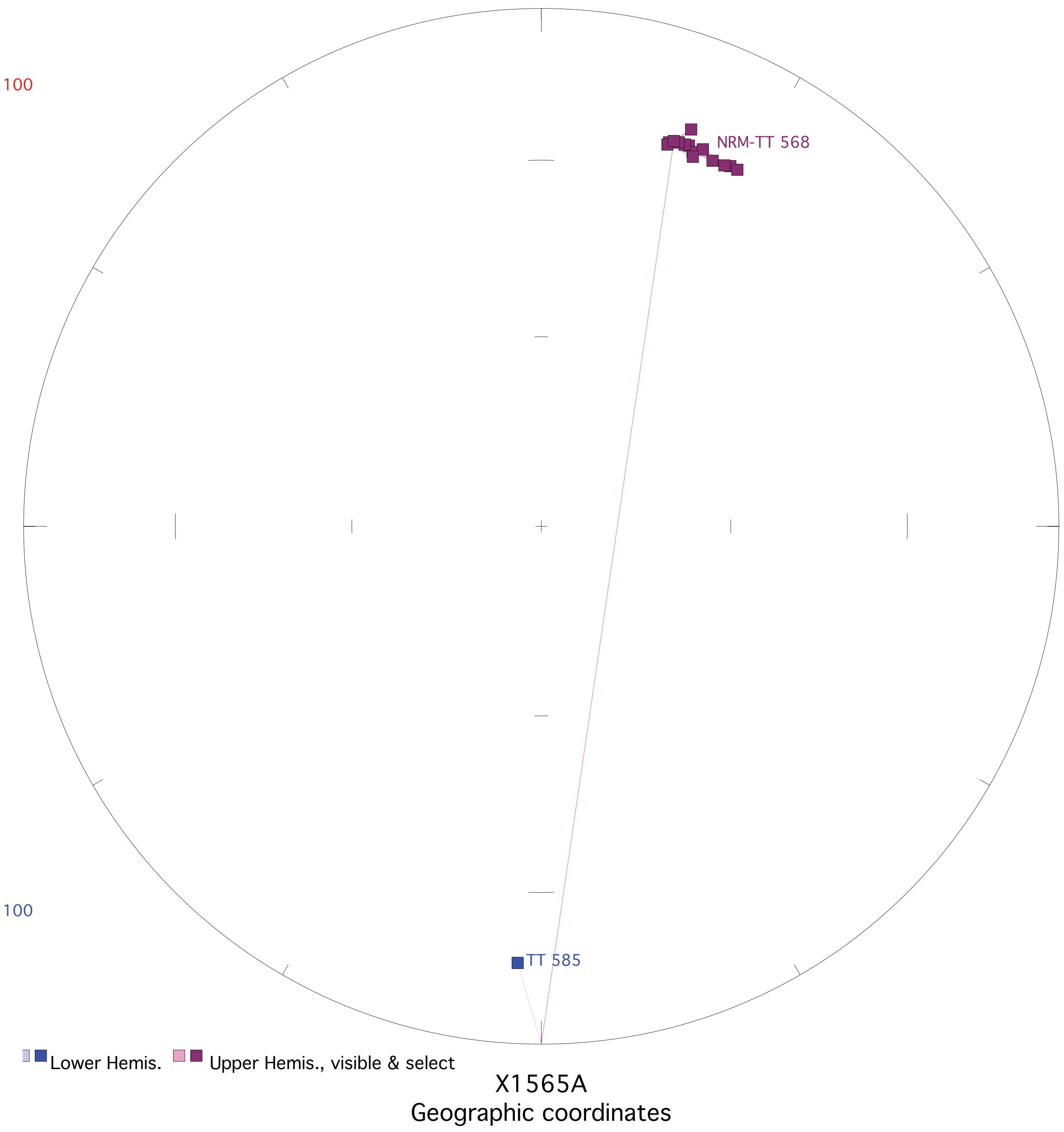

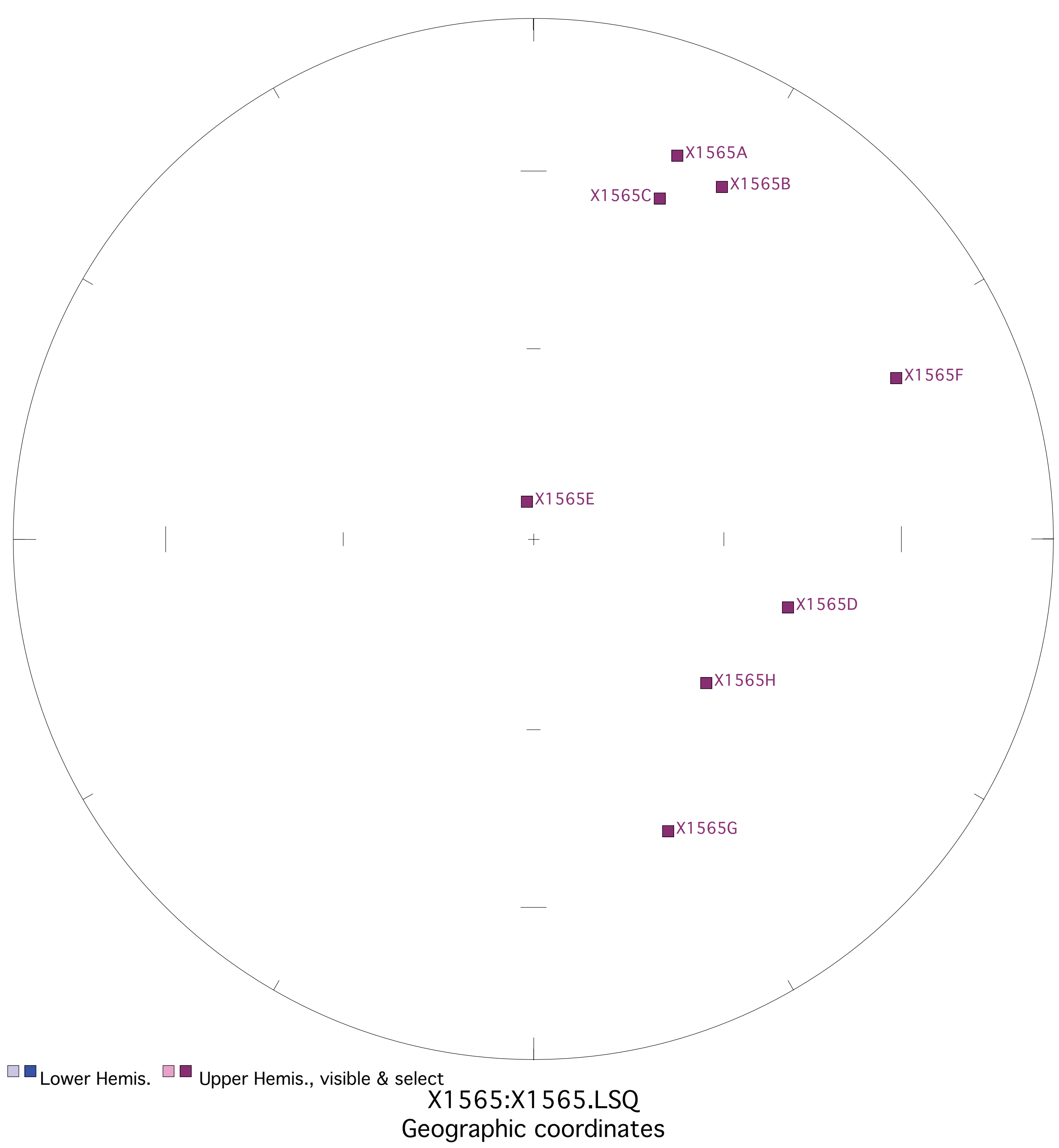

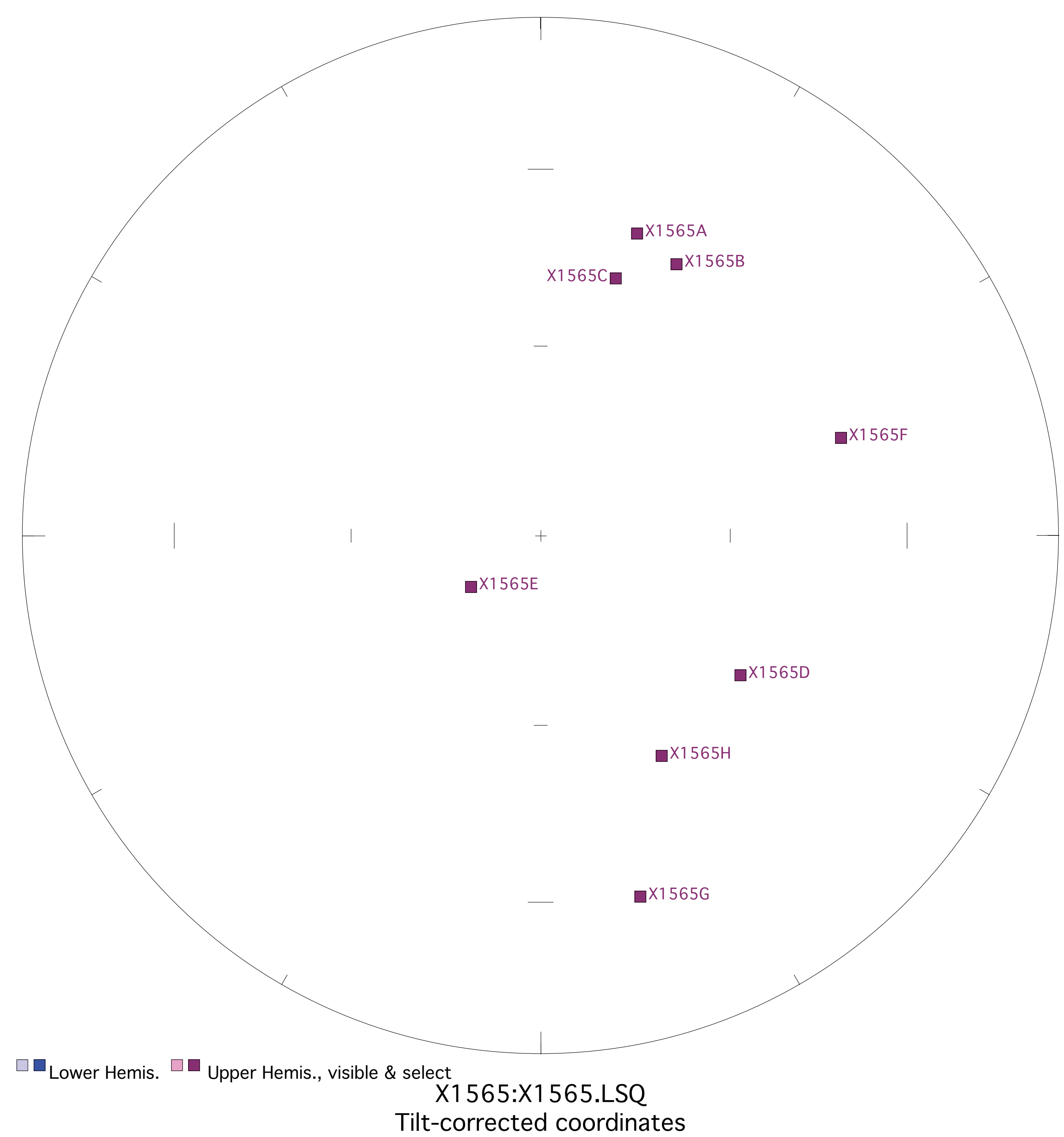

Figure X1566. Panel (a) shows the view of a representative sample in an orthographic projection in geographic coordinates. Blue=horizontal projection, red=vertical projection. Each pair of points represents a measurement step (natural remanent magnetization NRM, liquid nitrogen LN2, or thermal degrees C). Panel (b) shows the same sample in an equal-area projection in geographic coordinates. Blue=lower hemisphere, red=upper hemisphere. Panels (c) and (d) show equal-area projections of the site mean in geographic and tilt-corrected coordinates, respectively. Each point is a ChRM of a sample within the site. Blue=lower hemisphere, red=upper hemisphere. The circle represents the Fisher alpha 95-error of the site mean. Lighter colored points represent sample ChRMs that were not selected into the mean.

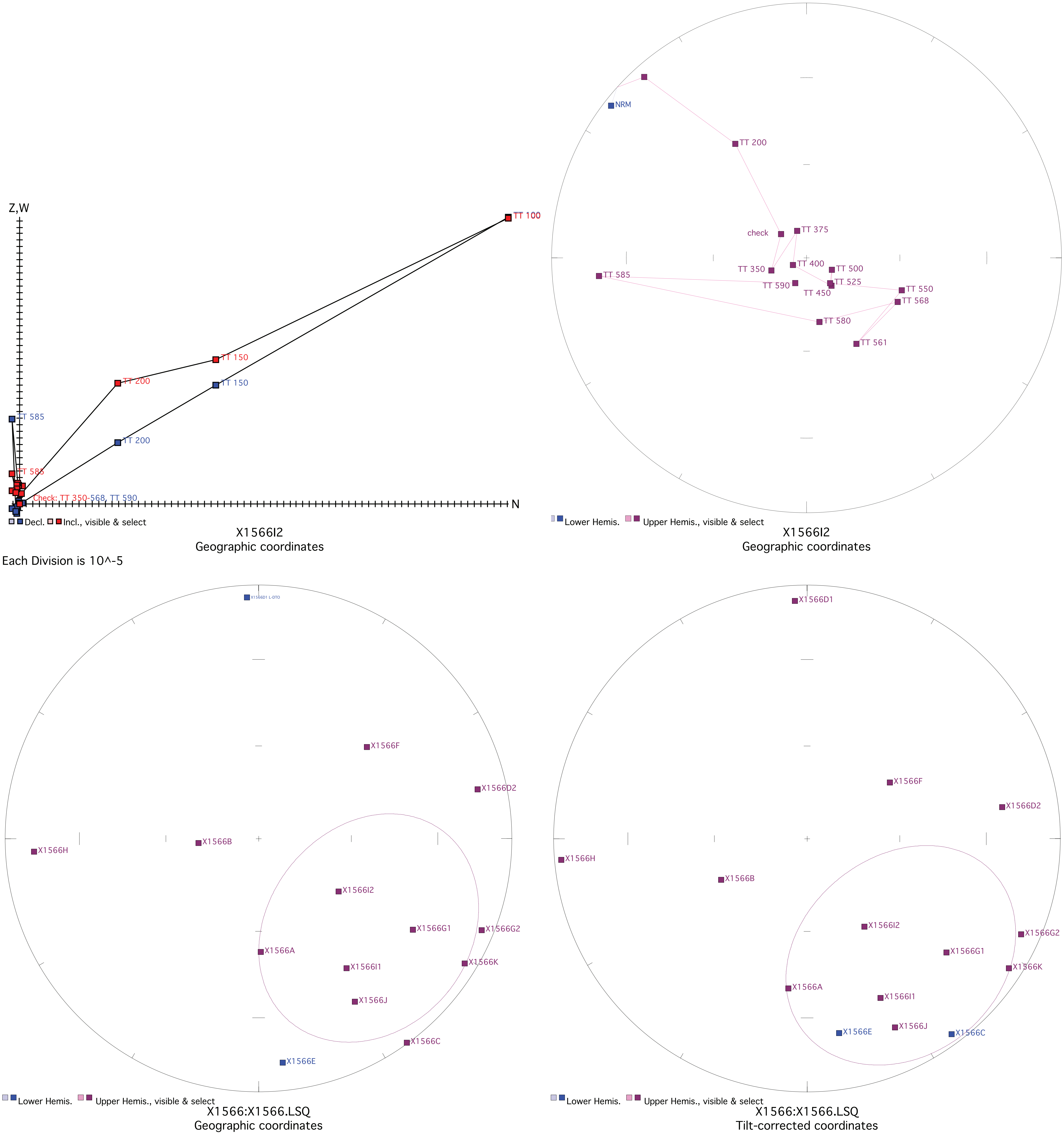

Fisher mean geog. decl.: 129.1, incl.: -40.5 a95 36.1, N: 14

Fisher mean strat. decl.: 141.1, incl.: -37.5 a95 36.1, N: 14

Figure X1567. Panel (a) shows the view of a representative sample in an orthographic projection in geographic coordinates. Blue=horizontal projection, red=vertical projection. Each pair of points represents a measurement step (natural remanent magnetization NRM, liquid nitrogen LN2, or thermal degrees C). Panel (b) shows the same sample in an equal-area projection in geographic coordinates. Blue=lower hemisphere, red=upper hemisphere. Panels (c) and (d) show equal-area projections of the site mean in geographic and tilt-corrected coordinates, respectively. Each point is a ChRM of a sample within the site. Blue=lower hemisphere, red=upper hemisphere. The circle represents the Fisher alpha 95-error of the site mean. Lighter colored points represent sample ChRMs that were not selected into the mean.

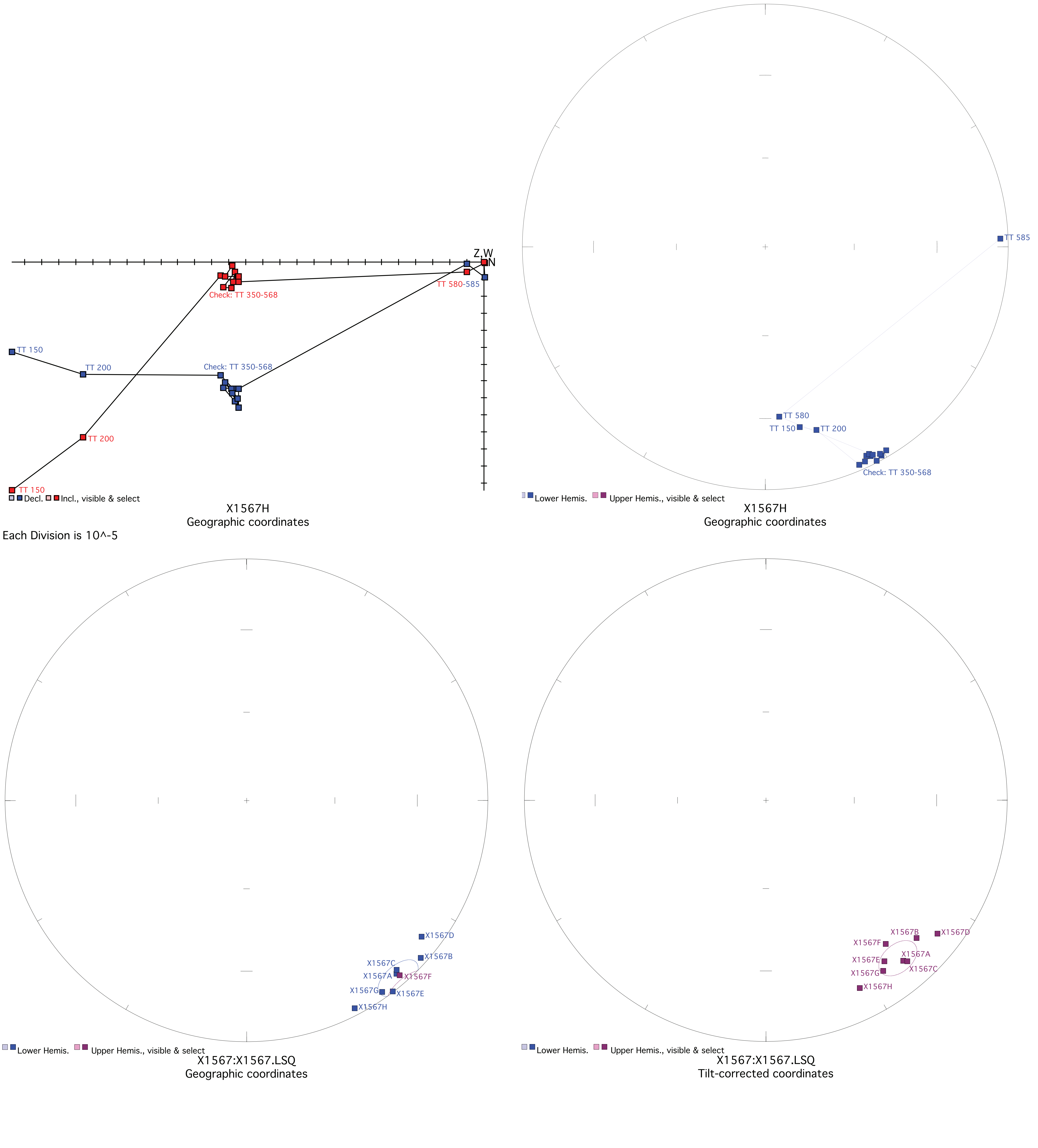

Fisher mean geog. decl.: 139.5, incl.: 3.5 a95 5.9, N: 8

Fisher mean strat. decl.: 140.1, incl.: -15.7 a95 5.9, N: 8